



UNIVERSIDAD NACIONAL AUTÓNOMA DE MÉXICO
PROGRAMA DE MAESTRÍA Y DOCTORADO EN INGENIERÍA
ENERGÍA–GEOTERMIA

EVALUACIÓN DEL POTENCIAL DE UTILIZACIÓN DE SISTEMAS DE ENFRIAMIENTO POR ABSORCIÓN DE UNA ETAPA Y AVANZADOS OPERANDO EN EL CAMPO GEOTÉRMICO DE CERRITOS COLORADOS, JALISCO, MÉXICO.

TESIS
QUE PARA OPTAR POR EL GRADO DE:
DOCTOR EN INGENIERÍA EN ENERGIA

PRESENTA:
JULIANA ISABEL SAUCEDO VELÁZQUEZ

TUTORES PRINCIPALES:

DR. WILFRIDO RIVERA GÓMEZ FRANCO, IER-UNAM
DRA. GEYDY LUZ GUTIÉRREZ URUETA, UASLP

COMITÉ TUTOR:
DR. JORGE ALEJANDRO WONG LOYA, IER-UNAM
DR. ROBERTO BEST Y BROWN, IER-UNAM
DR. JAVIER ALEJANDRO HERNÁNDEZ MAGALLANES, UANL

TEMIXCO, MORELOS, MÉXICO, ENERO 2023.



Universidad Nacional
Autónoma de México



UNAM – Dirección General de Bibliotecas
Tesis Digitales
Restricciones de uso

DERECHOS RESERVADOS ©
PROHIBIDA SU REPRODUCCIÓN TOTAL O PARCIAL

Todo el material contenido en esta tesis esta protegido por la Ley Federal del Derecho de Autor (LFDA) de los Estados Unidos Mexicanos (México).

El uso de imágenes, fragmentos de videos, y demás material que sea objeto de protección de los derechos de autor, será exclusivamente para fines educativos e informativos y deberá citar la fuente donde la obtuvo mencionando el autor o autores. Cualquier uso distinto como el lucro, reproducción, edición o modificación, será perseguido y sancionado por el respectivo titular de los Derechos de Autor.

*Cuando era niña te dije que sería doctora y ahora lo soy,
A mi madre.*

Agradecimientos

A mis asesores Dr. Wilfrido Rivera y Dra. Geydy Gutiérrez, por aceptarme bajo su tutela a pesar de mis circunstancias. Por su tiempo, enseñanzas y empatía que han marcado e inspirado mi camino.

A mi comité académico Dr. Alejandro Wong, Dr. Alejandro Magallanes y Dr. Roberto Best, por sus aportaciones a este trabajo.

A mi madre Rosa María, por cuidar de mis niños, de mi casa y de mí, sin su ayuda no lo hubiera logrado.

A mi esposo David, por no dejar que me rindiera y apoyarme en toda esta trayectoria.

A mis hijos Maya y Nicolas por ser mi luz y mayor motivación.

A mi hermana Anna, por sus consejos y su ayuda económica en esta última etapa.

A mi amiga Polar, por recibirme en su casa y por todos los favores.

A mi prima Erika, por cuidarme a mi bebe para poder terminar en tiempo.

A la vida, por darme las oportunidades para cumplir esta meta.

A mí Juliana, por haber enfrentado tanto cansancio físico y mental y no darme por vencida.

Índice general

Agradecimientos	3
Índice de figuras y tablas	6
Nomenclatura.....	6
Resumen	7
Abstract	8
Capítulo 1. Introducción	9
Introducción general.....	9
Objetivo general	10
Objetivos específicos	11
Estructura de la tesis	11
Capítulo 2. Marco conceptual.....	13
2.1 Generalidades de los sistemas de refrigeración por absorción.....	13
2.1.1 Principios de la refrigeración	13
2.1.2 Sistema convencional de compresión.....	14
2.1.3 Operación de los sistemas de refrigeración por absorción.....	15
2.1.4 Sistemas avanzados de absorción.....	17
2.1.5 Mezclas de trabajo	21
2.2 Energía geotérmica	23
2.2.1 Origen del calor geotérmico	23
2.2.2 Tipos de sistemas geotérmicos.....	23
2.2.3 Pozos geotérmicos.....	25
2.2.4 Aplicaciones de la energía geotérmica.....	26
2.2.5 Ventajas y desventajas energía geotérmica	28
2.2.6 México en el panorama mundial de la energía geotérmica	29
Capítulo 3. Evaluación del potencial de enfriamiento de un sistema de absorción en un campo geotérmico.....	32
3.1 Resumen.....	32
3.2 Artículo	33
Capítulo 4. Evaluación del potencial de enfriamiento de sistemas de absorción simples y avanzados en un campo geotérmico.....	53
4.1 Resumen.....	53

4.2 Artículo	54
Capítulo 5. Caso de estudio: Diseño un sistema de refrigeración por absorción para conservación de leche	74
5.1 Resumen.....	74
5.2 Artículo	75
Conclusiones.....	101
Referencias	104

Índice de figuras y tablas

Figura 1. Diagrama esquemático del sistema de refrigeración por compresión.....	15
Figura 2. Diagrama del sistema de refrigeración por absorción de simple efecto.....	17
Figura 3. Diagrama del sistema de refrigeración por absorción de doble efecto	19
Figura 4. Diagrama del sistema de refrigeración por absorción de triple efecto	20
Figura 5. Diagrama del sistema de refrigeración por absorción de medio efecto	21
Figura 6. Esquema general de un yacimiento geotérmico convencional	24
Figura 7. Esquema general de un yacimiento geotérmico de RDH.....	25
Figura 8. Principales usos de la energía geotérmica en función de su temperatura	27
Figura 9. Adiciones globales en la capacidad de energía geotérmica en 2019	30
Figura 10. Países con mayor potencia geotérmica instalada en 2021	30
Figura 11. Mapa de flujo de calor.....	31
Tabla 1. Sectores del mercado para las aplicaciones de refrigeración geotérmica.....	28
Tabla 2. Ventajas y desventajas de la energía geotérmica	28

Nomenclatura

COP = coeficiente de operación
Q = carga térmica
T = temperatura
W = trabajo

Subíndices

A = absorbedor
C = condensador
E = evaporador
G = generador
SHX = intercambiador de calor

Resumen

El uso de energías renovables permite disminuir el impacto al ambiente producto del consumo eléctrico para satisfacer necesidades humanas, entre ellas la refrigeración a nivel residencial o industrial. Los sistemas de refrigeración por absorción activados con una fuente de calor proveniente de la energía geotérmica son una alternativa para sobrellevar la demanda de enfriamiento a nivel mundial, ya que pueden ser utilizados para conservación de alimentos o acondicionamiento de espacios, entre otras aplicaciones de refrigeración.

Por tal motivo, en este trabajo se evalúa el potencial de utilización y viabilidad de sistemas de enfriamiento por absorción de una etapa y avanzados activados con energía geotérmica de baja, media y alta temperatura. El estudio se llevó a cabo usando datos reales de pozos del campo geotérmico Cerritos Colorados en el bosque de “La primavera”, Jalisco.

En primera instancia se analiza el rendimiento (COP) y el potencial de enfriamiento de un sistema de simple efecto que utiliza una mezcla $H_2O/LiBr$ para diferentes temperaturas de evaporación (T_E) de 6°, 8°, 10° y 12°C y para un rango de temperatura de generación (T_G) de 77-110°C. Se compara la variación en las temperaturas de condensación-absorción ($T_A=T_C$) para las distintas estaciones del año. Las temperaturas de generación se relacionan directamente con la profundidad a la que se podrían obtener mediante el uso de un intercambiador de calor en U dentro del pozo. Las simulaciones fueron realizadas utilizando el Engineering Equation Solver (EES).

Posteriormente se presenta una comparación de los sistemas simple y avanzados (doble, triple y medio efecto), se analiza el potencial de enfriamiento y del COP mediante la variación de la temperatura ambiente para las cuatro estaciones del año para una T_E fija de 8°C. El rango de temperaturas de funcionamiento fue de 59-80°C para el medio efecto, de 77°-110 °C para el simple efecto, de 135-162°C para el doble efecto y de 180-187°C para el triple efecto. Para este estudio se muestra un nuevo modelado del intercambiador de calor en U para la obtención de la temperatura dentro del pozo.

Por último, se analiza la problemática de un Ejido para mantener su actividad productiva a falta de red eléctrica y se propone una unidad de refrigeración por absorción $H_2O/LiBr$ de simple y doble efecto que utiliza el calor de un pozo geotérmico cercano e inoperante para la producción de potencia. Se presenta el diseño un almacén (cuarto frío) para conservar la leche que ordeñan a 10°C y el dimensionamiento del sistema de absorción, usando EnergyPlus, con una carga de enfriamiento de 5 kW. Además, se muestra un análisis económico para compararlo contra un sistema convencional y un sistema solar.

Abstract

Using renewable energies makes it possible to reduce the impact on the environment due to electricity consumption to satisfy human needs, including refrigeration at a residential or industrial level. Absorption refrigeration systems activated with a heat source from geothermal energy are an alternative to meet the global cooling demand since they can be used for food preservation or space conditioning, among other refrigeration applications.

For this reason, this work evaluates the potential use and feasibility of single-stage and advanced absorption cooling systems activated with low, medium, and high-temperature geothermal energy. The study was carried out using actual data from wells in the Cerritos Colorados geothermal field in the "La primavera" forest, Jalisco.

The coefficients of performance (COP) and the cooling potentials of a simple-effect system using an H₂O/LiBr mixture for different evaporation temperatures (T_E) of 6°, 8°, 10°, and 12°C and at a generation temperature range (T_G) of 77-110°C were analyzed. In addition, the variation in the condensation-absorption temperatures ($T_A=T_C$) for the different seasons of the year was compared. Generation temperatures are directly related to the depth at which they could be obtained by using a U-shaped heat exchanger within the wellbore. Simulations were performed using the Engineering Equation Solver (EES).

Subsequently, a comparison of the simple and advanced systems (double, triple, and half effect) was presented. The cooling potential and the COP were analyzed by varying the ambient temperature for the four seasons of the year at a fixed TE of 8°C. The operating temperature range was 59-80°C for the half-effect system, 77°-110°C for the single-effect, 135-162°C for the double-effect, and 180-187°C for the triple-effect. For this study, a new model of the U-shaped heat exchanger was shown to obtain the temperature inside the well.

Finally, the problem of a rural area maintaining its productive activity in the absence of an electrical network is analyzed, and a simple and a double effect H₂O/LiBr absorption refrigeration unit were proposed using the heat of a nearby and inoperative geothermal well for the power output. The design of a warehouse (cold room) to keep the milk that is milked at 10°C and the sizing of the absorption system, using EnergyPlus, with a cooling load of 5 kW, is presented. In addition, an economic analysis is shown to compare it against a conventional system and a solar cooling system.

Capítulo 1. Introducción

Introducción general

Dentro de las prioridades que actualmente la humanidad debe afrontar se encuentra de forma imprescindible el deterioro climático. Este gran problema, ocasionado por el aumento de población y la consecuente demanda de energía, es el motivo de numerosos temas de investigación relacionados a mitigación del daño ambiental. Los esfuerzos van encaminados a la búsqueda de procesos y materiales más limpios, y al uso de energías renovables, como alternativas que cubran el consumismo y las necesidades poblacionales.

En relación con dichas necesidades poblacionales se encuentra la refrigeración. Este es un proceso de uso cotidiano, tanto a nivel residencial para confort humano y conservación de alimentos como en la industria en procesos productivos y de almacenamiento. Aproximadamente el 50% de la energía consumida a nivel mundial se debe a procesos de refrigeración y más del 20% de la energía es usada en acondicionamiento térmico de espacios. Se estima que para 2024 la demanda de servicios de cadena de frío en Norteamérica aumentara un 76%, lo que conlleva a una demanda progresiva de servicios, energía, alimentos, medicamentos, etc., (IEA, 2018). Esta demanda de refrigeración es actualmente suministrada en su mayoría por sistemas convencionales de refrigeración y aire acondicionado, actualmente 2 mil millones operando en el mundo (IEA, 2018).

Con base a estas cifras se investigan sistemas alternos de refrigeración con menor impacto en el medio ambiente. En este campo adquieren importancia los sistemas de refrigeración por absorción, como una alternativa a los sistemas convencionales de refrigeración, al prescindir del trabajo de compresión (Sureshchandra Bhurat et al., 2022); y por ende el empleo de energía eléctrica. La consecuente reducción de la demanda de energía de enfriamiento es importante y la capacidad de estos sistemas para operar con aporte térmico, haciendo posible la introducción de energías renovables o calor residual de otros procesos (Ozcan et al., 2019). Adicionalmente, los sistemas de refrigeración por absorción son una tecnología que utiliza refrigerantes considerados “respetuosos” con el medio ambiente como el agua, amoníaco y algunas sales, los cuales se ajustan a los protocolos internacionales como el de Montreal y Kioto (Coskun et al., 2010). Asimismo, son sistemas con un bajo costo de mantenimiento según la fuente de energía térmica, con rango de temperaturas desde de 50 a 200 °C. En este rango puede usarse la energía geotérmica, la solar, el calor residual de plantas de cogeneración o proceso de vapor, entre otros (Keçeciler et al., 2000).

Entre las fuentes mencionadas en el párrafo anterior, la energía geotérmica se presenta como una opción poco explotada y con gran potencial, sobre todo en México. El término renovable describe una característica del recurso, su continuidad para producción de calor, es decir, la energía extraída del recurso se sustituye de manera continua, aun cuando su generación depende de la explotación del fluido geotérmico en el yacimiento, el volumen extraído se

puede llegar a recuperar logrando un explotación sostenible, lo que significa que el sistema de producción sería capaz de mantener un nivel de producción durante largos periodos de tiempo si se administra adecuadamente (Rybach & Mongillo, 2006).

Para mencionar datos de interés, se estima que el calor almacenado en el interior de la Tierra es de 12.6 billones de exajoules (12.6×10^{12} EJ), el cual se transfiere a la superficie terrestre a una tasa de 65 miliwatts por metro cuadrado (mW/m^2), con un flujo de calor global neto de 1,388 exajoules anuales (Gupta & S. Roy, 2007). Este flujo de calor es en gran parte de las regiones del mundo lo suficientemente alto para ser aprovechado mediante la perforación de pozos poco profundos o bombas de calor geotérmicas (Saemundsson et al., 2011). Se proyecta para el 2030 un crecimiento del 70% para la energía geotérmica, con 3.800 MWt de aplicaciones en usos directos los cuales procederán principalmente del uso en cascada en campos geotérmicos (Gutiérrez-Negrín et al., 2020). Debido a sus características, la energía geotérmica tiene un futuro prometedor para contribuir a satisfacer las necesidades energéticas del mundo, y puede ser ampliamente utilizada para operar sistemas de refrigeración por absorción. Con el uso de la energía geotérmica para calefacción y climatización se puede reducir el consumo energético entre un 30% y 70% en modo calefacción, y entre un 20 y 95% en modo refrigeración, en comparación con los sistemas convencionales (Sierra Rodríguez, 2016).

Considerando las ideas anteriores, esta tesis doctoral se enfoca en el uso de energía geotérmica como fuente de calor para operar los sistemas de refrigeración por absorción. A partir de la identificación de la demanda energética a nivel mundial para sostener la refrigeración/enfriamiento en todos los sectores, el enorme potencial que tiene la energía geotérmica en el país y revisando el estado del arte de los sistemas de refrigeración por absorción activados con energía geotérmica; el trabajo tiene como finalidad la evaluación del potencial de enfriamiento de los sistemas refrigeración por absorción de una etapa y avanzados para ser operados con pozos geotérmicos inoperantes para la producción de energía eléctrica, pero no así para el suministro de calor. De esta manera se pretende contribuir a la disminución de la demanda de refrigeración y al consumo de energía eléctrica, así como al aprovechamiento del potencial de recursos infrautilizados.

Objetivo general

Evaluar el potencial de utilización y viabilidad de sistemas de enfriamiento por absorción de una etapa y avanzados activados con energía geotérmica de baja, media y alta temperatura.

Objetivos específicos

- Investigar el estado del arte de los sistemas de refrigeración por absorción operados con energía geotérmica.
- Simular el potencial de enfriamiento y operación para los ciclos de absorción de una etapa y avanzados.
- Evaluar viabilidad operacional de ciclos de absorción de una etapa y avanzados mediante comparación de resultados de simulación.
- Definir caso de estudio para implementación teórica del sistema de enfriamiento.
- Realizar modelación y análisis técnico-económico para definir la factibilidad del aprovechamiento geotérmico para máquinas de absorción.

Estructura de la tesis

La presente tesis doctoral está conformada por cinco 6 capítulos estructurados de la siguiente manera:

El Capítulo 1 presenta una introducción general sobre el panorama de los sistemas de refrigeración por absorción operados con energías renovables, en específico con recursos geotérmicos como una alternativa a la demanda energética. Además, se plantean los objetivos generales y específicos de esta tesis de investigación doctoral.

El Capítulo 2 abarca el marco conceptual de la tesis, en el cual se describe los principios de la refrigeración por compresión y por absorción. Incluye una breve descripción de las mezclas de trabajo, principalmente Agua/Bromuro de litio (mezcla seleccionada para este estudio), se describe las características de energía geotérmica como fuente de calor renovable, su origen, aplicaciones, sus ventajas y desventajas. Por último, se presenta el panorama mundial de su uso y el potencial de esta alternativa en México.

El Capítulo 3 presenta el análisis del potencial de enfriamiento para un sistema de refrigeración por absorción de simple efecto operado con una fuente de calor geotérmica. Como cuerpo del capítulo se muestra el artículo correspondiente que describe a detalle el estudio realizado.

El Capítulo 4 muestra el análisis del potencial de enfriamiento para sistemas avanzados de refrigeración por absorción (doble, triple y medio efecto) operado con una fuente de calor geotérmica. Se ofrece el artículo correspondiente que describe a detalle el estudio realizado.

El Capítulo 5 exhibe el caso de estudio que considera el diseño, modelado y costos de un sistema de refrigeración por absorción para conservación de leche, el cual incluye el propio diseño del almacén, el dimensionamiento del sistema de refrigeración y el análisis económico de dos propuestas de sistemas de absorción. Se presenta el artículo correspondiente.

Finalmente, el Capítulo 6 presenta las conclusiones generales de proyecto doctoral.

Capítulo 2. Marco conceptual

En este capítulo se presenta las generalidades de los sistemas de refrigeración por absorción, principios de operación, clasificación, una breve descripción de las mezclas de trabajo y su comparación con un sistema convencional por compresión. Posteriormente se hace referencia a la energía geotérmica como fuente de calor renovable, su origen, aplicaciones, ventajas y desventajas. Además, se describe el panorama mundial de su uso y potencial en México.

2.1 Generalidades de los sistemas de refrigeración por absorción

2.1.1 Principios de la refrigeración

Los procesos de enfriamiento natural consisten en la pérdida o eliminación de calor de un cuerpo o espacio de manera espontánea. Naturalmente, los cuerpos pueden enfriarse hasta llegar a la temperatura del ambiente, pero se requieren de técnicas específicas para lograr mantener el cuerpo a una temperatura inferior al ambiente. Por otra parte, el enfriamiento artificial se basa en el uso de distintos procesos que utilizan fluidos conocidos como refrigerantes. Estas sustancias tienen propiedades termodinámicas que los sitúan como grandes absorbedores de calor, cuya función es extraer el calor de un cuerpo de manera constante, y con ello realizar el proceso de refrigeración (Dimas et al., 2018). El enfriamiento se puede realizar por medio de un abatimiento de la temperatura sin que el cuerpo sufra un cambio de estado físico a temperatura constante o mediante procesos que provocan un cambio de estado como la evaporación, fusión, sublimación, etc. (Dimas et al., 2018).

La refrigeración pertenece a las tecnologías que transfieren calor de una temperatura baja a una temperatura alta. Con base al enunciado de Clausius de la “Segunda Ley de termodinámica”, esta transferencia requiere una entrada termodinámica en forma de trabajo o de calor, es decir, demanda un gasto de energía (Herold Keith E. et al., 2016).

Los sistemas de absorción son un ejemplo de una tecnología impulsada por calor, en la cual es posible transferir calor de una temperatura baja a una alta temperatura mientras suministra sólo calor como energía impulsora. Al eliminar la necesidad de una entrada de trabajo, un ciclo de absorción proporciona una solución a las necesidades de enfriamiento y refrigeración.

El desempeño de los sistemas de refrigeración se define por el COP (coeficiente de operación o coefficient of performance), el cual se describe como la relación entre el beneficio obtenido y la energía requerida. En el caso de la refrigeración se define como la relación entre la capacidad de refrigeración Q_E y la potencia neta necesaria (Herold Keith E. et al., 2016).

$$COP = \frac{\text{potencia de enfriamiento producida}}{\text{trabajo neto suministrado}} = \frac{Q_E}{W_{neto}} \quad (2.1)$$

Existen características operativas que diferencian a los sistemas de refrigeración por absorción y los de compresión. En el siguiente apartado se describen y se comparan ambos sistemas.

2.1.2 Sistema convencional de compresión

Los sistemas de refrigeración por compresión de vapor constituyen aún la tecnología más utilizada en calefacción, refrigeración residencial o comercial, refrigeración de alimentos y aire acondicionado de automóviles, etc. (Herold keith E. et al., 2016). El ciclo de compresión está compuesto por cuatro elementos principales: un compresor, un condensador, una válvula de expansión y un evaporador. Utiliza un refrigerante de composición química fija, el cual es comprimido en el compresor. Para llevar a cabo esta compresión es necesario el consumo de una cantidad de energía eléctrica, con el fin de elevar la presión y temperatura de este refrigerante hasta las condiciones requeridas. Alcanzadas éstas, el refrigerante entra al condensador, en donde mediante la extracción de calor cambia de fase de vapor a líquido a alta presión. Pasa luego por la válvula de expansión en la cual se reduce la presión y por tanto la temperatura, de tal manera que se obtiene una mezcla líquido-vapor, a baja temperatura. En estas condiciones, la mezcla entra al evaporador en donde absorbe calor ya sea del espacio o productos a enfriar, produciéndose el efecto de enfriamiento. Por último, el refrigerante sale del evaporador como vapor saturado y es de nuevo comprimido, comenzando el ciclo nuevamente. En la Figura 1 se presenta el diagrama esquemático del sistema de refrigeración por compresión. En este sistema el compresor mecánico, normalmente accionado por un motor eléctrico, proporciona la entrada de trabajo que impulsa la transferencia de calor desde la temperatura baja a la alta temperatura.

Siguiendo la definición de COP, para el sistema de compresión (Herold keith E. et al., 2016):

$$COP = \frac{\text{potencia de enfriamiento producida}}{\text{energía suministrada al compresor}} = \frac{Q_E}{Q_C - Q_E} \quad (2.2)$$

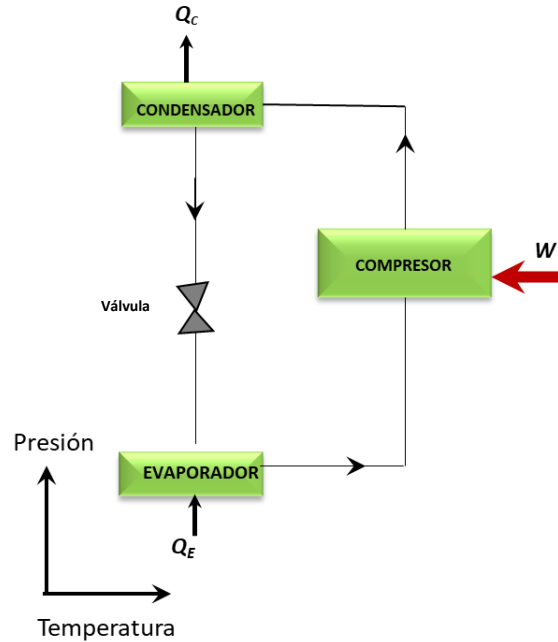


Figura 1. Diagrama esquemático del sistema de refrigeración por compresión.

2.1.3 Operación de los sistemas de refrigeración por absorción

La absorción se refiere a la capacidad que tienen algunas sustancias para absorber en fase líquida el vapor de otras sustancias. Termodinámicamente los ciclos de refrigeración por absorción se basan en el principio de condensación y evaporación de un refrigerante a diferentes presiones, al igual que los de compresión. Sin embargo, la diferencia entre estos ciclos se presenta en el proceso en el cual dicho fluido se traslada desde la zona de baja presión a la zona de alta presión. Además, se usa una mezcla (solución absorbente – refrigerante) cuya concentración varía durante todo el ciclo, en lugar de un solo refrigerante. El refrigerante vaporizado en la zona de baja presión es absorbido por una solución que tiene afinidad fisicoquímica por dicho fluido conocida como absorbente. La mezcla líquida resultante es bombeada a la zona de alta presión, donde el refrigerante es extraído de nuevo de la solución mediante la aportación de calor (Dimas et al., 2018). En el caso de los sistemas de compresión, este proceso se realiza mediante la acción mecánica de un compresor activado por energía eléctrica.

En la Figura 2 se muestra el diagrama de un sistema de refrigeración por absorción. Como se puede observar, algunos de los componentes los tienen ambos sistemas, como lo son el evaporador, condensador, y válvula de expansión; sin embargo, en un sistema de absorción se reemplaza el compresor por varios dispositivos siendo estos: un generador, un absorbedor, un intercambiador de calor de solución, una válvula de expansión y una bomba.

A continuación, se describen cada uno de los componentes del sistema de absorción:

- **Generador:** es un intercambiador de calor que recibe calor de una fuente externa de alta temperatura, con lo cual se evapora en primera instancia parte del refrigerante contenido en la solución.
- **Condensador:** intercambiador de calor cuya función es condensar el vapor de refrigerante proveniente del generador, mediante la eliminación de calor por intercambio entre el calor latente del refrigerante a alta presión y con el aire exterior o con agua fría.
- **Válvula de Expansión:** dispositivo cuya función es bajar la presión del líquido y producir una mezcla de líquido-vapor a baja temperatura y presión.
- **Evaporador:** es un intercambiador cuya función es llevar a cabo el proceso de enfriamiento o refrigeración, retirando el calor de los alimentos almacenados o del espacio a acondicionar.
- **Absorbedor:** intercambiador de calor donde se lleva a cabo el proceso de absorción del refrigerante por la solución proveniente del generador, liberando una cantidad calor.
- **Bomba:** dispositivo que se usa para circular la solución del absorbedor al generador elevando su presión.

Estos componentes operan de la siguiente manera. En el generador se tiene la solución con alta concentración de refrigerante, a la que se le suministra una cantidad de calor (de una fuente externa) para aumentar su temperatura y lograr vaporizar parte del refrigerante contenido en la solución en condiciones de alta presión y temperatura. Este vapor de refrigerante producido entra al condensador, y luego a la válvula de expansión y al evaporador de la misma forma que lo hace el sistema de compresión. Pero ahora y a diferencia del ciclo de compresión, el refrigerante en fase vapor que sale del evaporador, va a ser absorbido por la solución pobre de refrigerante proveniente del generador, de tal forma que una vez que se absorbe forma una a solución rica de refrigerante, lo que produce un cambio en su concentración (de débil a fuerte), y desprendimiento de calor. Por último, esta solución se vuelve a enviar al generador a través de la bomba, dando inicio nuevamente al ciclo.

El intercambiador de solución es un componente adicional que se coloca entre el absorbedor y el generador para hacer más eficiente el sistema, al precalentar la solución que va del absorbedor al generador, con la solución caliente y con ello aumentar la temperatura y eficiencia del generador al disminuir el calor transferido.

Para el COP del sistema de absorción, el término de la energía requerida involucra la energía que se suministra al generador más el trabajo que se consumen por el bombeo de la solución al generador (Herold Keith E. et al., 2016).

$$COP = \frac{\text{potencia de enfriamiento producida}}{\text{energía de entrada requerida}} = \frac{Q_E}{Q_G + W_B} \quad (2.3)$$

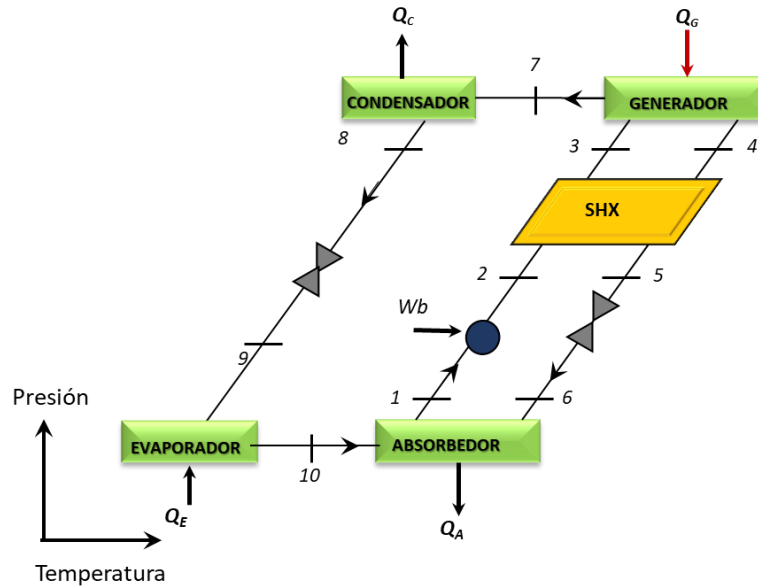


Figura 2. Diagrama del sistema de refrigeración por absorción simple efecto.

2.1.4 Sistemas avanzados de absorción

El sistema descrito en el apartado anterior es el sistema básico y corresponde al sistema más simple llamado sistema de una etapa o simple efecto, debido a que tiene una sola etapa de generación o producción de refrigerante y una de evaporación. Existen diferentes configuraciones o arreglos de estos sistemas de absorción.

Los sistemas de simple efecto tienen rangos de operación que van de temperaturas de generación de 80-120°C. y pueden llegar a obtenerse COP de 0.85- 1.1 (Best & Rivera, 2015) (Herold Keith E. et al., 2016).

Los sistemas avanzados son los sistemas de doble efecto, triple efecto y medio efecto (Herold Keith E. et al., 2016). A continuación, explica de forma general las configuraciones de estos sistemas. Una descripción detallada se presenta en el capítulo 4.

Sistema de doble efecto

El sistema de doble efecto se llama así por tener dos etapas de generación de refrigerante y una de evaporación, y opera de la siguiente manera: en la parte inferior se tienen los mismos dispositivos del ciclo de simple efecto (un generador que produce el vapor refrigerante, posteriormente se condensa, se produce el frío a través del evaporador, y se absorbe en el absorbedor) como ilustra la Figura 3. Sin embargo, y a diferencia del sistema de simple efecto, en alta presión el sistema de doble efecto se le adiciona un componente, un generador-condensador, que en una etapa la principal función es de generar refrigerante y en otra etapa su función es la de condensar.

Al tener un segundo generador (a más alta presión) se obtendrá una producción de refrigerante con una presión mayor que la se tenía con el simple efecto. Otra característica de este sistema es que el calor liberado en la condensación se utiliza directamente para suministrarse al generador del ciclo de presión menor, de tal manera que con un solo suministro de energía se está produciendo doble efecto de generación de refrigerante. Se llama de doble efecto porque se tienen dos etapas de generación de refrigerante y una de evaporación.

La ventaja de estos sistemas es que tienen un coeficiente de operación mayor que los de simple efecto, es decir son sistemas más eficientes, ya que al tener doble producción de refrigerante alcanzan valores de COP entre 0.9 y 1.33. La desventaja es que se requiere una temperatura de activación mayor a los de simple efecto, entre 130 y 185° C, para que cuando se realice la condensación se pueda hacer a 80°C y ese calor del condensado sea suficiente para activar la segunda etapa.

Los sistemas de doble efecto tienen diversas configuraciones, algunos de los más comunes son en serie, inverso y en paralelo.

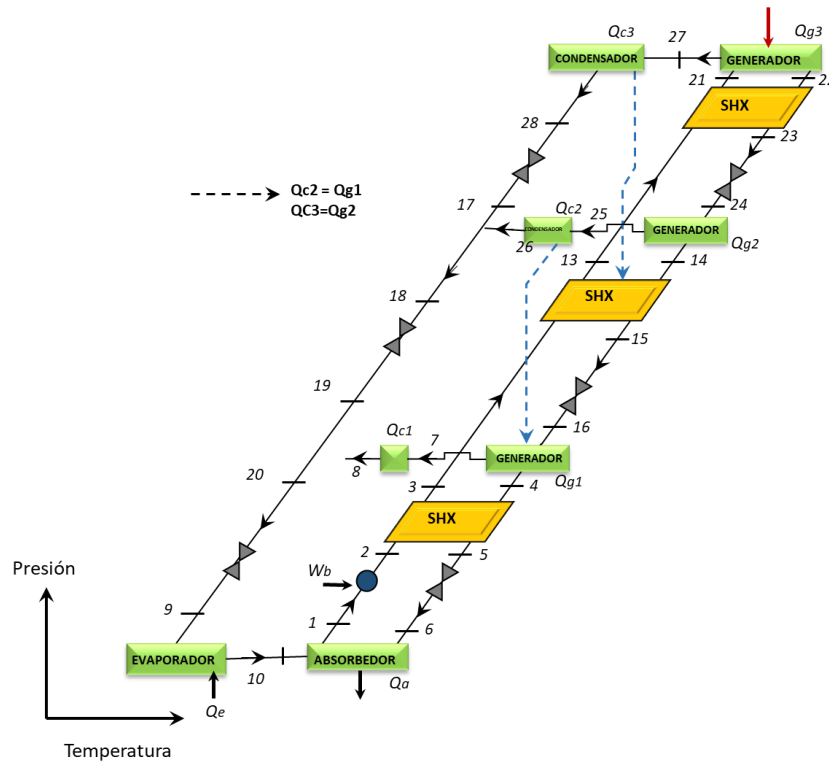


Figura 4. Diagrama del sistema de refrigeración por absorción de triple efecto.

Sistema de medio efecto

El sistema de medio efecto, a diferencia de los ciclos descritos anteriormente, tiene dos suministros de calor en los dos generadores y solo una etapa de enfriamiento. El generador de baja presión se utiliza para activar el circuito de la solución de alta, lo que hace que tenga dos circuitos de solución, uno de ellos a alta presión y el otro a baja presión. Por lo tanto, el ciclo de medio efecto tiene además de dos generadores, dos absorbedores, y dos intercambiadores de calor. Donde una sola corriente entra al condensador, pero se produce vapor refrigerante en los dos generadores y se suministran uno a otro.

La ventaja de este sistema es que utiliza menores temperaturas de activación 55-80° C, pero requiere mayor cantidad de energía a menor temperatura lo que lo hace menos eficiente con COP entre 0.4-0.5

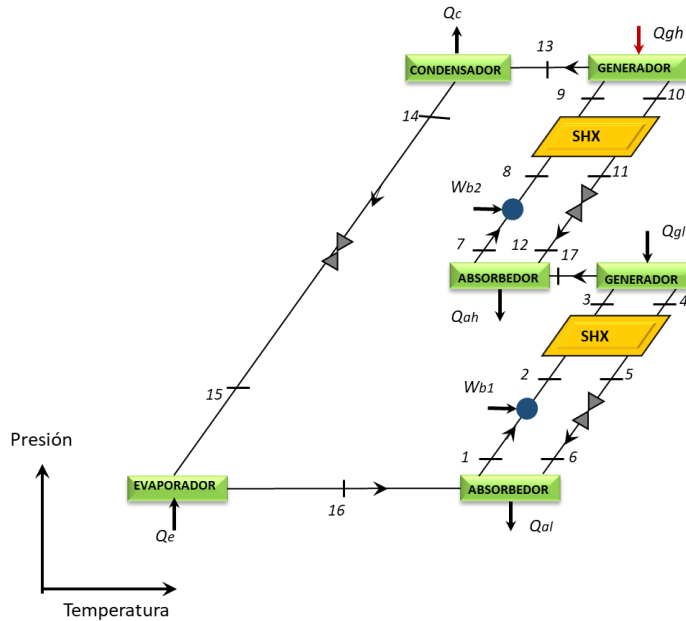


Figura 5. Diagrama del sistema de refrigeración por absorción de medio efecto.

2.1.5 Mezclas de trabajo

Como ya se había mencionado, los ciclos de absorción operan con mezclas de trabajo refrigerante-absorbente. El desempeño y costo de operación del sistema de absorción va a depender en su parte de las propiedades de las mezclas de trabajo (Pérez-Blanco, 1984).

Los refrigerantes son sustancias con la capacidad de producir el efecto de enfriamiento en el sistema de refrigeración, mediante la absorción de calor de otro cuerpo o sustancia. Estos van cambiando sus propiedades a lo largo del todo el ciclo. De manera general cualquier sustancia con la capacidad de cambiar de estado de líquido a vapor y viceversa puede actuar como refrigerante (Hernández Magallanes, 2017).

Por su parte los absorbentes debe tener ciertas propiedades para poder ser utilizado como fluido (Dimas et al., 2018):

- Tener una fuerte afinidad por el refrigerante.
- Menor volatilidad que el refrigerante para facilitar su separación en el generador.
- La presión de vapor en el generador debe ser despreciable o muy baja, en comparación con la presión de vapor del refrigerante.
- El absorbente debe permanecer en estado líquido durante todo el ciclo, para evitar el problema de cristalización.
- Estabilidad química.
- No corrosivo.

- No tóxico.
- El calor específico debe ser bajo para evitar pérdidas.
- La conductividad térmica alta.
- La viscosidad y la tensión superficial deben ser bajas para facilitar la transmisión del calor y la absorción.

El mecanismo de funcionamiento de los sistemas de refrigeración por absorción es el mismo, pero pueden utilizar diferentes tipos de mezclas de trabajo, es decir diferir entre el refrigerante y absorbente utilizado. Las mezclas más utilizadas y estudiadas son mezcla agua/bromuro de litio, amoníaco/agua.

En la mezcla agua/LiBr el agua actúa como refrigerante y el LiBr como absorbente. Presenta las siguientes ventajas: no tóxica ni inflamable, el refrigerante (agua) tiene una alta capacidad calorífica, la solución de LiBr no es volátil. Como desventajas presenta rangos más limitados de temperatura a los que puede trabajar debido a los problemas de cristalización del fluido, ya que el sistema no puede enfriar a temperaturas menores del punto de congelación del agua. Opera en condiciones de vacío y el costo del LiBr es elevado.

Por su parte, la mezcla amoníaco-agua tiene las ventajas de que puede alcanzar temperaturas de refrigeración muy bajas. Las desventajas son: toxicidad, necesita presiones muy altas y por ende tuberías más gruesas, presenta problemas de volatilidad del solvente por lo que es necesario adicionar un componente al sistema (rectificador) para realizar la separación de vapor.

La elección de la mezcla a utilizar dependerá de la aplicación que se requiere, es decir, del trabajo final en el que se empleara el sistema de absorción: para la refrigeración y almacenamiento de alimentos se requiere un rango de 0-7 °C, para aire acondicionado de 7-18 °C, para congelación y producción de hielo < 0°C (b. Dorgan et al., 1995).

En este trabajo se utiliza la mezcla agua-LiBr debido a las ventajas citadas, y a la aplicación requerida de acondicionamiento de espacios y almacenamiento de alimentos.

2.2 Energía geotérmica

2.2.1 Origen del calor geotérmico

La palabra geotermia se deriva del griego geo: "Tierra", y thermos: "calor"; literalmente "calor de la Tierra". La energía geotérmica es aquella energía natural térmica/calorífica que se encuentra en el interior de la Tierra, y que se transmite desde sus capas internas hacia la parte más externa de la corteza terrestre, a través de la roca y/o de fluidos. Este término de Geotermia se utiliza para designar tanto la ciencia que estudia los fenómenos térmicos internos del planeta, así como el conjunto de procesos industriales para producir energía eléctrica y/o calor útil para el ser humano (Trillo & Angulo, 2008).

El origen del calor interno de la tierra es el resultado de distintos fenómenos como:

- Desintegración de isótopos radiactivos presentes en la corteza y el manto, principalmente U235, U238, Th232 y K40.
- El calor inicial que se liberó durante la formación del planeta hace 4500 Ma y que todavía está llegando a la superficie.
- Los movimientos diferenciales entre las diferentes capas que constituyen la Tierra, principalmente entre el manto y núcleo.
- La liberación de calor por la continua cristalización tanto en el núcleo externo (líquido), como en la zona de transición del núcleo interno (sólido).

Este calor fluye debido al movimiento de las placas tectónicas (zonas de subducción, expansión del suelo oceánico y rift) las cuales, al chocar, separarse o moverse constituyen regiones geológicamente activas (Andraca Gutiérrez F. H. & Rodríguez Marian J. R., 2012), en las cuales se producen terremotos, erupciones volcánicas y fallas, que son las señales de la tectónica originada por los flujos de calor desde el interior de la tierra. En estas zonas los valores de flujo geotérmico son anómalos, donde el incremento del gradiente geotérmico es entre 15 y 30°C cada 100 m, por lo que se llegan a encontrar temperaturas desde 150 a 300°C a profundidades de 1.5 a 2 km, y es ahí, donde se encuentran los sistemas geotérmicos explotables o con potencial geotérmico (IDAE & IGME, 2008).

2.2.2 Tipos de sistemas geotérmicos

Se denomina yacimiento geotérmico al espacio de la corteza terrestre donde se encuentran materiales permeables que almacenan los recursos geotérmicos capaces de ser explotados por el hombre en condiciones técnicas disponibles y económicas adecuada (IDAE & IGME, 2008). Para que estos yacimientos geotérmicos logren ser explotados, es necesario que tengan suficiente calor natural que se transforme en presión y lleve el vapor a la superficie.

Por tanto, un sistema geotérmico se refiere a todas las partes que conforman el sistema, desde el sistema hidrológico, la superficie implicada y el flujo saliente del sistema. Se diferencia del campo geotérmico el cual se refiere a una zona geográfica definida, que indica un área donde se presenta actividad geotérmica en la superficie de la Tierra o en su caso al yacimiento geotérmico debajo de ella (Hiriart & Bert, 2011).

Con base a su tipo de explotación, los principales de yacimientos o sistemas geotérmicos son: los yacimientos hidrotermales conocidos también como sistema convencionales, y los yacimiento de roca caliente seca (HDR:Hot Dry Rock) o sistemas geotérmicos mejorados (EGS ,Enhanced or engineered geothermal systems,) conocidos también como sistema no convencionales (Hiriart & Bert, 2011). Los yacimientos hidrotermales conforman la mayoría de los sistemas geotérmicos, en los cuales el medio de transporte es el agua; las condiciones clásicas para que se conforme este yacimiento son: que se tenga una fuente de calor activo (cuerpo magmática en proceso de enfriamiento) , que se forme un acuífero con alta permeabilidad natural del cual circula un fluido, por lo general agua de origen meteórica ya sea en fase líquida o vapor la cual se encuentra dominados por los estratos o controlados por fracturas ,y por ultimo que tenga una cobertera o sello que impida o límite que escape del fluido (IDAE & IGME, 2008). Cuando el agua del acuífero se mezcla con los fluidos magmáticos y se calienta, da origen a estos yacimientos. En la Figura 6 se representa el esquema general de este tipo de yacimientos.

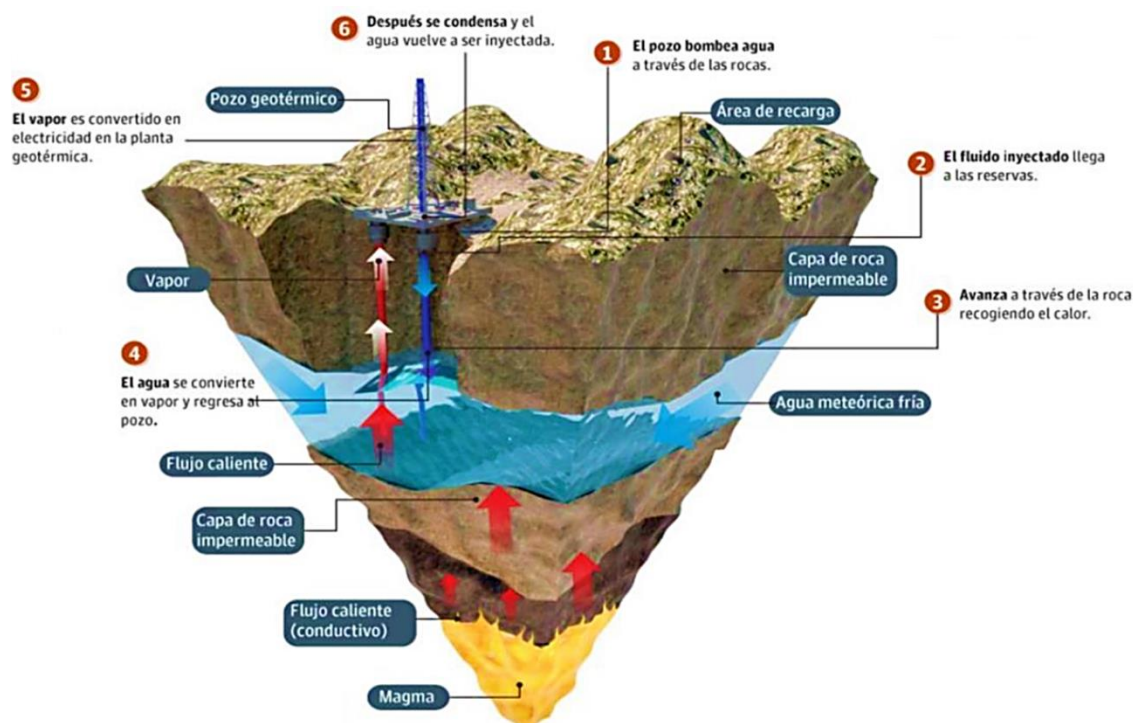


Figura 6. Esquema general de un yacimiento geotérmico convencional (tomado de (Hiriart, 2013).

Por su parte los yacimientos tipo HDR (Figura 7) son sistemas que se han calentado mediante volcanismo o flujo de calor anormalmente alto en volúmenes de roca, pero a diferencia de los hidrotermales, estos tienen baja permeabilidad o son impermeables, debido a esto, no se pueden explotar de la misma forma que un sistema hidrotermal (forma convencional). En los sistemas de HDR es necesaria la estimulación hidráulica y/o química de las rocas del subsuelo con patrones de flujo construidos artificialmente para mejorar las redes de fracturas; como es el caso del método hidro fracturado o “fracturado hidráulico” entre otras tecnologías (Hiriart, 2013). Estos campos aún están en etapa de desarrollo por la tecnología que requieren y por el aporte externo del recurso agua lo que limita su uso.

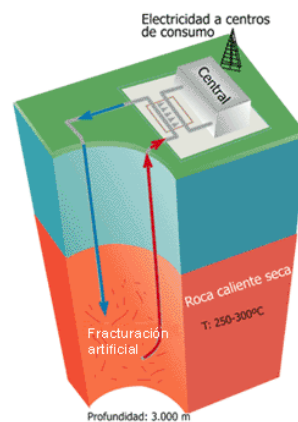


Figura 7. Esquema general de un yacimiento geotérmico de RDH tomado de (IGME, n.d.).

Otras de las clasificaciones más utilizadas de los sistemas geotérmicos es la relacionada con su temperatura, categorizándolos en recursos o sistemas de alta temperatura que alcanzan temperaturas $>150^{\circ}\text{C}$, de media temperatura con temperaturas entre 90 y 150°C , de baja temperatura con temperatura entre 30 y 90°C y de muy baja temperatura con temperatura $< 30^{\circ}\text{C}$ (Dickson & Fanelli, 2003).

2.2.3 Pozos geotérmicos

La explotación/extracción de la energía geotérmica se realiza mediante la perforación de pozos, llamados pozos geotérmicos, similares a los pozos petroleros. En la actualidad se cuenta con tecnología de perforación propia para la geotermia con algunas diferencias a las técnicas petroleras, debido a la naturaleza y a las características de los fluidos geotérmicos como son las altas temperaturas y presiones. Algunas de estas adaptaciones en la perforación son la necesidad de enfriamiento de los lodos de perforación, mayor diámetro en las tuberías de producción, aditivos especiales en la cementación (Morgado Ruiz, 2009).

Por definición la perforación de pozos geotérmicos es el conjunto de operaciones mediante las cuales se crea y acondiciona un ducto, medio por el cual los fluidos geotérmicos se transportan o extraen desde el yacimiento hasta la superficie para ser aprovechados; o en su caso transportar agua desde la superficie hasta el yacimiento (Delgado & Juarez, 2014).

La perforación de los pozos geotérmicos puede alcanzar distintas profundidades, dependiendo de la geología del yacimiento. A su vez, estos pueden ser perforados verticalmente o desviados. Dentro de una misma plataforma de perforación, se pueden perforar varios pozos, que se dirigen en diferentes direcciones para obtener un mayor volumen del recurso, y a su vez cortar estructuras permeables, y así reducir los impactos superficiales (Hiriart, 2013).

Existen pozos productores que descargan agua caliente (salmuera) y/o vapor. Y los pozos inyectoros los cuales se utilizan para regresar al yacimiento la salmuera recuperada con el fin de mejorar la recarga caliente profunda (Armstead & and J.W. Tester, 1987; Dickson & M. Fanelli, 2003).

Las perforaciones de pozos representan el 40% del costo total un proyecto geotérmico, esto es aproximadamente entre uno y dos millones de dólares. Y va a depender de diferentes factores como la geología del subsuelo (tipos de rocas y características de permeabilidad o fractura miento), el gradiente geotérmico, así como de las propiedades petrofísicas y termofísicas de las formaciones geológica (Augustine et al., 2006).

2.2.4 Aplicaciones de la energía geotérmica

A pesar de que la energía geotérmica se considera una energía renovable y abundante, sólo una fracción de los recursos a nivel mundial se aprovecha con la tecnología que existe actualmente (Santoyo & Barragán-Reyes, 2010).

El principal uso que se le da a la energía geotérmica es como uso indirecto, para la producción de electricidad a través de plantas o centrales geotermoeléctricas, las cuales pueden ser de distintos tipos dependiendo de las propiedades del fluido geotérmico, como son la temperatura, la profundidad, calidad del agua y del vapor (Dickson & Fanelli, 2003). Una clasificación estándar de estas centrales geotérmicas es: plantas de tipo binaria, de flash individual, de doble flash, de contrapresión y vapor seco (ESMAP, 2012).

Para que se produzca electricidad mediante energía geotérmica es necesario que los fluidos geotérmicos sean de alta o muy temperatura, es decir se encuentren por encima de los 150°C para tener calidad eléctrica. Estos recursos geotérmicos de alta temperatura se encuentran en zonas específicas de la tierra, y son escasos en comparación con los recursos de media y baja temperatura que se encuentran distribuidos más ampliamente, de aquí que a lo largo de ellos años se han desarrollado otras aplicaciones para el aprovechamiento en forma de calor de esta energía que y se denomina utilización o usos directos.

El uso directo del calor geotérmico es una de las aplicaciones más antiguas en balnearios, o aguas termales, posteriormente se expandió su uso a la agricultura, acuicultura, invernadero, para climatización calefacción, así como en la refrigeración, entre otros usos industriales. Otro de los usos directos es el uso en cascada, en el cual se puede reusar y beneficiarse de los distintos niveles térmicos del recuso geotérmico para diferentes aplicaciones, por ejemplo, después de la producción eléctrica, el fluido aún caliente puede ser aprovechado para calefacción o refrigeración; tras este segundo uso, el fluido puede ser nuevamente utilizado para otros usos con menores requerimientos de temperatura como climatización, etc., (IDAE & IGME, 2008).

A continuación, se presenta el diagrama clásico de los principales usos de la energía geotérmica en función de su temperatura.

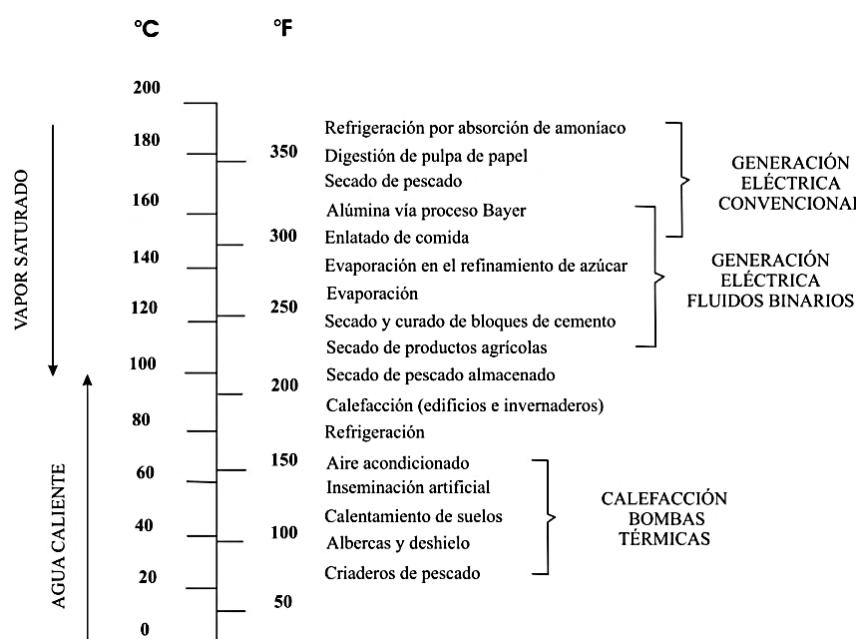


Figura 8. Principales usos de la energía geotérmica en función de su temperatura (tomado de (Sánchez-Upton et al., 2010).

En la relación a los usos específicos en procesos de refrigeración y/o enfriamiento, un compendio de los posibles sectores del mercado para las aplicaciones de refrigeración geotérmica se presenta en la siguiente tabla.

Tabla 1. Sectores del mercado para las aplicaciones de refrigeración geotérmica tomada de (Robins et al., 2021).

Aplicaciones de refrigeración	Sectores del mercado
Refrigeración de distrito	Aire acondicionado para ciudades, campus, bases militares etc.
Procesos de refrigeración y enfriamiento	Sector manufacturero Sector agrícola (procesos de comida y almacenamiento) Centros de datos Centros turísticos y otros usos misceláneos
Enfriamiento de la entrada de la turbina (turbine inlet cooling)	Sector energético, servicios públicos
Producción de hielo	Sector agrícola/pesquero almacenamiento de hielo

2.2.5 Ventajas y desventajas energía geotérmica

Existen diversas ventajas que distinguen la energía geotérmica de otras energías renovables, sin embargo, también presenta sus restricciones o inconvenientes. Estas se presentan en la siguiente tabla:

Tabla 2. Ventajas y desventajas de la energía geotérmica,(ESMAP, 2012).

Ventajas	Desventajas
La energía geotérmica es considerada una forma de energía natural y renovable. Aun cuando la generación de energía geotérmica depende del fluido geotérmico, el volumen extraído se puede reinyectar de manera continua.	Agotamiento de los recursos debido a una tasa de extracción insosteniblemente o errores al reinyectar el fluido geotérmico utilizado.
Su explotación es sostenible cuando se realiza en forma apropiada.	Algunos gases de efecto invernadero que se encuentran bajo la superficie terrestre pueden liberarse durante el aprovechamiento de la energía geotérmica y acabar en la atmósfera.

Es una fuente constante de energía, y con técnicas adecuadas se puede predecir la producción.	La construcción de plantas geotérmicas y pozos puede afectar a la estabilidad del terreno.
Su gran potencial Mundial.	Los proyectos geotermales son caros.
Para calefacción y enfriamiento se pueden aprovechar menores gradientes de temperatura entre la superficie y el interior del planeta.	El recurso geotérmico presenta restricciones de ubicación.
Las principales emisiones de las plantas geotermoeléctricas consisten en vapor de agua, con un contenido mínimo de gases.	
No depende de combustibles fósiles, por lo que no está sujeta a precios internacionales.	

2.2.6 México en el panorama mundial de la energía geotérmica

A pesar de su potencial, la energía geotérmica solo representa alrededor del 1% del total de energía renovables (REN21, 2020), en comparación con otras fuentes de energía.

La generación de electricidad geotérmica en 2019 sumó alrededor de 95 TWh, mientras que la producción térmica útil directa alcanzó 117 TWh (421 petjulios). El uso directo de la energía geotérmica para aplicaciones térmicas creció casi un 8% alcanzado de 30 GWth en promedio en los últimos años, principalmente en calefacción de espacios (alrededor del 13%). Los principales países en uso directo de energía geotérmica en el año 2019 fueron China, Turquía, Islandia y Japón, estos abarcan aproximadamente el 75%. El mercado más activo y de más rápida expansión fue China con 47% del total. (REN21, 2020).

México fue uno de los países que aumento su capacidad de energía geotérmica un 4% en 2019, como se presta en la Figura 9. Con una capacidad instalada en México de 1005.8 MWe, por los cinco campos geotérmicos en operación: Cerro Prieto, Los Azufres, Los Humeros, Las Tres Vírgenes y Domo de San Pedro. La generación eléctrica producida en esos campos fue 5.375 GWh, lo que representa el 1,7% de la producción eléctrica nacional. Los usos geotérmicos directos en México son en su mayoría subutilizados, con 156.1 MW instalada en piscinas calientes y spas (Gutiérrez-Negrín et al., 2020).

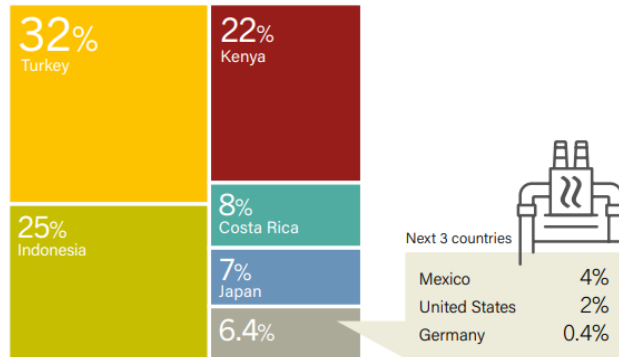


Figura 9. Adiciones globales en la capacidad de energía geotérmica en 2019 por país tomada de (REN21, 2020).

En relaciona la potencia geotérmica instalada a nivel mundial, en 2021, Estados Unidos se posiciono como mayor productor con aproximadamente 3.900 megavatios, seguido de Indonesia con 2.277, México ocupo el sexto lugar con 976 megavatios(Orús, 2022) como se observa en la Figura 10.

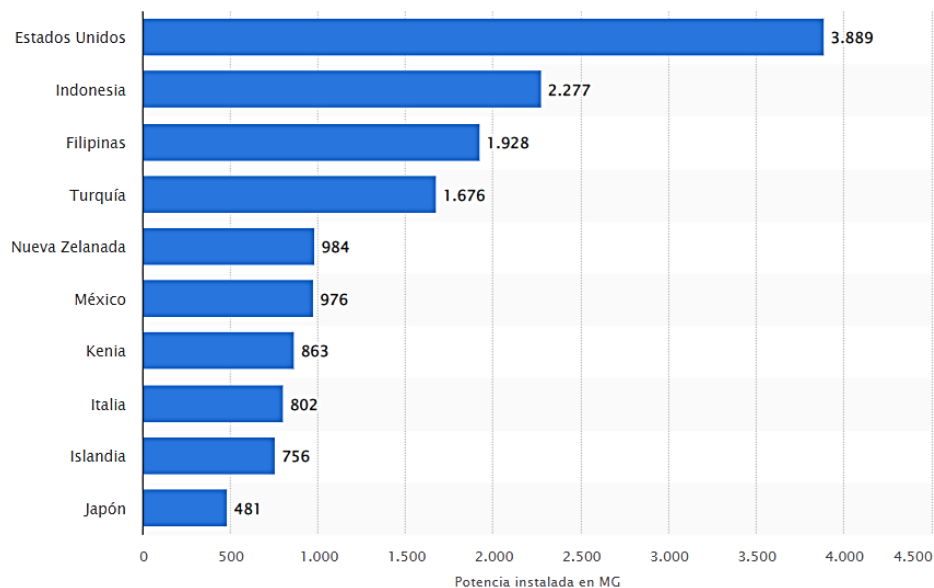


Figura 10. Países con mayor potencia geotérmica instalada en 2021 tomada de (Orús, 2022).

Con base a los datos anteriores, México es uno de los principales productores de energía geotérmica y con gran potencial, tanto para usos directos como para producción de electricidad. Este potencial se puede ver reflejado en la Figura 11 donde los valores del flujo de calor indican que en gran parte de México se tiene áreas óptimas para la explotación y utilización directa de la energía geotérmica (ProI-Ledesma et al., 2018).

Capítulo 3. Evaluación del potencial de enfriamiento de un sistema de absorción en un campo geotérmico.

3.1 Resumen

En este capítulo se presenta un análisis para determinar el potencial de enfriamiento y el rendimiento (COP) que se puede obtener de un pozo geotérmico ubicado en el campo geotérmico Cerritos Colorados, Jalisco, México. La introducción contiene los estudios relacionados con sistemas de absorción activados parcial o totalmente con energía geotérmica. Posteriormente se describe el sistema de absorción y la fuente geotérmica, la metodología utilizada para el cálculo del potencial de enfriamiento. Esta incluye cálculos para la estimación de la energía total del yacimiento, la simulación del sistema de absorción mediante balances de energía, la obtención del COP y las ecuaciones para el cálculo de transferencia del intercambiador de calor dentro del pozo. En la última sección se discuten los resultados que se obtuvieron y se presentan las conclusiones de este artículo.

Para este análisis se considera un sistema de refrigeración por absorción de simple efecto, o también conocido como de una sola etapa, que utiliza una mezcla $H_2O/LiBr$. El sistema de absorción se simuló usando el software EES, modelando un día típico de cada estación del año con base en la variación de la temperatura ambiente y la temperatura de condensación y absorción ($T_A=T_C$). Así mismo, se modeló el potencial de enfriamiento para diferentes temperaturas de evaporación (T_E) de 6° , 8° , 10° y $12^\circ C$ y para un rango de temperatura de generación (T_G) de $77-110^\circ C$. Estas temperaturas de generación se relacionaron directamente con la profundidad a la que se podrían obtener mediante el uso de un intercambiador de calor en U dentro del pozo.

Los resultados muestran la dependencia del potencial de enfriamiento y el COP con los valores suministrados en la $T_A=T_C$. Se observó que cuando la temperatura ambiente es mayor (en primavera y verano), y por ende la T_{AC} , se produce una disminución del potencial y del COP. Así mismo, los resultados mostraron que, para una temperatura de generación fija, se podría obtener un potencial de enfriamiento máximo de 71 594 GW, 70 649 GW, 71 164 GW, 70 859 GW en invierno, primavera, verano y otoño con una T_E de $12^\circ C$.

El análisis de transferencia de calor del intercambiador de calor de tubo en U fue evaluado por un código numérico escrito en Fortran, que permite estimar la temperatura máxima del agua a la salida del intercambiador de calor. Los resultados mostraron que la profundidad requerida para la mínima recuperación de calor a $77^\circ C$ se obtiene a 260 m en primavera, 270 m en verano, 290 m en otoño y 310 m en invierno. Para el caso de la temperatura máxima de $110^\circ C$, las profundidades obtenidas son 590 m en primavera, 600 m en verano, 620 m y 640 m, en otoño e invierno respectivamente.

3.2 Artículo

Evaluation of the cooling potential for a single effect absorption cooling system in the PR2 well of Cerritos Colorados geothermal field, Mexico

Energy Exploration & Exploitation



0(0) 1–20

© The Author(s) 2020

DOI: 10.1177/0144598720927458

journals.sagepub.com/home/eea



Juliana Isabel Saucedo Velázquez¹ ,
Wilfrido Rivera Gómez Franco¹,
Efraín Gómez-Arias² and
Geydy Gutiérrez Urueta³ 

Abstract

Conventional cooling systems consume a high percentage of the world's total electricity generation. Because absorption cooling systems can be mainly operated with thermal energy, they can be used to reduce such percentage. In the present paper, an analysis is carried out to determine the cooling potential that can be obtained from a geothermal well in a location of Mexico by using a single-stage absorption cooling system. The analysis has been carried out taking into account the desired cooling temperature, the ambient temperature, and the temperatures at different depths of the wells for a typical day of every season of the year. The results showed that, for a fixed generation temperature, a maximum cooling potential as big as 71,594 GW, 70,649 GW, 71,164 GW, 70,859 GW could be obtained in Winter, Spring, Summer, and Autumn, respectively. Using the temperatures obtained from the well, for a fixed depth, the results show that higher values are obtained in spring and summer. From the analysis, it is clear that absorption systems operating with geothermal energy could be an excellent alternative to reduce the electricity consumed by conventional systems.

¹Instituto de Energías Renovables, Universidad Nacional Autónoma de México, Temixco, México

²CONACYT-Centro de Investigación Científica y de Educación Superior de Ensenada, División de Ciencias de la Tierra, Baja California, México

³Facultad de Ingeniería, Universidad Autónoma de San Luis Potosí, San Luis Potosí, Mexico

Corresponding author:

Geydy Gutiérrez Urueta, Facultad de Ingeniería, Universidad Autónoma de San Luis Potosí, Av. Dr. Manuel Nava No. 8, Col. Zona Universitaria Poniente, C.P. 78290, San Luis Potosí, S.L.P., Mexico.

Email: geydy.gutierrez@uaslp.mx



Keywords

Single-effect absorption system, geothermal source, cooling potential, thermodynamic analysis, low enthalpy

Introduction

At present, the search for solutions for the environmental deterioration that humanity has caused is extremely important. There is no time to lose. The negative ecological impact of energy utilization, growing demand, and restricted resources accentuate the need to diminish emissions.

Conventional refrigeration systems, based on steam compression, require large amounts of electrical energy to operate. This, together with the environmental effect of chlorofluorocarbons, has stimulated interest in the development of absorption systems. These systems are attractive because they can use natural refrigerants (water, ammonia, etc.) and can also operate with renewable energy such as solar or geothermal, which reduces the consumption of fossil fuels.

Geothermal energy, unlike other renewable energy sources, has its origin in the gradient of temperatures that exist inside the earth. These range from 15°C of the surface to 4000°C in the core. The use of geothermal resources is strongly influenced by the nature of the system that produces them: in general, the resources of hot volcanic systems are mainly used for electric power generation, while the resources of lower temperature systems are mainly used for space heating and other direct uses. A number of factors should be considered to determine the optimal use of a geothermal resource. These include the type (water or hot steam), flow rate, temperature, chemical composition and pressure of the geothermal fluid, as well as the depth of the geothermal reservoir (ESMAP, 2012).

The importance of geothermal energy to the contribution of sustainable development for a country is well covered by Dursun and Gokcol (2012), for the case of Turkey. Mexico has a large number of areas that have high- and low-enthalpy geothermal potential. More than 1300 geothermal manifestations have been recorded. However, currently, geothermal energy in Mexico is used almost entirely as indirect energy to produce electricity. Direct uses of geothermal energy remain restricted for recreational purposes, and some of them with therapeutic uses (Gutiérrez-Negrin et al., 2015).

In the literature, both theoretical and experimental work on absorption cooling systems activated with renewable energy has been reported. A review of these works is presented in Best and Rivera (2015), which includes the use of solar energy as a thermal source to operate absorption systems. However, work on absorption cooling systems driven partially or totally by geothermal energy in Mexico is practically scarce.

Systems partially driven by geothermal energy include the joint operation of compression-absorption technologies or the use of geothermal energy in conjunction with another energy source, such as solar energy.

The first documented studies on systems operated entirely with geothermal energy date to 1970. Reynolds (1970) describes aspects of the design, control, and general installation of an air conditioning system using geothermal energy and a hot water system for the Tourist Hotel in New Zealand, by Fisher & Paykel Engineering. Rafferty Kevin (1986) presents some of the considerations for the use of absorption refrigeration equipment in geothermal

applications. The absorption cycle and performance for large and small tonnage machines are described, the capital and operating costs of steam absorption and compression equipment are compared, showing the data for a real geothermal installation. Breindel et al. (1978) conducted an economic analysis of the potato processing, freeze-drying, and large-scale meat packaging industries, using the geothermal resource in a cascade system. It was concluded that the use of cascade systems improves economic results. Rogowska and Szaflik (2005) designed a model for a 10 kW cooling machine with a one-stage absorption cycle, by calculating thermal parameters and fluid flow, for the production of air conditioning. The results were applied to more advanced design of 500 kW refrigeration units in the region studied. Ma et al. (2010) and Yilmaz (2017) analyze and evaluate different thermodynamic performance parameters, such as the cooling load and the coefficient of performance (COP). In addition, an economic analysis was performed to assess the cost structure, potential revenues and the recovery periods, for a geothermal absorption cooling system used for the cooling of buildings. The feasibility of using the absorption system for the case study was concluded. Uwera et al. (2015) designed an absorption cooling unit for the storage of agricultural products, which uses geothermal hot water as a heat source. The thermodynamic analysis of the cycle concluded that the COP of the absorption cooling cycle is 0.49, but it can reach 0.6 when a heat exchanger is used. Erickson et al. (2005) describe the installation of a chiller (“ThermoChiller”) that operates with a double-effect ammonia absorption cycle at the Aurora Ice Museum in Chena Hot Springs, Alaska. The ThermoChiller operates with thermal spring water and provides 15 tons of cooling at -20°F . Angrisani et al. (2016) carry out a dynamic simulation study to evaluate the energy, economy, and performance of a new heating and cooling system based on the coupling between a geothermal source of low or medium enthalpy, an Air Handling Unit and a desiccant wheel. Simulations demonstrated the technical and economic feasibility of the proposed system. Ramírez (2016) compares the performance of an absorption cooling cycle and a cycle ejector using data from a low enthalpy geothermal well. The evaluated data show that for the specific conditions, both systems are feasible as an alternative to conventional refrigeration. Arreola Núñez (2016) develops the thermodynamic model of a commercial absorption machine, replacing the gas heat supply with the geothermal resource. The thermodynamic feasibility of making this change in heat input is concluded, with a small decrease in the machine’s performance coefficient. Tugcu and Arslan (2017) analyzed parametrically the designs of an absorption cooling system using resources in a geothermal field, with the use of artificial neural networks. The results determined the best training architectures and algorithms and the optimal system. In Hernández-Magallanes et al. (2019), the results of the modeling of a medium-effect absorption system with a mixture of ammonia/lithium nitrate driven by a low enthalpy geothermal source from two geothermal wells are presented. The results showed that with the temperatures of the wells, the cooling system is operable, but obtained a low cooling effect. In a similar focus, Xu et al. (2020) reported a simulation of a heat pump system activated with a single well groundwater in China. The fluctuation range of the output temperatures was obtained. The system can supply heat for an area of approximately 9000 m^2 per year, saving an important quantity of coal. An analogous study was presented by Wang et al. (2018) introducing intermittent strategies for 25 years. They compared three operating conditions with positive results in favor of intermittent operation.

In relation to the work reported with partially driven systems with geothermal energy, Kairouani and Nehdi (2006) developed a combined cooling system to improve the overall efficiency of the conventional cascade steam compression refrigeration cycle with a

geothermal water-driven absorption system. The results showed that the COP of this combined system is significantly higher than that of a single-stage refrigeration system. Sikorska-Bączek (2015) analyzes the compression–absorption circuit of a refrigerator powered by geothermal energy, used for the production of suspended ice or binary ice for an air conditioning system. It is concluded, through the analysis of the physical and thermodynamic properties, that the conditions of the geothermal deposit studied have the temperature necessary to feed the generator of the absorption system. A more recent study is presented in Salhi et al. (2018), who perform a simulation that incorporates energy, exergy and economic factors in the development of an absorption–compression cycle for air conditioning. The simulation results showed a decrease in electricity consumption when the proposed system is used in opposition to the classic steam compression cycles. In addition, they showed that the COP varies according to the combination of working fluids used and the costs are related to depth. Equally, Galindo-Luna et al. (2018) propose a hybrid system by using a field of parabolic trough collectors coupled to a low enthalpy geothermal well, as a thermal source of an air conditioning absorption system to increase the temperature of the working fluid. A COP of 0.71 was obtained for a temperature in the generator of 90°C.

On the other hand, there have also been several studies on cooling systems related to complex energy systems; based on the use of geothermal energy, Mahmoudi and Akbari Kordlar (2018) and Parikhani et al. (2018) performed a parametric, exergy, and economic analysis to a combined cogeneration system to produce cooling and power, using geothermal energy as a heat source. The results of the analyses performed determined the most optimal operating characteristics of the proposed systems. Tesha (2010) models an integrated energy generation and absorption system, in which the residual heat from the power generation process feeds the heat demand of the absorption cooling system, which in turn supplies cooling water to the power plant. It was concluded that the integrated energy and absorption system could not meet the viability requirements because it requires a large cooling capacity, increasing the total investment cost. Nasruddin and Wibowo (2018) carry out an analysis of an integrated energy generation and absorption cooling system through the use of residual heat from the separation process of a geothermal power plant, and the implementation of an absorption cooling system, to improve the plant performance. Optimal values were identified to minimize energy efficiency and the annual cost for the integrated system. In Ghaebi et al. (2018), they perform energy, exergy, and economic analysis for a trigeneration system that includes the absorption refrigeration cycle, a heat pump system for heating, and cold natural gas energy. The results determined that the overall system performance can be optimized based on the state temperatures of the absorption cycle components. Ambriz-Díaz et al. (2017) analyze the cascade production of five integration alternatives of a system composed by three thermal levels: in the first level, an organic Rankine cycle for the production of electricity, in the second level, an absorption refrigeration cycle for the production of ice, and on the third level, a dehydrator for drying agricultural products. The results indicate that the dehydration process drastically improves the economic benefits of all alternatives, achieving recovery periods of around one year and reducing greenhouse gas emissions. In addition, the production of electricity alone is not desirable, because it has the worst energy and economic performance.

According to the literature review presented above, the cooling potential (CP) of the different absorption cycles (medium, single, double, and triple effect) operated solely with geothermal energy and for the same geothermal system has not been evaluated. In this article, we evaluate the CP that can be obtained from an inoperative geothermal wells

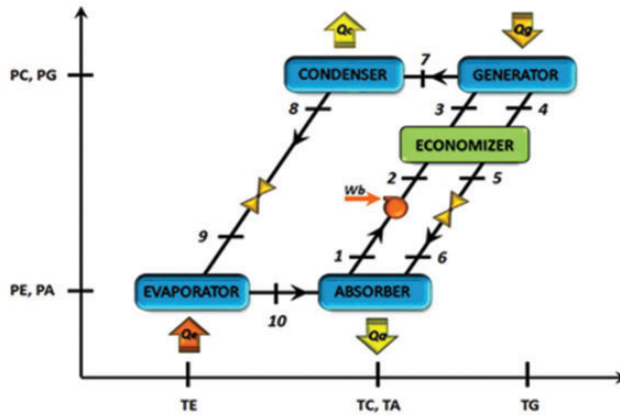


Figure 1. Schematic diagram of a single-stage absorption cooling system.

located in Cerritos Colorados geothermal field, Jalisco Mexico. The work developed is original and can have a great impact in areas where there are optimal conditions to explore the geothermal resource.

System description

A simple effect absorption cooling system (SEACS) consists of a generator, a condenser, an evaporator, an absorber, and an economizer, as shown in Figure 1. An amount of geothermal heat \dot{Q}_G is supplied to the generator at a high temperature T_G to separate part of the water from a lithium bromide solution. The vaporized water passes to the condenser, where it is condensed delivering an amount of heat \dot{Q}_C , at an intermediate temperature T_C . The water in a liquid phase is expanded through an expansion valve, decreasing its pressure and temperature. Then the water enters into the evaporator producing the cooling effect \dot{Q}_E , at the lowest system temperature. The water leaving from the evaporator in a vapor phase passes to the absorber where it is absorbed by the solution with high lithium bromide concentration coming from the generator, delivering an amount of heat \dot{Q}_A , at an intermediate temperature T_A . The solution with low lithium bromide concentration leaving the absorber returns to the generator starting the cycle again. An economizer is placed between the absorber and the generator to preheat the solution going from the absorber to the generator by means the heat supplied at higher temperature from the solution leaving the generator, thus reducing the amount of heat supplied to the generator.

Methods

Geothermal source

The study area is the Cerritos Colorados geothermal field, located in the central-southern portion of La Primavera Caldera or “La Primavera Forest” (Gutierrez-Negrin, 1988), 20 km west of the Guadalajara metropolitan area (Figure 2). It is located in the overlapping zone of two floristic provinces: Sierra Madre Occidental and Sierras Meridianos or

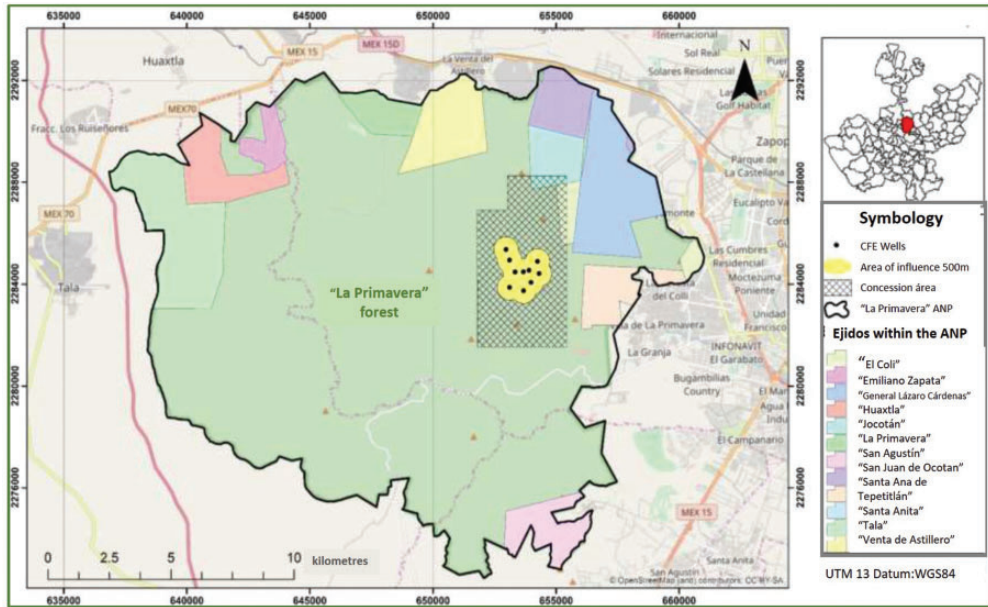


Figure 2. Location map of the Cerritos Colorado geothermal field (Zarate, 2017).

Transmexicano Volcanic Belt, one of the volcanic reliefs with the highest morphological wealth in Mexico. Volcanologically, this area is a volcanic caldera about 11 km in diameter, with an approximate age of 95,000 years (Mahood, 1980) and as a remnant of volcanic activity. It presents hydrothermal manifestations (fumaroles, hot springs, sulfates, and hot soils), which appear in various parts of the caldera (Villa Merlo et al., 1987).

Due to the expansion of the city, the surroundings of the forest are populated. In “La Primavera” forest, there are several lands (ejido) with active agrarian activity. For instance, the Santa Ana de Tepetitlán Indigenous Community resides permanently within the forest and the distance to the nearest well is 1.82 km (Zarate, 2017).

Given its geothermal potential, during the period 1980–1989 civil works were developed to explore this geothermal area, which includes the drilling of 12 geothermal wells (Universidad Autónoma de Chapingo, 2008). The location of such wells is presented in Figure 3.

The necessary data of depth, temperature, and geothermal gradient of wells PR2, PR8, PR10, and PR11 are available. For this first study, well PR2 is analyzed using data obtained from Table 1. The depth and geothermal gradient data were taken from Pról-Ledesma et al. (2018), and the temperature data from Gutierrez-Negrin (1988).

Calculation of total thermal energy

The volumetric method, also called the “volumetric heat” or “stored heat” method, is based on calculating the energy contained in a certain volume of rock, which contains a reservoir of water that can be exploited. The fraction of this energy that is recoverable is then estimated, and subsequently, the geothermal reservoirs are evaluated from the estimated thermal energies. This summarizes the physical and technological links that prevent the total

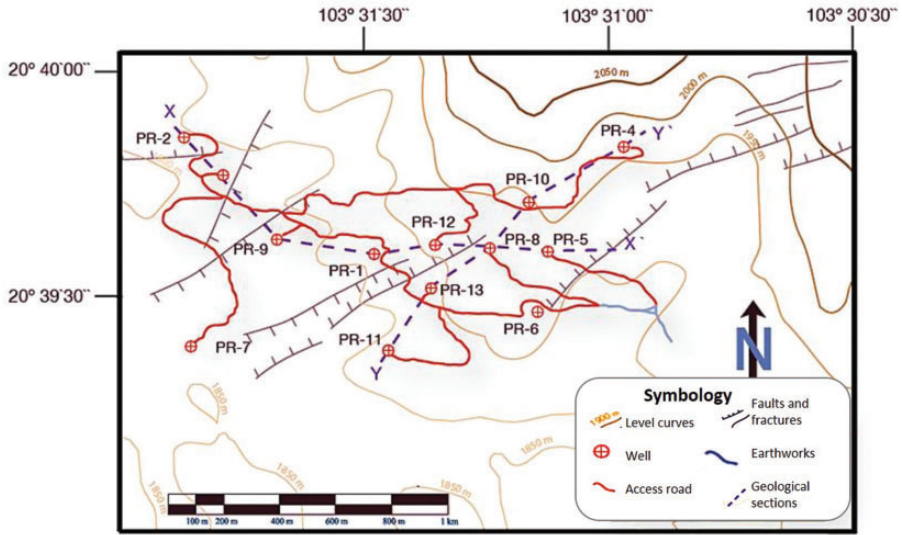


Figure 3. Location and access to the wells of the Cerritos Colorados field (Rocha Ruiz, 2013).

Table I. Data from geothermal wells in the geothermal field Cerritos Colorados.

Well	Latitude	Longitude	Geothermal gradient (°C/km)	Depth (m)	Temperature (°C)
PR2	20.66423	-103.53115	114.9	1988	320
PR8	20.66012	-103.52068	137.3	1855	262
PR10	20.66183	-103.51935	107	2086	301
PR11	20.65634	-103.52418	77.7	2125	300

extraction of thermal energy from the reservoir for its use in the production of electricity. The method evaluates the amount of heat stored in the rock and the heat obtained from the fluid, to obtain the heat available in the reservoir (Muffler and Cataldi, 1978). Equations (1) to (3) summarizes the calculation process.

Energy stored in the rock volume:

$$Q_r = AH(1 - \phi)p_r C_r (T_i - T_m) \quad (1)$$

Fluid energy:

$$Q_f = AHp_f C_f \phi (T_i - T_m) \quad (2)$$

Total thermal energy:

$$Q_t = Q_f + Q_r \quad (3)$$

Some of these parameters can be known with acceptable accuracy and others can be estimated with great uncertainty. However, it is important to remember that underground phenomena are always uncertain since detailed studies would need to be made, which give us exact values for each existing site. Uncertainties in geothermal energy result mostly in the estimated values for the area, reservoir thickness (H), and initial reservoir temperature (T_i). However, it is difficult to obtain areas of precise reservoirs, even in well-studied reservoirs, with extensive drilling in them. Therefore, because the only evidence obtained is the initial reservoir temperature, the evaluations are carried out considering a minimum area = 1 km^2 , probable = 2 km^2 and maximum = 3 km^2 (Muffler and Guffanti, 1979). In addition, for the majority of the reservoirs, the uncertainties regarding the depth are small compared with those of the respective area (Muffler and Guffanti, 1979). In equation (2), the area is considered as a probable area ($A = 2 \text{ km}^2$), in relation to the thickness of the reservoir (H), there is information on the depths of the geothermal wells drilled in the geothermal field Cerritos Colorados, where $H = 2000 \text{ m}$ and corresponds to the average depth of the four wells (PR2, PR8, PR10, PR11).

The porosity of the rock (\emptyset) is defined as the relationship between the volume of empty spaces in the host rock or spaces occupied by the water in it, and the total volume of the material (DiPippo, 2015). In equations (1) and (2) an intermediate value of $\emptyset = 10\%$ is contemplated. In relation to the type of rock, it is considered that the reservoirs are predominantly constituted by volcanic igneous rock of intermediate composition (DiPippo, 2015). For the case study, the values of density (ρ_r) and specific heat (C_r) of each type of rock were used according to the stratigraphic column of the Cerritos Colorados geothermal field (Figure 4). In the case of the fluid, the specific heat water values $C_f = 4.18 \text{ kJ/kg}^\circ\text{C}$ and a density $\rho_f = 1000 \text{ kg/m}^3$ are used.

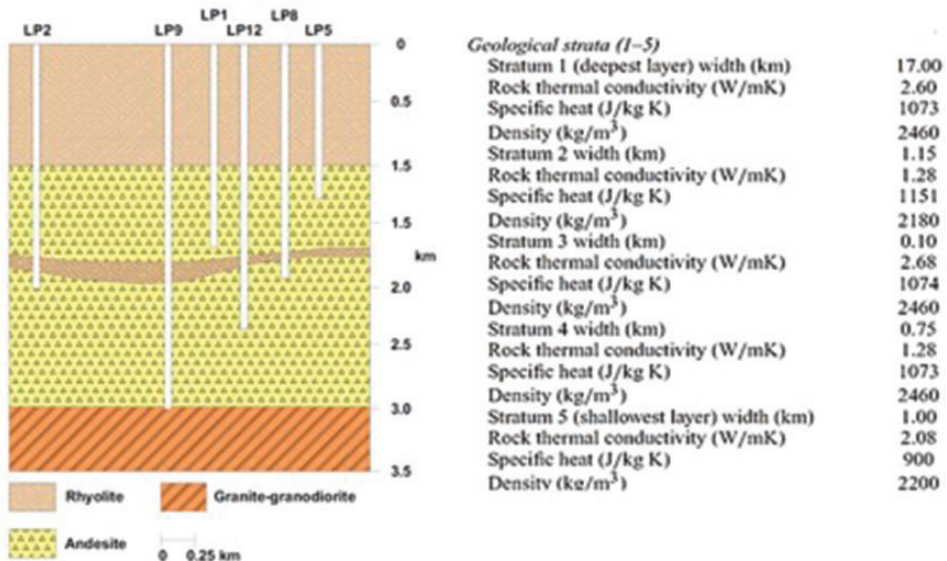


Figure 4. Simplified lithology based on core drilled wells from Cerritos Colorados geothermal field (taken and modified from Verma et al., 2012).

The minimum operating temperature (T_m) is set in relation to the technology used. In the case of geothermal power plants, a temperature of 135°C for a unit cycle and 90°C for a binary cycle is assumed (Hiriart, 2011). For the case study, the minimum temperature (T_m) was varied according to the requirements of each absorption cycle: for the SEACS, a minimum temperature of $T_m = 77^\circ\text{C}$ was considered; for the medium system effect, $T_m = 58^\circ\text{C}$; for the double effect, $T_m = 134^\circ\text{C}$; and for the triple effect, $T_m = 170^\circ\text{C}$. To define the reservoir initial temperature (T_i), an average of the temperatures recorded in the four wells (PR2, PR8, PR10, PR11) was taken based on the data in Table 1.

Calculation of the CP for a single effect absorption system

For this study, the CP is calculated based on the geothermal potential formula, equation (4), which is used to obtain the installable capacity of a geothermal plant. To convert stored thermal energy to an electrical potential, the amount of heat that could be recovered must first be estimated. The geo-thermoelectric potential is calculated from the estimated energy, using the volumetric method (Hiriart, 2011)

$$P = \frac{Q_t R_f C_e}{F_p t} \quad (4)$$

To obtain the CP, equation (4) was modified by replacing the efficiency factor (C_e) for the binary or unitary cycles with the COP of the cooling system (equation (5))

$$\text{CP} = \frac{Q_t R_f \text{COP}}{F_p t} \quad (5)$$

In equation (5), Q_t represents the total thermal energy, or heat, calculated in equation (3). In DiPippo (2015), it is reported that the heat recovery factor (R_f) under normal conditions of porosity and permeability can reach up to 25% in some convective systems, but most of the time, it is significantly lower. In many cases, it is known with very little precision, and it is often considered subjective. For the purposes of this evaluation, a conservative factor of $R_f = 12.5\%$ is considered. Hiriart (2011) reports that in recent geothermal units, the typical plant factor (F_p) is 90% or higher. This plant factor (F_p) of 90% is also considered for this calculation. The durability of the geothermal reservoir depends on the energy extracted from it, and therefore varies depending on the type of project to be carried out. For the case study, the calculation $t = 1$ h is performed.

Simulation of the single-effect LiBr-water absorption cooling system

To obtain the COP of the SEACS, a mathematical model was developed in the Software Engineering Equation Solver based on the first law of thermodynamics.

The assumptions for the thermodynamic modeling of the cycle were the following

- The system operates in thermodynamic equilibrium.
- The analysis is performed under steady-state conditions.
- The solution is in a saturated state when leaving the generator and absorber.
- The refrigerant is in a saturated state when it leaves the condenser and the evaporator.

- Heat losses and pressure drops in the pipe and components are considered insignificant.
- The flow through the valves is isenthalpic.
- Heat exchanger efficiencies = 0.8.
- Runs were made each hour for a representative day of every season.
- The inlet temperatures in the condenser–absorber (T_{AC}) are 7°C above the ambient temperature (presented in the Results section).
- For the case base, a generator temperature of 100°C is considered.

Table 2 shows the steady-state mass and energy balances for each of the components of the SEACS.

Heat transfer analysis in a U-tube heat exchanger

The convective heat transfer analysis between the geothermal wells (PR2, PR8, PR10, PR11) from Cerritos Colorados geothermal field and the U-tube heat exchanger was evaluated by using a numerical code written in Fortran, which allows estimating the maximum water temperature to the heat exchanger outlet. The heat transfer was solved following the empirical relationship for pipe and tube flow given by the following expression (Galindo-Luna et al., 2018; Holman, 1986)

$$\dot{Q} = h\pi dL \left(T_W - \frac{T_1 + T_2}{2} \right) = \dot{m} C_P (T_2 - T_1) \quad (6)$$

Table 2. Mass and energy balance for each of the components of the SEACS.

Component	Balances
Generator	$\dot{m}_3 = \dot{m}_7 + \dot{m}_4$ $\dot{m}_3 X_3 = \dot{m}_7 X_7 + \dot{m}_4 X_4$ $Q_g = \dot{m}_4 H_4 + \dot{m}_7 H_7 - \dot{m}_3 H_3$
Condenser	$\dot{m}_7 = \dot{m}_8$ $\dot{m}_7 X_7 = \dot{m}_8 X_8$ $Q_c = \dot{m}_7 (H_7 - H_8)$
Evaporator	$\dot{m}_9 = \dot{m}_{10}$ $\dot{m}_9 X_9 = \dot{m}_{10} X_{10}$ $Q_e = \dot{m}_{10} (H_{10} - H_9)$
Absorber	$\dot{m}_1 = \dot{m}_{10} + \dot{m}_6$ $\dot{m}_1 X_1 = \dot{m}_{10} X_{10} + \dot{m}_6 X_6$ $Q_a = \dot{m}_{10} H_{10} + \dot{m}_6 H_6 - \dot{m}_1 H_1$
Efficiency of the solution heat exchanger	$\varepsilon_{SHX} = \frac{H_3 - H_2}{H_4 - H_2}$
Pump work	$W_b = V_1 (P_8 - P_{10})$
COP	$COP = \frac{Q_c}{Q_g + W_b}$

COP: coefficient of performance.

where h is the convective heat transfer coefficient ($\text{W}/\text{m}^2\text{°C}$), d is the tube diameter (m), L is the length of well (m), T_W is the wall temperature along the depth of the tube, \dot{m} is the mass flow (kg/s), C_P is the fluid heat capacity ($\text{J}/\text{kg °C}$), and T_1 and T_2 are the inlet and outlet water temperatures. For this study, T_2 is the heating temperature of water at depth and the one supplied to the generator ($T_{G,i}$). The turbulent flow inside the U-tube was estimated using the empirical relation proposed by Dittus and Boelter (1930)

$$N_{\mu d} = 0.023\text{Re}_d^{0.8}\text{Pr}^n \quad (7)$$

where Re_d and Pr correspond to Reynolds and Prandtl numbers, respectively, and the exponent n is equal to 0.4 for heating and 0.3 for cooling (Dittus and Boelter, 1930). The thermodynamic properties of water at temperatures between 20 and 300°C were used.

Results and discussion

Results

Ambient temperature data per hour. For the analysis, the station closest to the site to be evaluated is “La Primavera” station, with coordinates 20°40′34.6″, 103°38′38.7″, and altitude 1468.15 msl. The ambient temperature data for the entire year 2018 were obtained directly from the National Water Commission (Comisión Nacional del Agua, CONAGUA, in Spanish).

A representative day of each season (spring, summer, autumn, and winter) was chosen. Subsequently, an average temperature per hour was obtained for each selected day. Figure 5 illustrates a comparison of ambient temperatures for a representative day of each season.

This information is basic for the subsequent cooling system analysis. This will define the condenser–absorber inlet temperature T_{AC} , considering 7°C above the ambient temperature.

Total thermal energy. Using equations (1) to (3) and lithological parameters based on Figure 4, the total energy can be obtained from the reservoir. Table 3 presents the results for simple and advanced absorption cycles. As can be seen, the values of Q_t are different for each absorption system because the total energy, related to the minimum operating temperature of the system (equation (1)), varies according to the thermal requirements of it. For this work, we present the results corresponding to the SEACS.

Cooling potential. Using equation (5), the CP was calculated based on Q_t and COP for an SEACS. The hourly results for a representative day of each season are presented in Figure 6 (a) to (d), for a fixed generation temperature and different evaporation temperatures.

Figure 6(a) to (d) illustrates the dependency of CP with the season, due to the variation of the ambient temperature throughout the day. As already mentioned, this is directly related to the T_{AC} , which affects the COP.

The effect of ambient temperature is observed in Figure 7, which shows that the CP is proportional to the COP. This is illustrated in Figure 8 for the different seasons.

CP against depth. Based on the calculation of the temperature with depth profile, the thermal requirements to operate an SEACS can be obtained, depending on the installation depth of

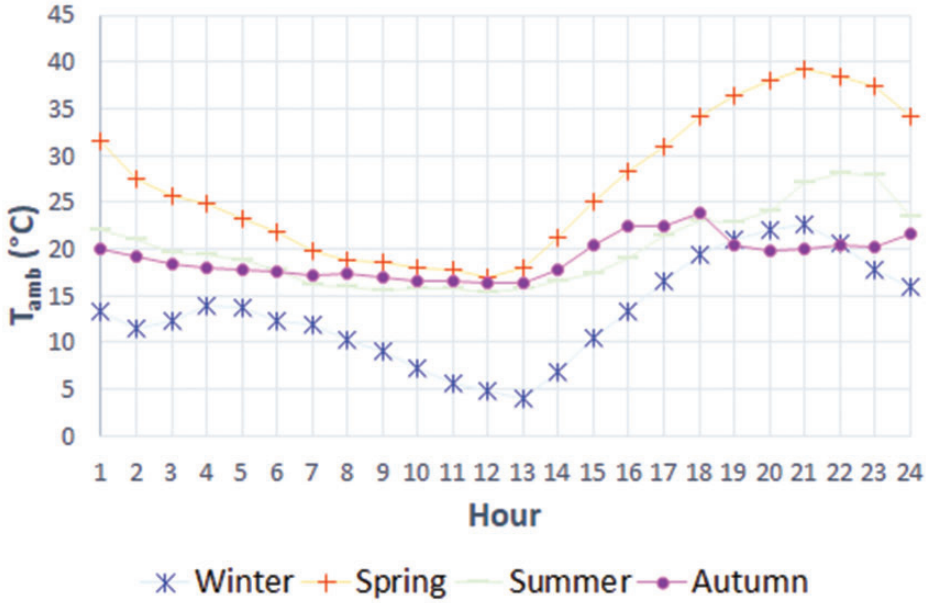


Figure 5. Ambient temperatures for a representative day of each season.

Table 3. Total energy.

System	Q_t (kJ)
Single effect	1.8832E+15
Half effect	2.0416E+15
Double effect	1.74322E+15
Triple effect	1.34094E+15

the heat exchanger. The temperature supplied to the generator in the SEACS, $T_{G,i}$, using a thermally insulated U exchanger (section 3.5) at different depths is shown in Figure 9, according to the season. Knowing the resulting COP, the cooling capacity for the entire temperature profile was calculated using equation (5). A generation temperature ranging from 77°C to 110°C (see Figure 9) was considered for the SEACS.

From the values of $T_{G,i}$ at different depths, the CP for the entire temperature profile was calculated every 10 m, considering 24 h, see Figure 10.

Figure 11 shows the behavior for a fixed T_e , which shows the variation of the annual potential according to the season.

Discussion

The Results section presented the results corresponding to CP analyses from two approaches: for a fixed $T_{G,i}$, observing the influence variations in the ambient temperature, and for $T_{G,i}$ varying according to the depth along the well and according to the average seasonal temperature.

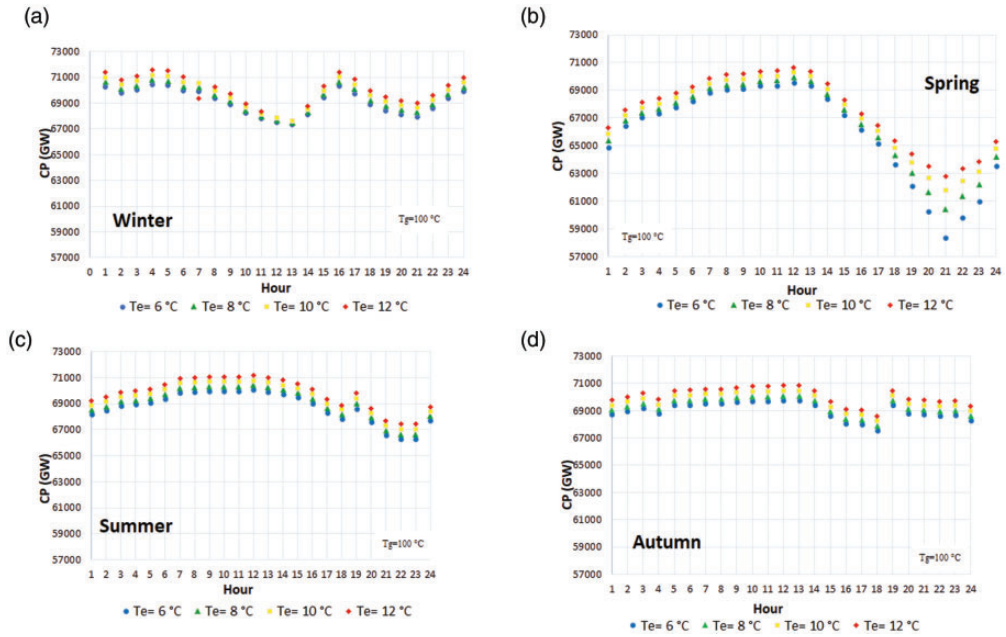


Figure 6. Cooling potential per hour for a representative day of (a) winter, (b) spring, (c) summer, (d) autumn, at different evaporation temperatures for a simple effect absorption system.

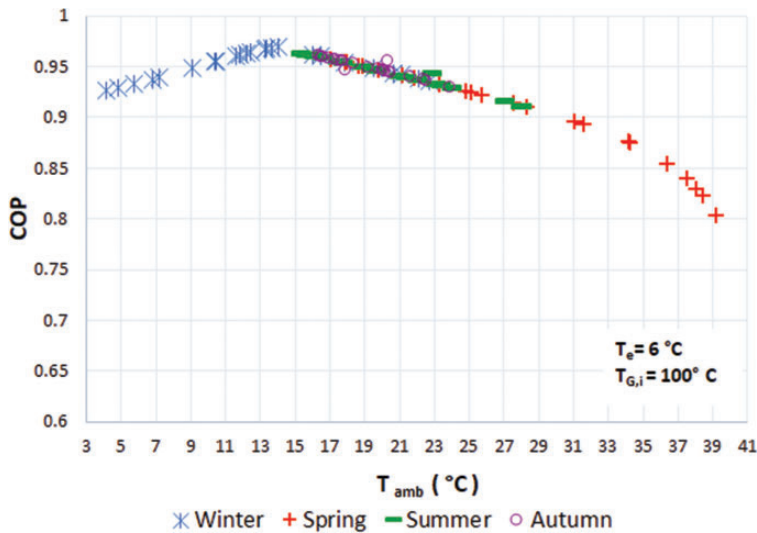


Figure 7. COP vs. T_{AC} for the different seasons.

Figure 6(a) to (d) illustrates the first approach. It is observed that the CP, and therefore the energy recovered, increases as the evaporation temperature (T_e) increases. The maximum CP is obtained with $T_e = 12^\circ\text{C}$ (Figure 6(a)), which reaches a maximum value as big as 71,594 in winter. The corresponding values for spring, summer, and autumn are 70,649,

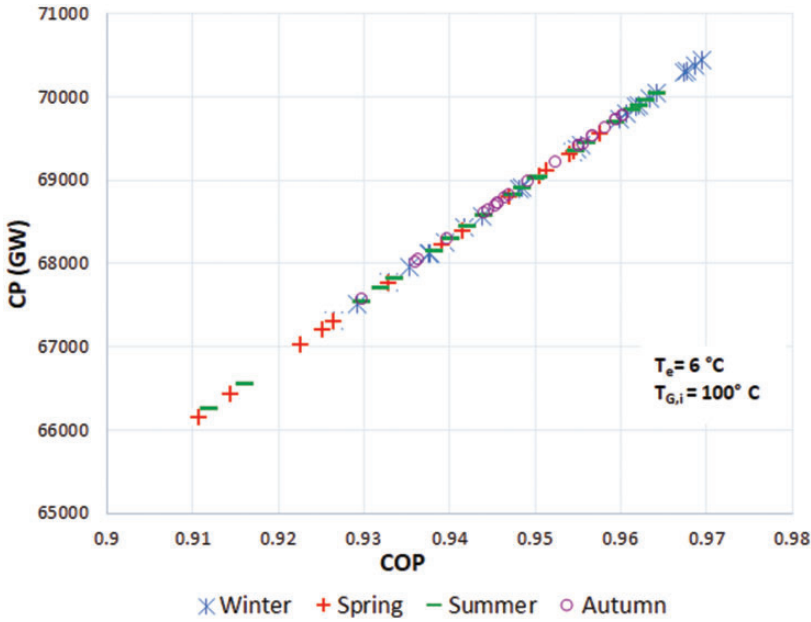


Figure 8. Cooling potential vs. COP for the different seasons.

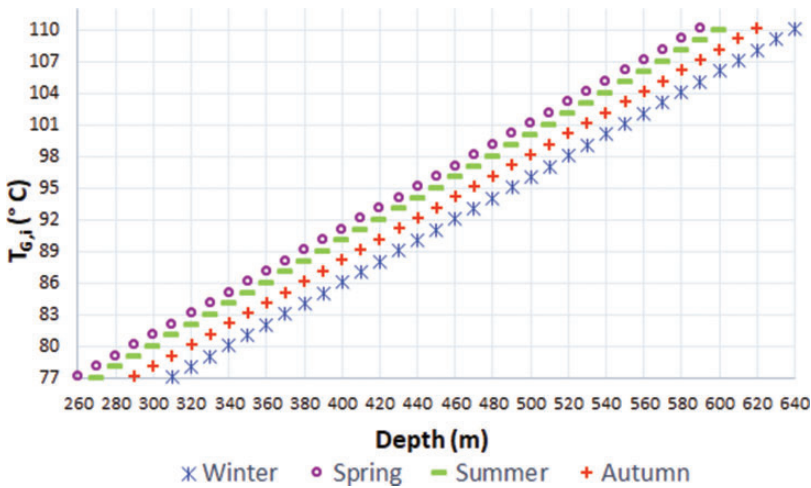


Figure 9. Temperature supplied to the generator in the SEACS against well depth, for each season.

71,164, 70,859 GW, respectively. In addition, Figure 6 illustrates that in autumn, the results have less variation compared to the other seasons. In winter, when ambient temperatures are lower (see Figure 5 between 11 and 14h), the cooling system cannot be simulated due to crystallization conditions. Likewise, in spring, when the ambient temperature is higher, and therefore the T_{AC} , there is a decrease in the COP and CP (equation (5)).

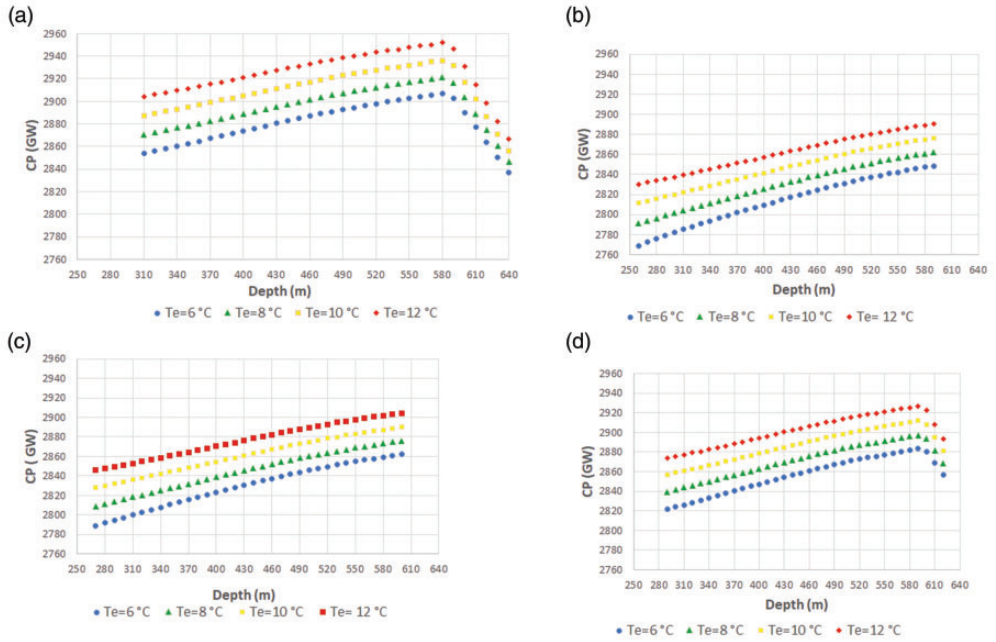


Figure 10. Cooling potential (CP) vs. depth for (a) winter, (b) spring, (c) summer, (d) autumn, at different evaporation temperatures for a simple effect absorption system.

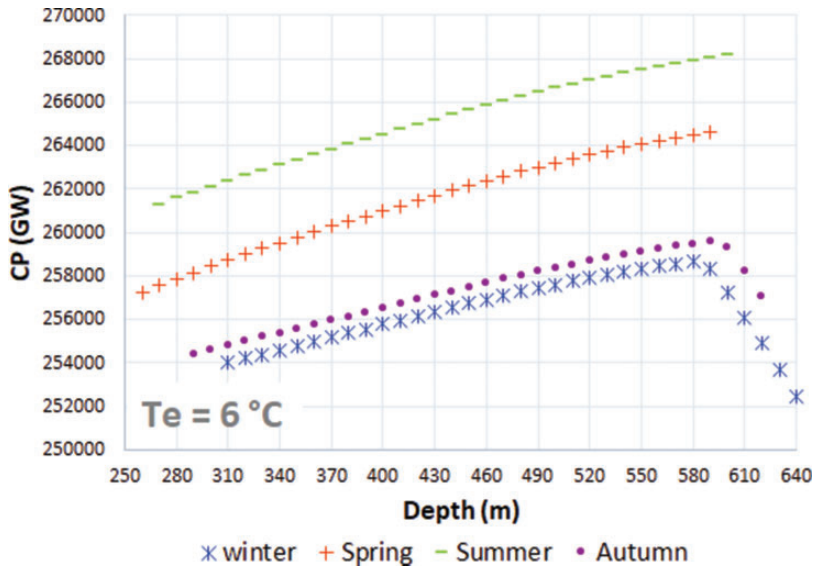


Figure 11. Cooling potential (CP) vs. depth for each station at a fixed evaporation temperature.

From Figure 9, it can be appreciated that the ambient temperature influences the depth at which heat is recovered in the exchanger. In winter, when the temperature is lower, the heating temperature of water recovered is 110°C ($T_{G,i}$), by installing an exchanger at a depth of 640 m. In spring, the same temperature is recovered at 590 m. The corresponding depth at $T_{G,i}=77^{\circ}\text{C}$ was 310 m in winter and 260 m in spring.

For the temperature range considered, Figure 10 demonstrates that the CP increases linearly with the depth in summer and spring. However, in winter and autumn, the CP exhibits a small decrease in the COP, related to lower values of generation inlet temperature obtained for the same depth. As in the previous analysis, it was observed that the ambient temperature (T_{AC}) influences the COP, and therefore the CP. For a fixed evaporation temperature (Figure 11), the results of CP vs. depth show that the greatest potential is obtained in spring and summer, with an average seasonal temperatures of 22.6°C and 21.4°C , respectively.

The advantage of the system proposed in this work is that the energy supplied to the absorption system is obtained from a drilled and inoperative well, so the installation costs are negligible because only the cost associated with the process (pumping) is considered. This makes this option cost-effective if it is compared, for instance, with solar energy. This is because the acquisition of other technology such as solar collectors is not required to obtain the heat used to activate the absorption system since it is already available in this case.

In Mexico, there are several inoperative geothermal and oil wells, which can meet the thermal requirements for various applications (Caulk and Tomac, 2017), such as absorption systems. According to the economic study developed by Hernández-Magallanes (2017), in which the costs of different cooling systems in Mexico are compared (absorption, a solar absorption, and a conventional compression system), the absorption cooling machine was the most profitable system. This was concluded considering a useful life period of 20 years, for the three systems. The payback period resulted in seven years, compared with the solar absorption cooling system with a payback almost equal to the lifetime period.

Conclusions

An SEACS, fed by a geothermal well, was used to evaluate the CP of a geothermal field in Mexico. The absorption system was simulated using actual data from the site and the PR2 well.

The CP of the geothermal site was estimated for each season of the year, based on the variation of the ambient temperature. The dependence of the COP and the CP with the T_{AC} is manifested in the variations throughout the day and season of the year. The obtained CP values are of great magnitude considering an area of 2 km^2 . For a fixed generation temperature, the maximum CP is obtained with $T_e=12^{\circ}\text{C}$, with a value of 71,594 GW in winter. When the ambient temperature is higher (spring and summer), and hence the T_{AC} , there is a decrease in the COP and CP.

On the other side, using the temperatures obtained from the well, for a fixed depth the results show that higher CP is obtained in spring and summer, with an average seasonal temperature of 22.6°C and 21.4°C , respectively. The required depth for heat recovery at 77°C was obtained at 260 m in spring, 270 m in summer, 290 m in autumn, and in 310 m winter. For the case of 110°C , the depths are 590 m, 600 m, 620 m, and 640 m, respectively.

Acknowledgements

J Saucedo is thankful for the scholarship provided by CONACYT through the National Graduate Scholarship Program.

Declaration of conflicting interests


The author(s) declared no potential conflicts of interest with respect to the research, authorship, and/or publication of this article.

Funding

The author(s) received no financial support for the research, authorship, and/or publication of this article.

ORCID iDs

Juliana Isabel Saucedo Velázquez  <https://orcid.org/0000-0002-1445-5669>

Geydy Gutiérrez Urueta  <https://orcid.org/0000-0002-4314-8254>

References

- Ambriz-Díaz VM, Rubio-Maya C, Pacheco Ibarra JJ, et al. (2017) Analysis of a sequential production of electricity, ice and drying of agricultural products by cascading geothermal energy. *International Journal of Hydrogen Energy* 42: 18092–18102.
- Angrisani G, Diglio G, Sasso M, et al. (2016) Design of a novel geothermal heating and cooling system: Energy and economic analysis. *Energy Conversion and Management* 108: 144–159.
- Arreola Núñez M (2016) *Aprovechamiento de Calor Geotérmico de Mediana y Baja Entalpía Para la Producción de Frío*. Master's Thesis, Universidad Michoacana de San Nicolás de Hidalgo. Mexico.
- Best R and Rivera W (2015) A review of thermal cooling systems. *Applied Thermal Engineering* 75: 1162–1175.
- Breindel B, Harris RL and Olson GK (1978) *Geothermal Absorption Refrigeration for Food Processing Industries*. Sacramento, CA: Aerojet Energy Conversion Company.
- Caulk RA and Tomac I (2017) Reuse of abandoned oil and gas wells for geothermal energy production. *Renewable Energy* 112: 388–397.
- DiPippo R (2015) *Geothermal Power Plants: Principles, Applications, Case Studies and Environmental Impact*. 4th ed. Butterworth-Heinemann, USA, ISBN: 9780081008799.
- Dittus FW and Boelter LMK (1930) Heat transfer in automobile radiators of the tubular type. Berkeley: University of California, p.2.
- Dursun B and Gokcol C (2012) The role of geothermal energy in sustainable development of Turkey. *Energy Exploration & Exploitation* 30(2): 207–222.
- Erickson DC, Kyung I and Holdmann GP (2005) Geothermal powered absorption chiller for Alaska Ice Hotel. *Geothermal Resources Council Transactions* 29: 57–59.
- ESMAP (Energy Sector Management Assistance Program) (2012) Manual de geoterminia: cómo planificar y financiar la generación de electricidad. Informe Técnico 0 0 2/1 2. Washington: Energy Sector Management Assistance Program, pp.12–62.
- Galindo-Luna YR, Gómez-Arias E, Romero RJ, et al. (2018) Hybrid solar-geothermal energy absorption air-conditioning system operating with NaOH-H₂O-Las tres vírgenes (Baja California Sur), “La Reforma” case. *Energies* 11(5): 1268.
- Ghaebi H, Parikhani T and Rostamzadeh H (2018) A novel trigeneration system using geothermal heat source and liquefied natural gas cold energy recovery: Energy, exergy and exergoeconomic analysis. *Renewable Energy* 119: 513–527.

- Gutierrez-Negrin L (1988) The La Primavera, Jalisco, México, Geothermal Field. *Geothermal Resources Council Transactions* 2: 35–38.
- Gutiérrez-Negrin L, Maya-González R and Quijano-León JL (2015) Present situation and perspectives of geothermal in Mexico. In: *Proceedings, world geothermal congress, 2015*, 10p. Melbourne: Australia International Geothermal Association.
- Hernández-Magallanes JA (2017) *Desarrollo y evaluación de un sistema de enfriamiento solar tipo vertical operando con la mezcla nitrato de litio-amoniaco*. Ph.D. Thesis, Instituto de energías renovables, Universidad Nacional Autónoma de México, Temixco, Mexico.
- Hernández-Magallanes JA, Ibarra-Bahena J, Rivera W, et al. (2019) Thermodynamic analysis of a half-effect absorption cooling system powered by a low-enthalpy geothermal source. *Applied Sciences* 9, 1220.
- Hiriart G (2011) *Evaluación de la Energía Geotérmica en México*. Washington: Inter-American Development Bank.
- Holman JP (1986) *Heat Transfer*. 6th ed. Singapore: McGraw-Hill Book Co.
- Kairouani L and Nehdi E (2006) Cooling performance and energy saving of a compression-absorption refrigeration system assisted by geothermal energy. *Applied Thermal Engineering* 26: 288–294.
- Ma W, Chao L and Gong Y-L (2010) An absorption refrigeration system used for exploiting mid-low temperature geothermal resources. In: *Proceedings of the world geothermal congress 2010*, Bali, Indonesia, 25–29 April 2010, pp.1–4. Available at: <https://www.geothermal-energy.org/pdf/IGASTandard/WGC/2010/2911.pdf>
- Mahmoudi SMS and Akbari Kordlar M (2018) A new flexible geothermal based cogeneration system producing power and refrigeration. *Renewable Energy* 123: 499–512.
- Mahood GA (1980) Geological evolution of a pleistocene rhyolitic center – Sierra La Primavera, Jalisco, México. *Journal of Volcanology and Geothermal Research* 8: 199–230.
- Muffler L and Cataldi R (1978) Methods for regional assessment of geothermal resources. *Geothermics* 7: 53–89.
- Muffler LJP and Guffanti M (1979) Introduction to Muffler, L.J.P, ed., Assessment of geothermal resources of the United States – 1978. Geological Survey Circular 790, pp. 1–7.
- Nasruddin N and Wibowo AS (2018) Utilization of waste heat from separation process of Ulubelu's geothermal power plant by implementing an Absorption Refrigeration System (ARS) to improve plant performance. *IOP Conference Series: Earth and Environmental Sciences* 105.
- Parikhani T, Ghaebi H and Rostamzadeh H (2018) A novel geothermal combined cooling and power cycle based on the absorption power cycle: Energy, exergy and exergoeconomic analysis. *Energy* 153: 265–277.
- Pról-Ledesma RM, Carrillo-de la Cruz JL, Torres-Vera MA, et al. (2018) Heat flow map and geothermal resources in Mexico. *Terra Digitalis* 2: 1–15.
- Rafferty Kevin PE (1986) Absorption refrigeration: Cooling with hot water. *Geothermal Resources Council Transactions* 10: 25–29.
- Ramírez SR (2016) *Refrigeración Térmica con Geotermia de Baja Entalpía*. Thesis, Universidad Nacional Autónoma De México, Mexico.
- Reynolds G (1970) Cooling with geothermal heat. *Geothermics* 2: 1658–1661.
- Rocha Ruiz DA (2013) *Distribución de la alteración Hidrotermal del campo Geotérmico cerritos colorados*. Thesis, Universidad Nacional Autónoma de México, México
- Rogowska A and Szaffik W (2005) Cooling load production in sorption cycles supplied by a geothermal heat source for air. *Proceedings World Geothermal Congress 2005 Antalya*, Turkey, 24–29 April 2005. Available at: <https://www.geothermal-energy.org/pdf/IGASTandard/WGC/2005/1445.pdf>
- Salhi K, Korichi M and Ramadan KM (2018) Thermodynamic and thermo-economic analysis of compression-absorption cascade refrigeration system using low-GWP HFO refrigerant powered by geothermal energy. *International Journal of Refrigeration* 94: 214–229.

- Sikorska-Bączek R (2015) The use of geothermal energy in absorption refrigeration circuits. *Czas. Tech* 119–125.
- Tesha (2010) *Absorption Refrigeration System as an Integrated Condenser Cooling Unit in Geothermal. Proceedings World Geothermal Congress 2010 Bali*, Indonesia, 25-29 April. Available at: <https://www.geothermal-energy.org/pdf/IGAstandard/WGC/2010/3808.pdf>
- Tugcu A and Arslan O (2017) Optimization of geothermal energy aided absorption refrigeration system – GAARS: A novel ANN-based approach. *Geothermics* 65: 210–221.
- Universidad Autónoma de Chapingo (2008) *Manifestación de impacto ambiental modalidad Regional proyecto geotermoeléctrico Cerritos Colorados (25 MW – primera etapa)*. Mexico: Universidad Autónoma de Chapingo, pp.1–399.
- Uwera J, Itoi R, Jalilinasrabad S, et al. (2015) Design of a cooling system using geothermal energy for storage of agricultural products with emphasis on Irish potatoes in Rwanda, Africa. *Geothermal Resources Council Transactions* 39: 157–164.
- Verma SP, Arredondo-Parra UC, Andaverde J, et al. (2012) Three-dimensional temperature field simulation of a cooling of a magma chamber, La Primavera caldera, Jalisco, Mexico. *International Geology Review* 54: 833–843.
- Villa Merlo SJ, Chacón-Franco MY and Orozco-Medina G (1987) Utilización de la relación atómica Na+/K+ para identificar zonas de mayor actividad hidrotermal en el campo geotérmico de La Primavera, Jalisco. *Geotermia, Revista Mexicana de Geoenergía* 3: 241–244.
- Wang W, Luo J, Wang G, et al. (2018) Study of the sustainability of a ground source heat pump system by considering groundwater flow and intermittent operation strategies. *Energy Exploration & Exploitation* 37(2): 677–690.
- Xu T, Li F, Feng B, et al. (2020) Numerical evaluation of the performance of a single-well groundwater source heat pump system in Beijing, China. *Energy Exploration & Exploitation* 38: 201–222.
- Yilmaz C (2017) Thermodynamic and economic investigation of geothermal powered absorption cooling system for buildings. *Geothermics* 70: 239–248.
- Zarate, AA (2017) Necesidad energética y aceptación social de las energías renovables. Estudio de caso: Campo Geotérmico “Cerritos Colorados” en el Bosque La Primavera, Jalisco, México. Master’s thesis, Instituto Politécnico Nacional, CIEMAD, México.

Appendix

Notation

A	area
C_e	efficiency factor
C_f	specific heat of the fluid
C_p	heat capacity
C_r	specific heat of the rock
d	diameter
F_p	plant factor
h	heat transfer coefficient
H	thickness of the reservoir
L	well length
\dot{m}	mass flow

p_f	density of the fluid
p_r	density of the rock
Q_t	total energy
R_f	recovery factor
t	time
T_{AC}	condenser–absorber temperature
$T_{G,i}$	temperature supplied to the generator
T_m	minimum temperature
T_i	initial deposit temperature
T_1	inlet temperatures water
T_2	outlet temperatures water
T_W	wall temperature
\emptyset	porosity of the rock

Capítulo 4. Evaluación del potencial de enfriamiento de sistemas de absorción simples y avanzados en un campo geotérmico

4.1 Resumen

En este capítulo se evalúa y compara el potencial de enfriamiento y el rendimiento de los sistemas de enfriamiento avanzados, utilizando una mezcla H₂O/LiBr, accionados con energía geotérmica. Esta última proviene de un pozo inoperante en el campo Cerritos Colorados, y para su aprovechamiento se hace uso un intercambiador de calor de tubo en U dentro del pozo.

En la introducción se presentan los estudios relacionados con sistemas avanzados de refrigeración por absorción activados parcial o totalmente con energía geotérmica. Después se presenta una descripción del funcionamiento de cada uno de estos sistemas (simple, doble, triple y medio efecto), se describe la fuente geotérmica, la metodología utilizada para el cálculo del potencial de enfriamiento y las simulaciones para cada uno de los sistemas de software EES. Consecutivamente se presenta un nuevo modelo para la obtención de la temperatura dentro del pozo mediante intercambiador de calor en U. Por último se discuten los resultados obtenidos y se muestran las conclusiones respectivas.

Los resultados revelaron que este pozo puede alcanzar temperaturas de 59° C a 190° C, dependiendo de la profundidad del tubo en U y el espesor del aislamiento. Para una T_E=8°C, el rango de temperaturas de funcionamiento fue de 59-80°C para el medio efecto, de 77°-110 °C par el simple efecto, de 135-162°C para el doble efecto y de 180-187°C para el triple efecto. El máximo potencial de refrigeración fue de 99,334 GW el cual se obtuvo con el sistema de doble efecto, seguido de 92,995 GW con el sistema de triple efecto, 70,939 GW con el sistema de simple efecto y 38,721 GW con el sistema de medio efecto. El rango de COP fue: 0.43–0.49 para el sistema de medio efecto, de 0.89–0.97 para el de simple efecto, de 1.27–1.47 para el de doble efecto y 1.78–1.95 para el de triple efecto. Los valores máximos de los COPs obtuvieron en otoño e invierno cuando las temperaturas ambientales eran más bajas.

Del análisis del pozo geotérmico se determinó que, sin colocar una capa aislante en el tubo de retorno, es posible obtener temperaturas alrededor de los 60°C, las cuales son suficientes para accionar un sistema de medio efecto. Sin embargo, es necesario el aislamiento para alcanzar temperaturas más altas y así poder impulsar los otros sistemas, especialmente los sistemas de doble y triple efecto.

4.2 Artículo

Article

Cooling Potential for Single and Advanced Absorption Cooling Systems in a Geothermal Field in Mexico

Juliana Saucedo-Velázquez¹, Geydy Gutiérrez-Urueta² , Jorge Alejandro Wong-Loya¹ ,
Ricardo Molina-Rodea¹  and Wilfrido Rivera Gómez Franco^{1,*} 

¹ Instituto de Energías Renovables, Universidad Nacional Autónoma de México, Privada Xochicalco S/N, Col. Centro, Temixco C.P. 62580, Morelos, Mexico; jusave@ier.unam.mx (J.S.-V.); jawol@ier.unam.mx (J.A.W.-L.); rmr@ier.unam.mx (R.M.-R.)

² Facultad de Ingeniería, Universidad Autónoma de San Luis Potosí, Av. Dr. Manuel Nava No. 8, Col. Zona Universitaria Poniente, San Luis Potosí C.P. 78290, San Luis Potosí, Mexico; geydy.gutierrez@uaslp.mx

* Correspondence: wrgf@ier.unam.mx

Abstract: Climate change is one of the main problems humanity is currently facing due to the use of fossil fuels. At present, 20% of the total electricity consumed in buildings worldwide is for air conditioning. The development and use of thermally driven cooling systems is very important, since they can be activated by renewable energies, such as geothermal, reducing the consumption of electricity produced by fossil fuels. In this paper, we analyze a geothermal field located in the state of Jalisco, Mexico, with the aim of comparing the performance of different advanced absorption cooling systems driven by a geothermal heat source. The analysis includes the influence of water temperature obtained from an abandoned geothermal well, using a U tube heat exchanger inside the well. The results show that this well can reach temperatures from 59 °C to 190 °C, depending on the depth of the U tube and the insulation thickness. At a $T_E = 8$ °C, the operating range temperatures were 59–80 °C, 77–110 °C, 135–162 °C, and 180–187 °C for the half-effect, single-effect, double-effect and triple-effect systems, respectively. The maximum cooling potential was 99,334 GW obtained with the double-effect system, followed by 92,995 GW with the triple-effect system, 70,939 GW with the single-effect system, and 38,721 GW with the half-effect system.

Keywords: absorption cooling systems; geothermal cooling; cooling potential



Citation: Saucedo-Velázquez, J.; Gutiérrez-Urueta, G.; Wong-Loya, J.A.; Molina-Rodea, R.; Rivera Gómez Franco, W. Cooling Potential for Single and Advanced Absorption Cooling Systems in a Geothermal Field in Mexico. *Processes* **2022**, *10*, 583. <https://doi.org/10.3390/pr10030583>

Academic Editor:
Ahmad Arabkoohsar

Received: 22 February 2022

Accepted: 15 March 2022

Published: 17 March 2022

Publisher's Note: MDPI stays neutral with regard to jurisdictional claims in published maps and institutional affiliations.



Copyright: © 2022 by the authors. Licensee MDPI, Basel, Switzerland. This article is an open access article distributed under the terms and conditions of the Creative Commons Attribution (CC BY) license (<https://creativecommons.org/licenses/by/4.0/>).

1. Introduction

Climate change is one of the main problems humanity is currently facing due to the use of fossil fuels for different applications. Currently, 20% of the total electricity consumed in buildings worldwide is for air conditioning [1]. In 2018 it was estimated that refrigeration systems consumed 3900 TWh/year of electricity worldwide, and this energy is mainly produced by the consumption of fossil fuels [2]. Therefore, it is important that alternative cooling systems capable of operating with renewable energies, such as geothermal, are used.

A geothermal resource is the portion of heat released from the interior of the Earth that can be used in the appropriate technical and economic conditions available [3]. The potential of the Earth's geothermal resources is enormous, considering their current use and prospects, given the energy needs of humanity. The total heat content of the Earth is estimated to be around 1013 EJ (1 EJ = 1018 J) and it would take more than 109 years to deplete it, through a current global terrestrial heat flux of 40 million MW [4]. Therefore, the geothermal resource base is large enough and is practically everywhere. In 2020, the total global electricity production was 26,000 TWh, of which geothermal energy supplied an estimated 225 TWh (97 TWh of electricity and the rest in the form of heat) [5]. These amounts represent a low contribution to the total energy consumed around the world, even with the known potential.

The distribution of thermal energy used by category is approximately 58.8% for geothermal heat pumps, 18.0% for bathing and swimming, 16.0% for space heating, 3.5% for greenhouse heating, 1.6% for industrial applications, 1.3% for aquaculture pond and raceway heating, 0.8% for other applications [6].

In Mexico, the indirect use of geothermal energy almost entirely encompasses electricity production. Its direct uses are still restricted to bathing and swimming in recreational facilities and some of them for therapeutic uses (reported in 20 locations), including the geothermal field studied in this work, La Primavera. Likewise, Mexico's Federal Electricity Commission developed some of the direct uses of geothermal resources in the Los Azufre field, including a wood dryer, a fruit and vegetable dehydrator, a greenhouse, and a heating system of offices [7]. National studies related to geothermal energy and absorption cooling systems are presented next. Galindo-Luna et al. [8] proposed a hybrid system using a parabolic-trough collector field coupled to a low-enthalpy geothermal well to drive an absorption air conditioning system. A coefficient of performance (COP) of 0.71 was obtained for a generator temperature of 90 °C. The results of the modeling of a half-effect absorption system were reported using an ammonia/lithium nitrate mixture driven by a low-enthalpy geothermal source from two geothermal wells [9]. The results showed that at the wells temperatures, the cooling system can operate but obtaining low cooling effects. The potential that can be obtained from a geothermal well to operate a single-effect system was presented considering seasonal variations [10]. The COP values varied between 0.91 and 0.97. Ambriz-Díaz et al. [11] analyzed a cascade hybrid system operating in different modes. The system was composed in the first thermal level by an organic Rankine cycle to produce electricity, in the second level by an absorption refrigeration cycle to produce ice, and on the third level by a dehydrator for drying agricultural products. The results indicated that the dehydration process significantly improved the economic benefits of all the alternatives, achieving payback periods of around one year and reducing greenhouse emissions. Also, it was reported that the production of electricity alone was undesirable because it had the worst energy efficiencies and payback periods.

At an international level, several studies have been realized using geothermal energy to drive cooling systems or hybrid systems to produce cooling and an extra output. These studies are mainly based on single-effect, half-effect, and double-effect systems. Rogowska et al. [12] modeled a 10 kW single-stage absorption cooling system to produce air conditioning. The results were applied to a more advanced design of 500 kW refrigeration units in the studied region. An absorption refrigeration unit for the storage of agricultural products driven by geothermal hot water [13] reported a COP of 0.49, reaching a maximum value of 0.6 by using an extra heat exchanger. A dynamic simulation study to evaluate the performance of a new heating and cooling system was made based on the coupling between a low or medium-enthalpy geothermal source, an air handling unit, and a desiccant wheel [14]. The analysis demonstrated the technical and economic feasibility of the proposed system. The performance of an absorption refrigeration cycle and an ejector cycle using data from a low-enthalpy geothermal well were compared [15], deducing that at specific conditions, both systems were feasible as alternatives to conventional refrigeration systems. Arreola Núñez [16] modeled a commercial absorption machine driven by geothermal energy instead of gas. The results showed the thermodynamic feasibility of the system operating with geothermal energy but obtaining slightly lower coefficients of performance. Two works [17,18] have performed a parametric exergy and economic analysis of a combined cogeneration system to produce cooling and power using geothermal energy as a heat source. The results determined the most optimal operating conditions of the proposed systems. An integrated power and absorption cooling system was modeled including the waste heat from the power generation process as heat input in the cooling system, which in turn supplied the cooling water to the power plant [19]. It was concluded that it was not feasible, since it required a larger cooling capacity, increasing the total investment costs. Regarding advanced absorption cooling systems, a study presented a performance comparison of four different configurations for water/LiBr absorption cooling systems,

being these a single-effect, a half-effect, a double-effect in series, and a double-effect in reverse [20]. The maximum COPs achieved were 0.89, 0.4, 1.5, and 1.48, respectively. Similarly, calculations of the COPs and exergy analysis for single, double, triple, and half-effect water/LiBr absorption cycles were performed in another work [21]. It was observed that the COP significantly increased with the double and triple-effect cycles with values of 1.65 and 2.32, respectively. In the last two studies, the authors did not consider a special heat source, they only analyzed the performance of the systems at different operating temperatures. Shirazi et al. [22] analyzed the feasibility of single, double, and triple-effect heating and cooling absorption systems operating with solar collectors. The most favorable results were obtained with the double-effect system. The influence of various operating parameters on the COP and exergy efficiencies of the system were evaluated in [23]. The COPs for the single, double, and triple-effect chillers were in the range of 0.73–0.79, 1.22–1.42, and 1.62–1.90, respectively, while the maximum exergy efficiencies were in the range of 12.5–23.2%, 14.3–25.1%, and 17.7–25.2%, respectively. Best and Rivera [24] carried out a review analyzing both theoretical and experimental studies on absorption refrigeration systems operated with renewable energies such as geothermal. It was observed that the studies on absorption cooling systems driven partially or totally by geothermal energy in Mexico were very scarce. The installation of a thermo-chiller was described [25] operating with a double-effect ammonia absorption cycle at the Aurora Ice Museum in Chena Hot Springs, Alaska. The thermo-chiller was powered by thermal spring water providing 52.8 kW of cooling at $-29\text{ }^{\circ}\text{C}$. Han et al. [26], proposed a double-effect water/LiBr absorption cooling system, based on an enhanced geothermal system (EGS) using concentric circle wells. The influence of key parameters such as well depth and injection rates in the cooling system were analyzed. The results showed that the driven temperature of EGS hot water can reach more than $150\text{ }^{\circ}\text{C}$ steadily for 20 years. A thermodynamic analysis of a parallel-flow water/LiBr double-effect absorption system powered by geothermal energy was performed by using the Engineering Equation Solver (EES) software [27]. The results showed the behavior of the chiller at different operating conditions. A COP of up to 1.43 and a cooling load of 420 kW were obtained. Another thermodynamic study to utilize an existing low-temperature geothermal heat source was presented including six different models, with simple and half-effect systems [28]. The COP obtained with the half-effect system was approximately half (0.424) of the COP obtained with single-effect chillers (0.825). The results showed that the geothermal heat source can be used to drive both single and half-effect systems.

This bibliographic review showed that several studies have been carried out to compare the performance of advanced systems (half, double, and triple-effect systems) operating with solar energy. However, studies related to advanced absorption systems directly operating with a geothermal heat source are very scarce. Specifically, no studies were found for double and triple-effect systems driven by geothermal energy in which the geothermal well was analyzed.

The purpose of this article is to compare different configurations of absorption cooling systems driven by a geothermal field located in Mexico. The analysis includes the temperatures that can be obtained from a geothermal well considering different cases, and the variation of the cooling potential and COP for each one of the systems over the course of the year as a function of the driven and ambient temperatures. Real ambient temperatures were used in the analysis obtained from a meteorological station installed in the geothermal field.

2. Systems Description

2.1. Single-Effect Cooling System

A single-effect water/LiBr refrigeration system is mainly integrated by two circuits: a refrigerant circuit formed by a condenser, an expansion valve, and an evaporator, and a solution circuit integrated by a generator, an absorber, a solution heat exchanger, a pump, and a valve. Figure 1 shows a schematic diagram of the system.

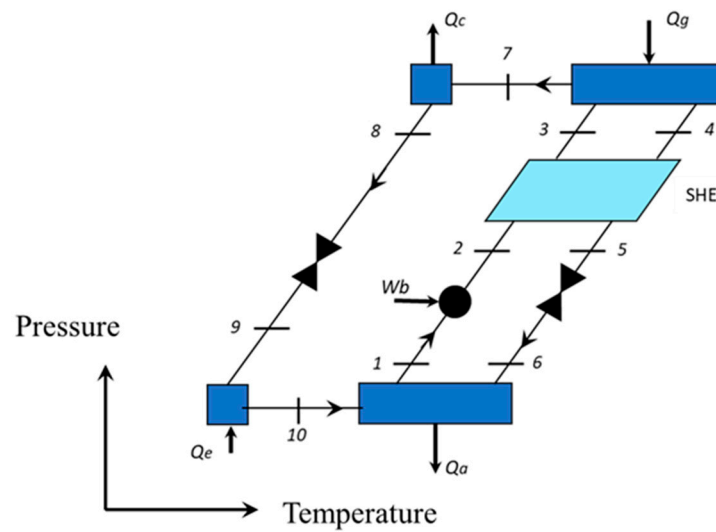


Figure 1. Schematic diagram of a single-effect absorption cooling system.

A solution with a high amount of refrigerant leaving the absorber (1) is pumped (2) to the generator, passing first through the solution heat exchanger, where it is preheated before entering the generator (3). In this component, an amount of heat Q_g is supplied to separate part of the water from the water/LiBr solution. The water in a vapor phase (7) goes to the condenser where it is condensed by means of an amount of heat removed Q_c . The liquid leaving this component (8) passes through an expansion valve reducing its pressure and temperature (9) and then to the evaporator producing the cooling effect Q_e . The water in a vapor phase leaving the evaporator (10) goes to the absorber where it is absorbed by the solution coming from the generator (4). The solution leaving the generator passes through the solution heat exchanger (5), preheating the solution going to the generator, and then through the valve reducing its pressure before entering the absorber (6). In the absorber, an amount of heat Q_a is delivered due to the exothermic reaction from the water absorption process. The solution with a high amount of refrigerant formed is then ready to be pumped to the generator starting the cycle again.

2.2. Half-Effect Cooling System

As can be seen in Figure 2, the half-effect cycle has one refrigerant circuit and two water/LiBr solution circuits, one of them at high pressure and the other one at low pressure. The refrigerant produced in the high-pressure generator passes through the condenser, the expansion valve, the evaporator, and the absorber similarly to the single-effect system. The solution low-pressure circuit also operates in the same way as previously described but with the difference that the refrigerant produced in the low-pressure generator is absorbed in the high-pressure absorber to produce a solution with a high amount of refrigerant which is used in the high-pressure circuit. Because in this system the heat is supplied into the two generators and produces only one stream of refrigerant which passes to the evaporator to produce the cooling effect, this system is called half-effect.

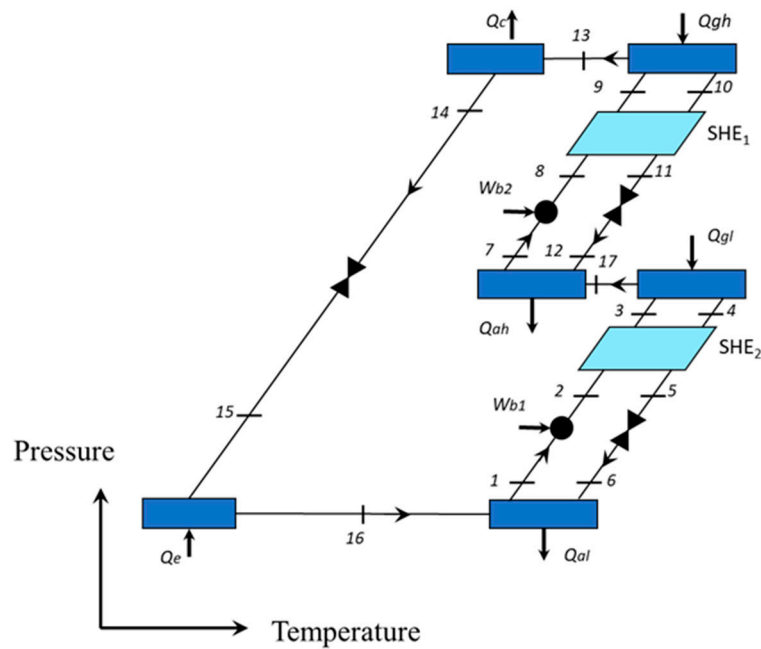


Figure 2. Schematic diagram of a half-effect absorption cooling system.

2.3. Double-Effect Cooling System

A double-effect system is shown in Figure 3. In the low part of the schematic diagram, it can be observed a single-stage system as described in Figure 1 but additionally, it has a second generator (Q_{g2}) operating at higher pressure and temperature, and a second solution heat exchanger (SHE_2). Although a second condenser appears in the diagram (Q_{c2}), this component and Q_{g1} is the same component. The shell part of a heat exchanger operates as a generator, while the side tubes operates as a condenser. As will be seen, the objective of adding the components above mentioned is to improve the system COP.

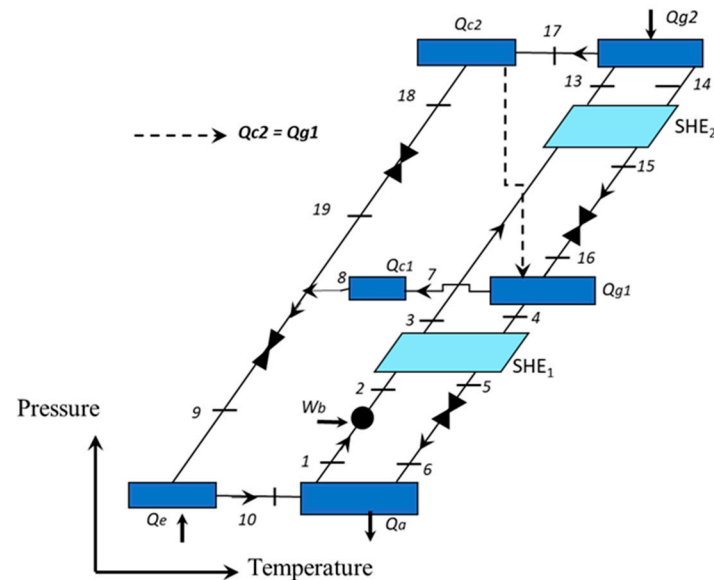


Figure 3. Schematic diagram for a double-effect absorption cooling system.

In this system, an amount of heat is supplied to Q_{g2} at a higher temperature than that supplied to a single-stage system to produce the refrigerant. The water in a vapor phase is then condensed in Q_{c2} leaving as a saturated liquid. The heat removed from the condensation processes is used as heat input to Q_{g1} to produce an extra amount of

refrigerant which is then condensed in Q_{c1} . Both condensed streams join before passing through the expansion valve and the evaporator. The rest of the cycle operates similarly to the single-stage system with the difference that the solution leaving from the absorber is pumped to Q_{g2} to produce the refrigerant at the highest pressure, and the solution leaving this component passes to Q_{g1} to produce more refrigerant. The two solution heat exchangers SHE_1 and SHE_2 are used to preheat the solution going from the absorber to the generator to reduce the heat supplied to Q_{g2} .

As can be seen from Figure 3, and the above explained, the heat is supplied to this system only in Q_{g2} , since Q_{g1} uses the heat delivered from the condensation process in Q_{c2} . Because the heat is supplied in only one component and produces two refrigerant streams, this system is denominated as a double-effect.

2.4. Triple-Effect Cooling System

A triple-effect system is shown in Figure 4. This system is similar to the double-effect system previously described but additionally, it has a third generator (Q_{g3}) and a third solution heat exchanger (SHE_3). The operation of this system is analogous to the double-effect system but in this case, the heat source is supplied to Q_{g3} at an even higher temperature than the second-stage system to produce the first stream of refrigerant. The other two streams of refrigerants are produced in Q_{g2} and Q_{g1} , using the heat delivered from the condensation processes in Q_{c3} and Q_{c2} . Because this system has the capability of producing three streams of refrigerant by supplying heat in only one component, this system is called a triple-effect system.

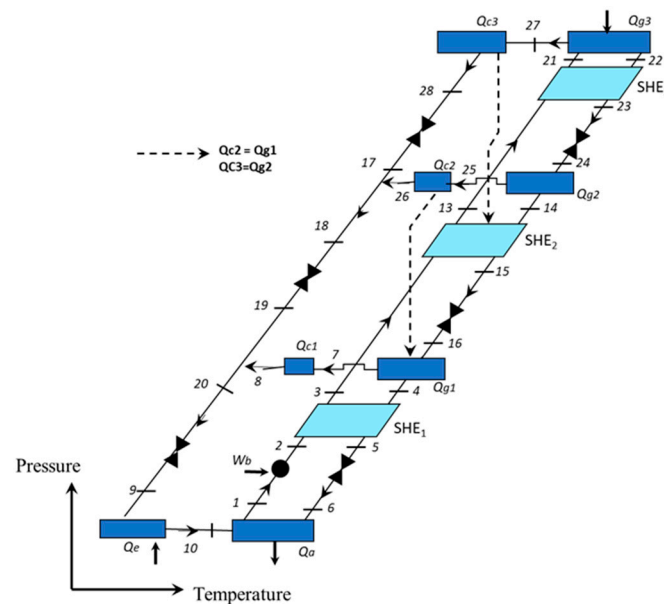


Figure 4. Schematic diagram of a triple-effect absorption cooling system.

3. Location and Solution Methods

3.1. Geothermal Source

The “Cerritos Colorados” geothermal field is located in the central-southern portion of the “La Primavera forest” [29] which is located 20 km west of the city of Guadalajara, in the state of Jalisco, between the extreme coordinates $103^{\circ}28'$ to $103^{\circ}42'$ West longitude and $20^{\circ}32'$ to $20^{\circ}44'$ North latitude (Figure 5).

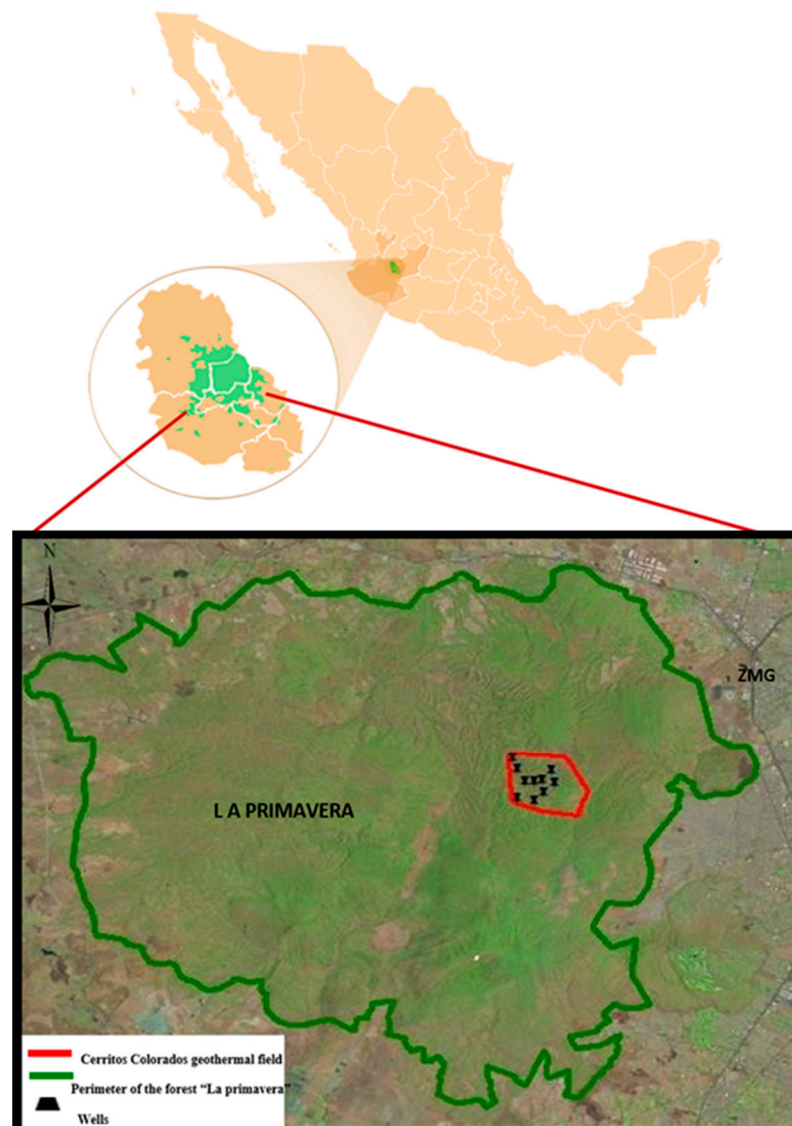


Figure 5. Location map of the Cerritos Colorado geothermal field [30].

In the present study, the data of the PR2 well are used. This well was chosen due to all the necessary data for analysis were available [31]. In Table 1 the characteristics of the well are presented, and Figure 6 presents its lithology.

Table 1. Data from PR2 geothermal well in the geothermal field Cerritos Colorados [29,31].

Well	Latitude	Longitude	Geothermal Gradient ($^{\circ}\text{C}/\text{km}$)	Depth (m)	Temperature ($^{\circ}\text{C}$)
PR2	20.66423	−103.53115	114.9	1988	320

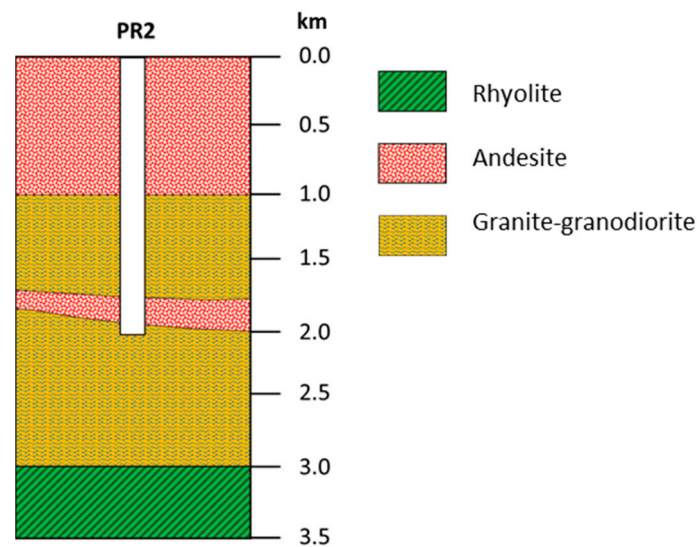


Figure 6. Simplified lithology based on core drilled wells from Cerritos Colorado geothermal field.

3.2. Calculation of Total Thermal Energy

To determine the energy gained by the fluid circulating through the well, the volumetric method was used. This method takes into consideration the energy contained in a certain volume of rock containing a hot water reservoir which supplies the energy to the fluid circulating through the pipe. The energy gained by the fluid is determined by using heat transfer equations and energy balances [32]. The procedure is repeated again for each control volume.

The energy stored in the rock volume (Q_r) can be determined by

$$Q_r = AH(1 - \phi)\rho_r C_r (T_i - T_m) \quad (1)$$

where A is the area of the control volume; H is the thickness of the reservoir; ρ_r is the density of the rock; C_r the specific heat of the rock; ϕ the porosity of the rock, defined as the relationship between the volume of empty spaces in the host rock or spaces occupied by the water in it and the total volume of the material [33]; and T_i and T_m , the initial and minimum temperatures, respectively.

The fluid energy Q_f can be estimated by Equation (2)

$$Q_f = AH\rho_f C_f \phi (T_i - T_m) \quad (2)$$

where ρ_f and C_f represent the density and specific heat of the rock, respectively.

Thus, the total energy is calculated as:

$$Q_t = Q_f + Q_r \quad (3)$$

Some of these parameters can be known with acceptable accuracy, but others, such as the area and thickness of the well, are uncertain even with extensive drilling, due to underground phenomena and morphology. Therefore, study areas of 1 km², 2 km², and 3 km², were considered as a minimum, probable, and maximum areas, respectively. For the majority of the reservoirs, the uncertainties regarding the depth are small compared with those of the respective area [34].

In Equations (1) and (2) H was considered as 2000 m which is an average value of divers well of the geothermal field. ϕ was established as 10%, which is related to the type of rock which is predominantly constituted by a volcanic igneous rock of intermediate composition [35]. The values of ρ_r and C_r of each type of rock were used according to the stratigraphic column of the Cerritos Colorado geothermal field (Figure 6). In the case of the fluid, the specific heat water values $C_f = 4.18$ kJ/kg°C and a density $\rho_f = 1000$ kg/m³

are used. T_m is set according to the technology used. For geothermal power plants, a temperature of 135 °C for single cycles and 90 °C for binary cycles are assumed in general [36]. For the present study, T_m varied according to the requirements of each absorption cycle. From the modeling of each one of the systems, it was found that for the specified conditions, T_m was 58 °C, 77 °C, 134 °C and 170 °C for the half, single, double, and triple-effect systems, respectively, and T_i was taken from the recorded temperatures of the analyzed geothermal well. It is important to mention that although a T_m of 58 °C for the half-effect cycle seemed to be a low temperature to drive an absorption cooling system, the double solution circuit used in this cycle (see Figure 2), allows the system to operate at such low temperature.

To define the reservoir initial temperature (T_i), an average of the temperatures recorded in the well PR2 was taken based on the data in Table 1.

3.3. Calculation of the Cooling Potential (CP) for the Absorption Cooling Systems

The power (P) produced by a geothermal power plant can be calculated by Equation (4) using the volumetric method [36].

$$P = \frac{Q_t R_f C_e}{F_p t} \quad (4)$$

where Q_t is the total energy obtained by Equation (3), R_f is the recovery factor, which represents the fraction of the energy that could be recovered, C_e is the efficiency factor, F_p is the plant factor, and t the operation time in hours. Values of R_f up to 25% have been reported for good conditions of porosity and permeability into the well but normally lower values are reported [35]. For the present study, an R_f of 12.5% and an F_p of 90% were considered since they are typical values reported in the literature [36].

Based on this equation, the cooling potential (CP) can be estimated by Equation (5) as:

$$CP = \frac{Q_t R_f COP}{F_p t} \quad (5)$$

where the efficiency factor (C_e) is replaced by the COP for each one of the cooling analyzed systems.

3.4. Simulation of the Water/LiBr Absorption Cooling Systems

To obtain the COP of each system, mathematical models were developed based on the first-law of thermodynamics, and then the simulation was carried out by using the Engineering Equation Solver (EES) software.

The following assumptions were considered in the modeling of each one of the cooling cycles:

- There is thermodynamic equilibrium in the cycles.
- The cycles operate under steady-state conditions.
- The solution is saturated at the exit of the generators and absorbers.
- The refrigerant is saturated at the exit of the condensers and evaporators.
- Heat losses and pressure drops in piping and components are negligible.
- The flow through the valves is isenthalpic.
- The effectiveness of the heat exchangers was 0.8.
- A $\Delta T = 7$ °C was considered between the ambient temperature and the temperature of the condensers and absorbers.
- The evaporation temperature T_E was 8 °C.

The value of $T_E = 8$ °C was chosen since it was the optimum value of the evaporation temperature obtained from the analysis of diverse absorption cooling systems [10]. These authors also reported that the values of CP and COP are directly proportional to T_E . However, higher values of T_E were not considered in the present study, since higher temperatures cannot provide good air condition temperatures.

Appendix A shows the tables with the energy balances for each one of the components integrating the four analyzed systems [20].

3.5. Heat Transfer Analysis in a U-Tube Heat Exchanger

The heat transfer analysis inside the “U” type heat exchanger was performed using a mathematical model developed with the finite volume numerical method and implemented in Fortran 90 programming language. This computational mathematical method consists of dividing the study domain into a finite quantity of control volumes. The equation which models the physical phenomena is discretized and solved for each control volume [37]. The main advantage of this mathematical model is that allows the estimation of fluid temperature through the heat exchanger based on pipe diameter, fluid velocity, boundary temperatures, the total length of the heat exchanger, the total length of the insulator, and soil thermo-physical characteristics. The study domain includes the soil, the well, the heat exchanger walls, the insulator material, and the space inside the heat exchanger where the fluid flows. Figure 7 shows a schematic diagram of the underground U tube heat exchanger.

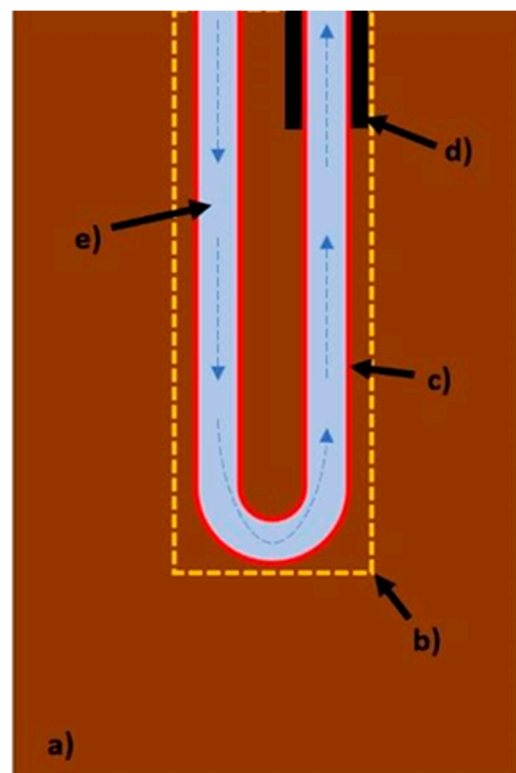


Figure 7. Study domain: (a) soil (brown), (b) well (yellow), (c) heat exchanger walls (red), (d) insulator (black), and (e) space inside the heat exchanger (blue).

In total, 1400 control volumes were used to represent the study domain. These control volumes are organized irregularly, presenting a greater density near the pipe walls of the heat exchanger.

The assumptions considered for the mathematical model are:

- The fluid viscosity is neglected, thus, the fluid velocity profile inside the heat exchanger is constant.
- The space inside the heat exchanger is represented as one-dimensional due to the constant fluid velocity.
- Inside the heat exchanger, the convection is the main heat transfer phenomenon; therefore, the conduction heat transfer among the fluid and the pipe walls is neglected.

- Outside the heat exchanger, the conduction is the main heat transfer phenomenon; therefore, the convection heat transfer through the soil porous is neglected.
- The heat exchanger walls thickness is neglected as the thermal dynamic is led by the soil.
- The soil thermal diffusivity changes as a function of the soil type presented in the lithology [32].
- The boundary temperature is equal to the temperature calculated with the geothermal gradient.
- The inlet fluid temperature remains constant.
- Environmental factors are neglected in soil surface temperature.
- Condensation and phase change for the fluid are omitted.

The energy equation (Equation (6)) is used for modeling purposes. All the terms in this equation (temporal, convective, and diffusive) are discretized for each node in the mesh represents the study domain [38].

$$\frac{\partial T}{\partial t} + \nabla \cdot (vT) = \alpha \cdot \nabla^2 T \quad (6)$$

In the previous equation, v and α represent the fluid velocity and thermal diffusivity, respectively. When Equation (6) is discretized, and the coefficients are arranged for each mesh node, a linear equation system results. This equations system is solved using an iterative Tridiagonal Matrix Algorithm (TDMA), which solves each dimension separately [39].

4. Results and Discussion

To determine the CP and COP for each of the systems driven with the energy provided by the geothermal well, first it is necessary to know the ambient temperatures in the zone since the geothermal well temperatures and the systems cooling performance depend upon these.

4.1. Ambient Temperature Data per Hour

The ambient temperature data used for the analysis were requested from the National Water Commission, CONAGUA. The data from the meteorological station “La Primavera” was used since it is the nearest station to the geothermal field.

Figure 8 shows the average ambient temperature per hour for the entire year 2018 for Spring, Summer, Autumn, and Winter. As can be seen, the temperatures varied between 10.3 °C and 33 °C for the whole year.

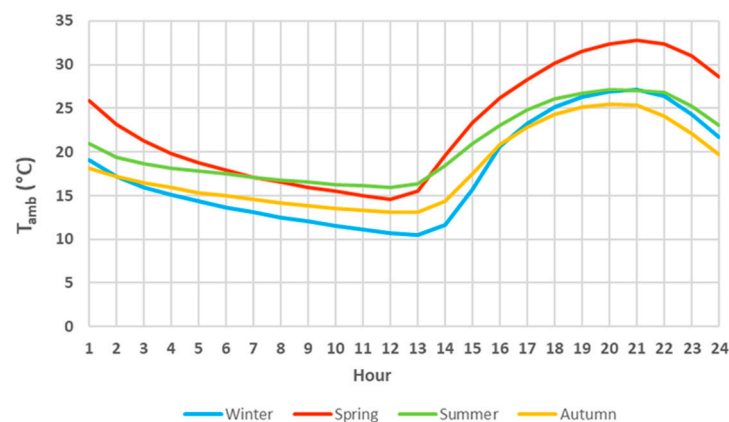


Figure 8. Average temperature per hour for each season.

4.2. Determination of the Geothermal Well Temperature

As stated in the assumptions, the initial temperature distribution is equal to the geothermal gradient for the specific site, which is equal to the boundary temperature.

Equations (7) and (8) show temperature correlations used in this study as a function of depth z .

$$T_{(z,t=0)} = 20 + (0.115 \cdot z), 0 < z < 2000 \quad (7)$$

$$T_{(z,t=0)} = 480 - (0.115 \cdot z), 2000 < z < 4000 \quad (8)$$

Six different cases were simulated changing the fluid velocity, the heat exchanger total length, the insulator length, and thickness. The thermal diffusivity for each type of soil used in the simulations was calculated using data from the stratigraphic column presented previously (Figure 6) and is constant for each test. The thermal diffusivity of the insulator material was considered equal to 1.08×10^{-9} (m^2/s). For all the tests carried out, the fluid inlet temperature was fixed at 20 °C, which is the average value of the seasonal environmental temperature. Finally, a “U” tube heat exchanger with a 3” pipe diameter was considered for the 6 cases. This value is considered because this is the maximum allowable diameter to cover the largest contact area inside the well. Table 2 shows the values of total length (TL), insulator length (IL), insulator thickness (IT), and fluid velocity (v) for each one of the 6 tests. The outlet fluid temperature is also reported (T_O).

Table 2. Values considered for the simulations of the geothermal well.

Case	TL (m)	IL (m)	IT(in)	v (m/s)	T_O (°C)	Cooling System Possible to Activate
1	4000	-	-	6	60.8	half-effect
2	4000	1000	1	6	174.7	triple-effect
3	4000	500	2	6	116.2	single-effect
4	4000	1000	1	4	160	double-effect
5	3000	1000	1	6	145.9	double-effect
6	3000	-	-	6	59.6	half-effect

The base case (first) was done without insulation, resulting in a temperature of 60.8 °C. This outlet temperature is enough to be used in a half-effect cooling system and was set as the starting point to compare subsequent results. Afterward, distinct values of total length, insulator length, insulator thickness, and air velocity were used to analyze their effects on the outlet fluid temperature, which is used to drive the absorption systems.

For the second case, insulator material was considered with 1000 m length and 1 ” of thickness, keeping the remaining parameters as in the first case. The result shows that the fluid outlet temperature was 174.7 °C.

The insulator material was considered again for the third case but changing the length and thickness. As result, the outlet fluid temperature was 116.2 °C. Compared with the first one, simulating 500 m less insulator material, allows the fluid to continue exchanging energy with its surroundings.

The fourth case considers 1000 m of insulator material, 1 ” of insulator thickness but a fluid velocity of 4 m/s. The result shows that the change in the velocity caused less turbulence, but the outlet fluid temperature was greater compared with the first case achieving a temperature of 160 °C.

Figure 9 illustrates the results obtained for cases 1 to 4. It shows the initial temperature condition in blue, equal to the temperature at the boundary obtained with the geothermal gradient. The fluid temperature profile is also shown, along with the heat exchanger for examples 1 to 4 (all 4000 m in total length). It is observed that the energy gain occurs in the first 2000 m, which is the downward section of the exchanger, while, depending on the simulator conditions, the energy gained was different.

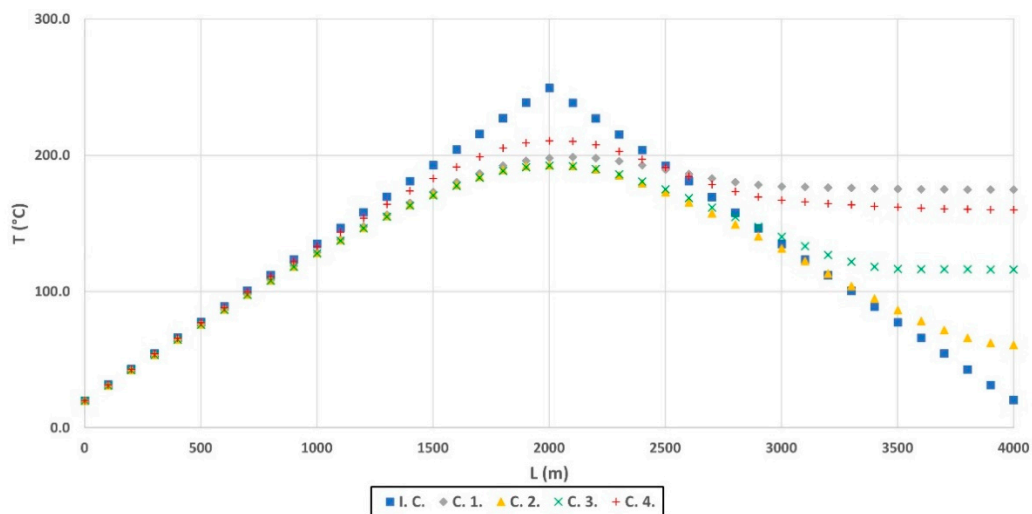


Figure 9. Fluid temperature inside the exchanger: I.C. initial condition (blue), C.1 (orange), C.2 (grey), C.3 (green), C.4. (red).

For the fifth case, the total length of the heat exchanger was reduced, while in the sixth one the insulator material was omitted. The results showed that both cases' temperature for were 145.9 °C and 59.6 °C, respectively. As in the first 2 cases, there is a difference of almost 100 °C in the final temperature of the fluid caused by the absence of the insulator material. Figure 10 shows the results for cases 5 and 6 (3000 m total length).

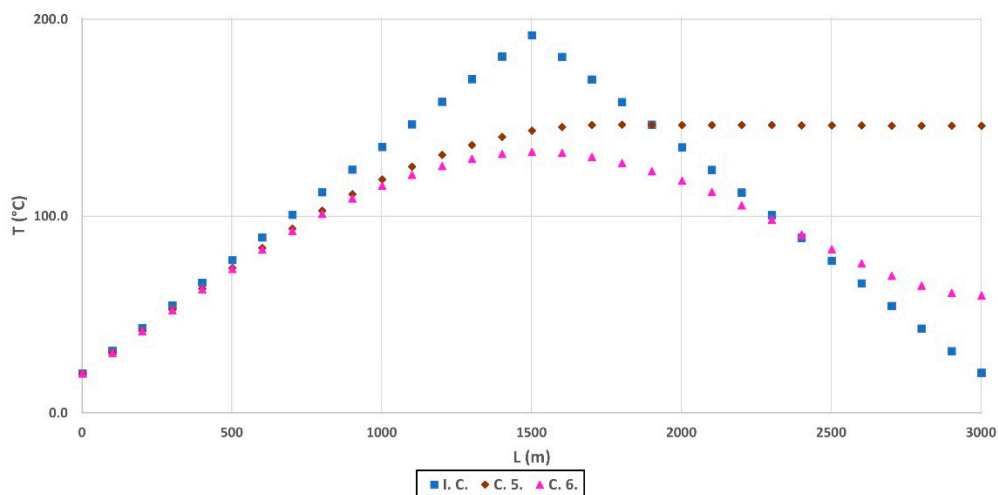


Figure 10. Fluid temperature inside the exchanger: I.C. initial condition (blue), C.5. (coffee), C.6. (pink).

4.3. Determination of the Cooling Potential (CP)

The CP can be determined for each one of the proposed systems by using Equation (5). The hourly results for the four seasons are presented in Figure 11a–d at a $T_E = 8$ °C. It can be observed that the CP is higher for the double-effect system with a maximum cooling potential of 99,334 GW, followed by the triple-effect with 92,995 GW, 70,939 GW for simple-effect, and 38,721 GW for the half-effect system. These maximum potentials are obtained in winter when the ambient temperature is lower. For the double and triple-effect system, when the environmental temperatures are very high, the systems cannot operate. This happened since the absorber and condenser temperatures were fixed 7 °C above the ambient temperature, and at considerably high absorber temperatures and low pressures, a crystallization phenomenon occurs.

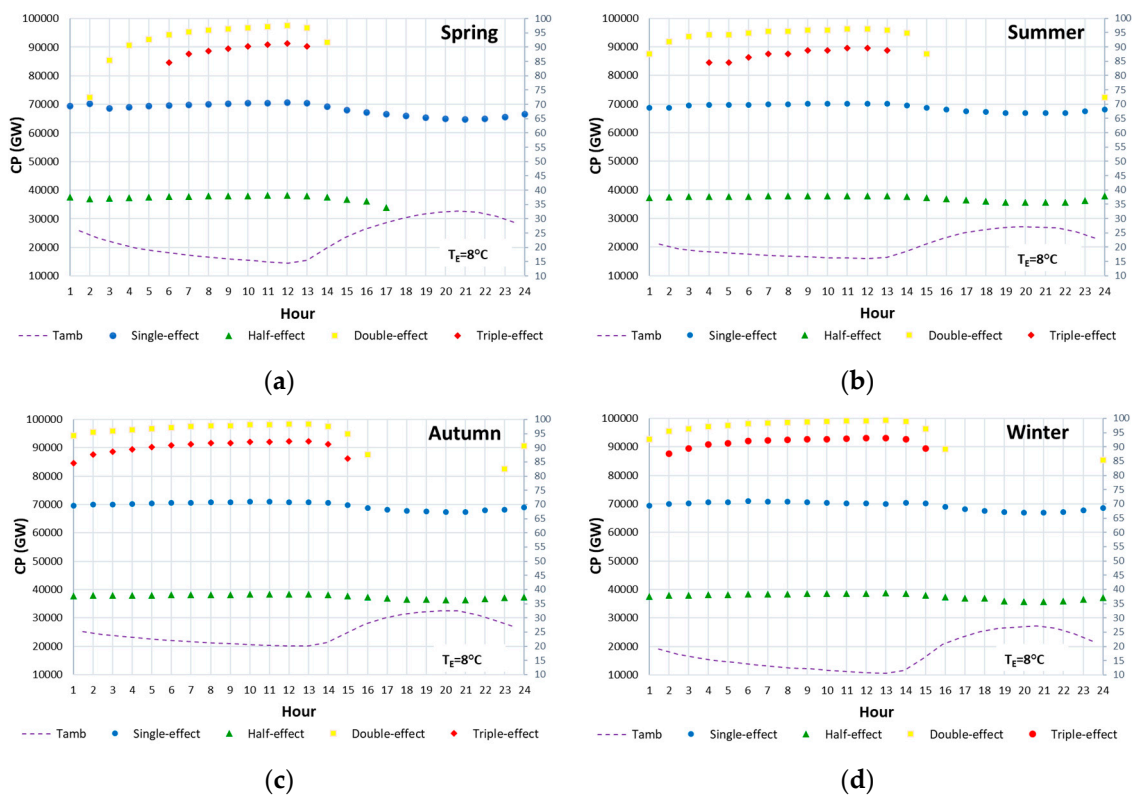


Figure 11. Cooling potential per hour for each absorption system for the season, (a) Spring, (b) Summer, (c) Autumn, and (d) Winter.

From the analysis carried out in Section 4.2, it was clear that the geothermal well can produce useful heat at temperatures up to 175 °C, depending on the analyzed case as it was shown in Table 2 and in Figures 9 and 10. Figure 12a–d show the cooling potential for each one of the proposed systems at a $T_E = 8$ °C for Spring, Summer, Autumn, and Winter, respectively. First, it is noticeable that the triple-effect system cannot operate in the Spring and Summer seasons due to the high ambient temperatures. The rest of the systems may operate for all seasons. Although it was expected that with the triple-effect system the highest cooling potential could be reached, due to its limited operating ranges the CP values are slightly lower than those obtained with the double-effect system. So, the highest potentials are obtained with the double-effect system, followed by the triple-effect system, and then for the single-effect system. The lowest CP values are obtained with the half-effect system, but with the advantage that these type of system may operate at very low temperatures from 59 °C to 79 °C. The single-effect system operates at temperatures between 77 °C and 112 °C, while the other systems require temperatures higher than 140 °C to operate, which can be only obtained for the analyzed cases 2, 4, and 5.

Figure 13a–d show the coefficients of performance for each one of the systems for Spring, Summer, Autumn, and Winter, respectively. As it was expected, according to the data reported in the literature [21], the highest $COPs$ are obtained with the triple-effect system. However, this system has a more limited operating temperature range in contrast to the other systems. The lowest COP values were obtained for the half-effect system varying from 0.43 to 0.49. For the single-effect system, the $COPs$ varied between 0.89 and 0.97, while for the double-effect and triple-effect systems varied from 1.27 to 1.47, and from 1.78 to 1.95, respectively. The maximum $COPs$ are obtained in the Winter and Autumn seasons.

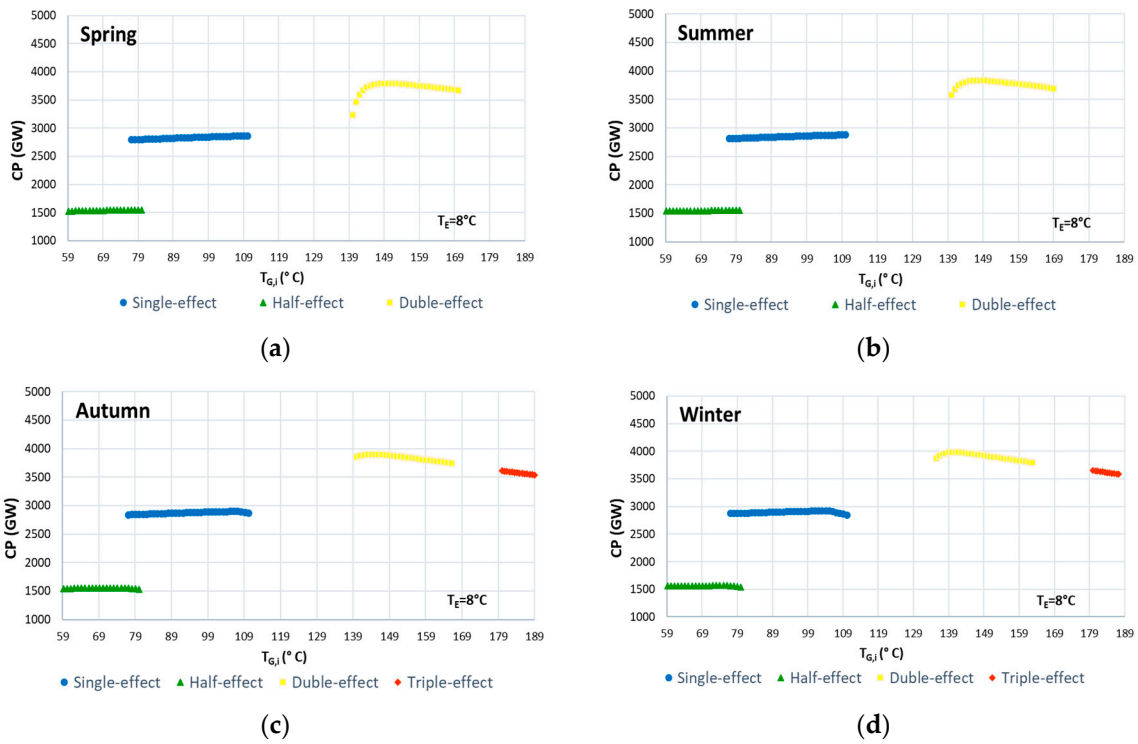


Figure 12. Cooling Potential per hour for each absorption system for the season, (a) Spring, (b) Summer, (c) Autumn, and (d) Winter.

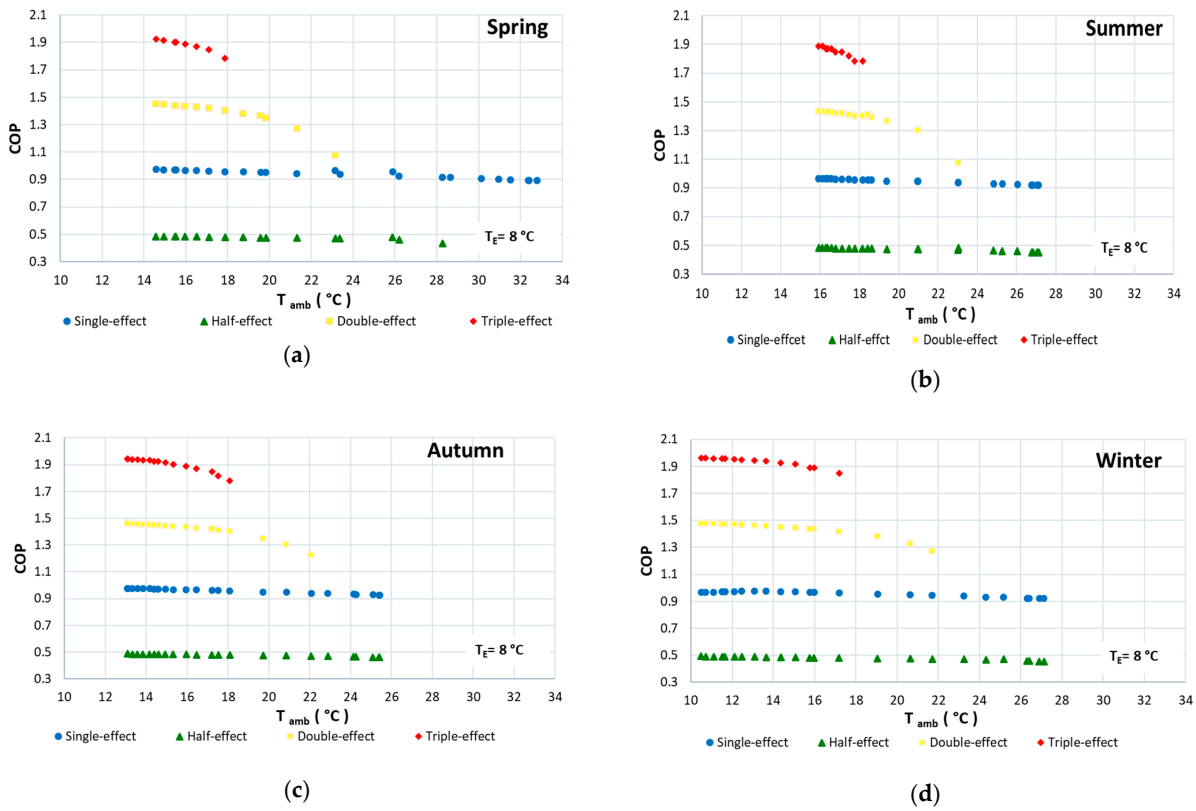


Figure 13. COP as a function of the T_{amb} for each absorption system for (a) Spring, (b) Summer, (c) Autumn, and (d) Winter.

5. Conclusions

A geothermal field located in Mexico was studied with the purpose to assess the performance of the four advanced absorption cooling systems driven by a geothermal heat source.

From the analysis of the geothermal well, it was found that without placing an insulation layer in the tube of return, it is possible to obtain temperatures around 60 °C, which are enough to drive a half-effect system; however, it is necessary the insulation to reach higher temperatures to drive the other systems, especially the double-effect and triple-effect systems.

At a $T_E = 8$ °C, the operating range temperatures were 59–80 °C, 77–110 °C, 135–162 °C, and 180–187 °C, with the half-effect, single-effect, double-effect, and triple-effect systems, respectively.

The range of the coefficients of performance for the four systems were: 0.43–0.49 for the half-effect system, 0.89–0.97 for the single-effect system, 1.27–1.47 for the double-effect, and 1.78–1.95 for the triple-effect system. The maximum values of the coefficients of performance were obtained in Autumn and Winter when the ambient temperatures were the lowest. This occurs since at low ambient temperatures, the condenser and absorber temperatures are also lower, thus reducing the operating pressures of the systems. The lower operating pressures cause an increase of the refrigerant production and therefore an increase of the coefficients of performance.

The maximum cooling potential was obtained with the double-effect system, achieving values up to 99,334 GW, followed by the triple-effect system with 92,995 GW. With the single-effect and half-effect systems the cooling potentials were up to 70,939 GW and 38,721 GW, respectively.

From the analysis, it was demonstrated that the triple-effect system does not present any advantage over the double-effect system, since it is more complex, it requires higher operating temperatures, it has a more limited operating range, and achieved lower cooling potentials.

The technical feasibility to produce cooling at temperatures as low as 58 °C by using geothermal energy was also demonstrated. This fact is very important because around the world there are numerous geothermal wells which can be used for these purposes. However, it is important to consider both the distance from the wells to towns and the possible applications. This is relevant since long distance result in the economic infeasibility because the geothermal areas (hydrothermal) are, in many cases, located far from urban areas.

Author Contributions: Conceptualization, J.S.-V., G.G.-U. and W.R.G.F.; methodology, J.S.-V., G.G.-U. and W.R.G.F.; geothermal well modeling, J.A.W.-L. and R.M.-R.; formal analysis, J.S.-V., G.G.-U. and W.R.G.F.; writing—original draft preparation, J.S.-V., G.G.-U., W.R.G.F., J.A.W.-L. and R.M.-R.; writing—review and editing, J.S.-V. and W.R.G.F.; visualization, W.R.G.F. and G.G.-U.; supervision, W.R.G.F. All authors have read and agreed to the published version of the manuscript.

Funding: This research received no external funding.

Institutional Review Board Statement: Not applicable.

Informed Consent Statement: Not applicable.

Data Availability Statement: The data presented in this study are available in the article.

Conflicts of Interest: The authors declared no potential conflict of interest with respect to the research, authorship, and/or publication of this article.

Nomenclature

A	area
C_e	efficiency factor
C	specific heat
COP	coefficient of performance
CP	cooling potential

F_p	plant factor
h	enthalpy
H	thickness of the reservoir
IL	insulator length
IT	insulator thickness
\dot{m}	mass flow
p	pressure
P	geothermoelectric potential
Q	heat load
Q_t	total energy
R_f	recovery factor
SHE	solution heat exchanger
T	temperature
TL	total length
t	time
W	work
v	fluid velocity
Z	depth

Subscripts

a	absorber
b	pump
c	condenser
e	evaporator
f	fluid
g	generator
G,I	introduced to the generator
i	initial
m	minimum
o	outlet
r	rock
w	wall

Greek letters

α	thermal diffusivity
ρ	density
ε	effectiveness
v	volume
\emptyset	porosity of the rock

Appendix A**Table A1.** Energy balances for each one of the components of the single-effect absorption cooling system.

Component	Balances
Generator	$Q_g = \dot{m}_4 h_4 + \dot{m}_7 h_7 - \dot{m}_3 h_3$
Condenser	$Q_c = \dot{m}_7 (h_7 - h_8)$
Evaporator	$Q_e = \dot{m}_{10} (h_{10} - h_9)$
Absorber	$Q_a = \dot{m}_{10} h_{10} + \dot{m}_6 h_6 - \dot{m}_1 h_1$
Effectiveness of the SHE	$\varepsilon_{SHE} = \frac{h_3 - h_2}{h_4 - h_2}$
Pump Work	$W_b = v_1 (P_8 - P_{10})$
COP	$COP = \frac{Q_e}{Q_g + W_b}$

Table A2. Energy balances for each one of the components of the half-effect absorption cooling system.

Component	Balances
Generator	$Q_{gh} = \dot{m}_{13}h_{13} + \dot{m}_{10}h_{10} - \dot{m}_9h_9$ $Q_{gl} = \dot{m}_4h_4 + \dot{m}_{17}h_{17} - \dot{m}_3h_3$
Condenser	$Q_c = \dot{m}_{13}(h_{13} - h_{14})$
Evaporator	$Q_e = \dot{m}_{16}(h_{16} - h_{15})$
Absorber	$Q_{al} = \dot{m}_6h_6 + \dot{m}_{16}h_{16} - \dot{m}_1h_1$ $Q_{ah} = \dot{m}_{17}h_{17} + \dot{m}_{12}h_{12} - \dot{m}_7h_7$
Effectiveness of the SHE	$\varepsilon_{SHE1} = \frac{h_3-h_2}{h_4-h_2}$ $\varepsilon_{SHE2} = \frac{h_9-h_8}{h_{10}-h_8}$
Pump Work	$W_{b1} = v_1(P_2 - P_1)$ $W_{b1} = v_7(P_8 - P_7)$
COP	$COP = \frac{Q_e}{Q_{gh}+W_{b1}+Q_{gl}+W_{b2}}$

Table A3. Energy balances for each one of the components of the double-effect absorption cooling system.

Component	Balances
Generator	$Q_{g2} = \dot{m}_{14}h_{14} + \dot{m}_{17}h_{17} - \dot{m}_3h_3$
Condenser	$Q_{c1} = \dot{m}_7h_7 - \dot{m}_8h_8$
Generator-Condenser	$Q_{g1} = \dot{m}_7h_7 + \dot{m}_4h_4 - \dot{m}_{16}h_{16}$ $Q_{c2} = \dot{m}_{17}h_{17} - \dot{m}_{18}h_{18}$
Evaporator	$Q_e = \dot{m}_{10}(h_{10} - h_9)$
Absorber	$Q_a = \dot{m}_6h_6 + \dot{m}_{10}h_{10} - \dot{m}_1h_1$
Effectiveness of the SHE	$\varepsilon_{SHX} = \frac{h_3-h_2}{h_4-h_2}$ $\varepsilon_{SHX} = \frac{h_{13}-h_3}{h_{14}-h_3}$
Pump Work	$W_b = v_1(P_2 - P_1)$
COP	$COP = \frac{Q_e}{Q_{g2}+W_b}$

Table A4. Energy balances for each one of the components of the triple-effect absorption cooling system.

Component	Balances
Generator	$Q_{g3} = \dot{m}_{22}h_{22} + \dot{m}_{27}h_{27} - \dot{m}_{21}h_{21}$
Condenser	$Q_{c1} = \dot{m}_7h_7 - \dot{m}_8h_8$
Generator-Condenser	$Q_{g2} = \dot{m}_{25}h_{25} + \dot{m}_{14}h_{14} - \dot{m}_{24}h_{24}$ $Q_{c3} = \dot{m}_{27}(h_{27} - h_{28})$ $Q_{g1} = \dot{m}_7h_7 + \dot{m}_4h_4 - \dot{m}_{16}h_{16}$ $Q_{c2} = \dot{m}_{25}(h_{25} - h_{26})$
Evaporator	$Q_e = \dot{m}_{10}(h_{10} - h_9)$
Absorber	$Q_a = \dot{m}_6h_6 + \dot{m}_{10}h_{10} - \dot{m}_1h_1$
Effectiveness of the SHE	$\varepsilon_{SHE 1} = \frac{h_3-h_2}{h_4-h_2}$ $\varepsilon_{SHE 2} = \frac{h_{13}-h_3}{h_{14}-h_3}$ $\varepsilon_{SHE 3} = \frac{h_{21}-h_{13}}{h_{22}-h_{13}}$
Pump Work	$W_b = v_1(P_2 - P_1)$
COP	$COP = \frac{Q_e}{Q_{g3}+W_b}$

References

1. International Energy Agency (IEA). *The Future of Cooling Opportunities for Energy-Efficient Air Conditioning*; IEA: Paris, France, 2018; p. 92. Available online: https://iea.blob.core.windows.net/assets/0bb45525-277f-4c9c-8d0c-9c0cb5e7d525/The_Future_of_Cooling.pdf (accessed on 10 October 2021).
2. United Nations Environment Programme; International Energy Agency. *Cooling Emissions and Policy Synthesis Report*; UNEP, Nairobi and IEA: Paris, France, 2020.
3. IGME; IDEA. *Manual de Geotermia*; Instituto para la Diversificación y Ahorro de la Energía- Instituto Geológico y Minero de España: Madrid, Spain, 2008; Available online: http://geoatlantic.eu/portfolio/wp-content/uploads/2020/06/10952_manual_geotermia_a2008.pdf (accessed on 12 August 2021).
4. Rybach, L.; Mongillo, M. Geothermal Sustainability—A Review with Identified Research Needs. *GRC Trans.* **2006**, *30*, 1083–1090.
5. Renewable Supply and Demand. Available online: <https://www.c2es.org/> (accessed on 11 January 2022).
6. Lund, J.W.; Boyd, T.L. Direct Utilization of Geothermal Energy 2015 Worldwide Review. In Proceedings of the World Geothermal Congress 2015, Melbourne, Australia, 19–24 April 2015.
7. Gutiérrez-Negrín, L.C.A.; Maya-González, R.; Luis Quijano-León, J. Present Situation and Perspectives of Geothermal in Mexico. *Proc. World Geotherm. Congr.* **2015**, *2015*, 19–25.
8. Galindo-Luna, Y.; Gómez-Arias, E.; Romero, R.; Venegas-Reyes, E.; Montiel-González, M.; Unland-Weiss, H.; Pacheco-Hernández, P.; González-Fernández, A.; Díaz-Salgado, J. Hybrid Solar-Geothermal Energy Absorption Air-Conditioning System Operating with NaOH-H₂O—Las Tres Virgenes (Baja California Sur), “La Reforma” Case. *Energies* **2018**, *11*, 1268. [\[CrossRef\]](#)
9. Hernández-Magallanes, J.A.; Ibarra-Bahena, J.; Rivera, W.; Romero, R.J.; Gómez-Arias, E.; Dehesa-Carrasco, U.; Espinoza-Ojeda, O.M.; Chandran, S.K. Thermodynamic Analysis of a Half-Effect Absorption Cooling System Powered by a Low-Enthalpy Geothermal Source. *Appl. Sci.* **2019**, *9*, 1220. [\[CrossRef\]](#)
10. Saucedo Velázquez, J.I.; Rivera Gómez Franco, W.; Gómez-Arias, E.; Gutiérrez Urueta, G.G. Evaluation of the cooling potential for a single effect absorption cooling system in the PR2 well of Cerritos Colorados geothermal field, Mexico. *Energy Explor. Exploit.* **2020**, *38*, 2521–2540. [\[CrossRef\]](#)
11. Ambriz-Díaz, V.M.; Rubio-Maya, C.; Pacheco Ibarra, J.J.; Galván González, S.R.; Martínez Patiño, J. Analysis of a sequential production of electricity, ice and drying of agricultural products by cascading geothermal energy. *Int. J. Hydrog. Energy* **2017**, *42*, 18092–18102. [\[CrossRef\]](#)
12. Rogowska, A.; Szaflik, W. Cooling Load Production in Sorption Cycles Supplied by a Geothermal Heat Source for Air. *Proc. World Geotherm. Congr.* **2005**, *2005*, 24–29.
13. Uwera, J.; Itoi, R.; Jalilinasrabad, S.; Jóhannesson, T.; Benediktsson, D.Ö. Design of a cooling system using geothermal energy for storage of agricultural products with emphasis on Irish potatoes in Rwanda, Africa. *Trans.—Geotherm. Resour. Counc.* **2015**, *39*, 157–164.
14. Angrisani, G.; Diglio, G.; Sasso, M.; Calise, F.; Dentice d’Accadia, M. Design of a novel geothermal heating and cooling system: Energy and economic analysis. *Energy Convers. Manag.* **2016**, *108*, 144–159. [\[CrossRef\]](#)
15. Ramírez Sanchez, R. *Refrigeración Térmica con Geotermia de baja Entalpía*; Universidad Nacional Autónoma de México: Manzanilla, Mexico, 2016.
16. Arreola Núñez, M. *Aprovechamiento de Calor Geotérmico de Mediana y baja Entalpía para la Producción de Frío*; Universidad Michoacana de San Nicolás de Hidalgo: Morelia, Mexico, 2016.
17. Akbari Kordlar, M.; Mahmoudi, S.M.S.; Talati, F.; Yari, M.; Mosaffa, A.H. A new flexible geothermal based cogeneration system producing power and refrigeration, part two: The influence of ambient temperature. *Renew. Energy* **2019**, *134*, 875–887. [\[CrossRef\]](#)
18. Parikhani, T.; Ghaebi, H.; Rostamzadeh, H. A novel geothermal combined cooling and power cycle based on the absorption power cycle: Energy, exergy and exergoeconomic analysis. *Energy* **2018**, *153*, 265–277. [\[CrossRef\]](#)
19. Tesha. Absorption Refrigeration System as an Integrated Condenser Cooling Unit in Geothermal Power Plant. MSc Thesis, Department of Mechanical and Industrial Engineering, University of Iceland, Reykjavík, Iceland, 2010; pp. 25–29.
20. Domínguez-Inzunza, L.A.; Sandoval-Reyes, M.; Hernández-Magallanes, J.A.; Rivera, W. Comparison of the Performance of Single Effect, Half Effect, Double Effect in Series and Inverse Absorption Cooling Systems Operating with the Mixture H₂O-LiBr. *Energy Procedia* **2014**, *57*, 2534–2543. [\[CrossRef\]](#)
21. Gebreslassie, B.H.; Medrano, M.; Boer, D. Exergy analysis of multi-effect water–LiBr absorption systems: From half to triple effect. *Renew. Energy* **2010**, *35*, 1773–1782. [\[CrossRef\]](#)
22. Shirazi, A.; Taylor, R.A.; White, S.D.; Morrison, G.L. A systematic parametric study and feasibility assessment of solar-assisted single-effect, double-effect, and triple-effect absorption chillers for heating and cooling applications. *Energy Convers. Manag.* **2016**, *114*, 258–277. [\[CrossRef\]](#)
23. Gomri, R. Investigation of the potential of application of single effect and multiple effect absorption cooling systems. *Energy Convers. Manag.* **2010**, *51*, 1629–1636. [\[CrossRef\]](#)
24. Best, R.; Rivera, W. A review of thermal cooling systems. *Appl. Therm. Eng.* **2015**, *75*, 1162–1175. [\[CrossRef\]](#)
25. Erickson, D.C.; Kyung, I.; Holdmann, G.P. Geothermal powered absorption chiller for Alaska Ice Hotel. *Trans.—Geotherm. Resour. Counc.* **2005**, *29*, 57–59.
26. Han, B.; Li, W.; Li, M.; Liu, L.; Song, J. Study on LiBr/H₂O absorption cooling system based on enhanced geothermal system for data center. *Energy Reports* **2020**, *6*, 1090–1098. [\[CrossRef\]](#)

27. El Haj Assad, M.; Said, Z.; Khosravi, A.; Salameh, T.; Albawab, M. Parametric study of geothermal parallel flow double-effect water-LiBr absorption chiller. In Proceedings of the 2019 Advances in Science and Engineering Technology International Conferences (ASET), Dubai, United Arab Emirates, 26 March–10 April 2019; IEEE: Piscataway, NJ, USA, 2019; pp. 1–6.
28. Masheiti, S.; Agnew, B. Thermodynamic Simulation Modelling of Low-Temperature Geothermal Source Located in Arid-Zone Area North Africa. *Jordan J. Mech. Ind. Eng.* **2010**, *4*, 61–68.
29. Gutierrez-Negrin, L.C.A. The La Primavera, Jalisco, Mexico, Geothermal Field. In Proceedings of the Geothermal Resources Council Transactions; Geothermal Resources Council, San Diego, CA, USA, 9–12 October 1988.
30. Saucedo Velazquez, J.I. *Propuesta para el Desarrollo de un Proyecto Geotérmico Sustentable en el Bosque de la Primavera*; Universidad Autónoma de San Luis Potosí: San Luis Potosí, Mexico, 2017.
31. Prol-Ledesma, R.M.; Carrillo-de la Cruz, J.L.; Torres-Vera, M.A.; Membrillo-Abad, A.S.; Espinoza-Ojeda, O.M. Heat flow map and geothermal resources in Mexico. *Terra Digit.* **2018**, *2*, 1–15. [[CrossRef](#)]
32. Verma, S.P.; Arredondo-Parra, U.C.; Andaverde, J.; Gómez-Arias, E.; Guerrero-Martínez, F.J. Three-dimensional temperature field simulation of a cooling of a magma chamber, La Primavera caldera, Jalisco, Mexico. *Int. Geol. Rev.* **2012**, *54*, 833–843. [[CrossRef](#)]
33. Muffler, P.; Cataldi, R. Methods for regional assessment of geothermal resources. *Geothermics* **1978**, *7*, 53–89. [[CrossRef](#)]
34. Muffler, L.J.P. Assessment of geothermal resources of the United States -1978. In *Geological Survey Circular 790*; Geological Survey: Reston, VA, USA, 1979; Volume 2.
35. Dippippo, R. *Geothermal Power Plants: Principles, Applications, Case Studies and Environmental Impac*, 4th ed.; Butterworth-Heinemann: Oxford, UK, 2015; ISBN 978-0081008799.
36. Hiriart, G. Evaluación de la Energía Geotérmica en México. 2011. Available online: <https://www.cre.gob.mx/documento/2027.pdf> (accessed on 3 July 2021).
37. Serageldin, A.A.; Abdelrahman, A.K.; Ookawara, S. Earth-Air Heat Exchanger thermal performance in Egyptian conditions: Experimental results, mathematical model, and Computational Fluid Dynamics simulation. *Energy Convers. Manag.* **2016**, *122*, 25–38. [[CrossRef](#)]
38. Liu, Q.; Du, Z.; Fan, Y. Heat and Mass Transfer Behavior Prediction and Thermal Performance Analysis of Earth-to-Air Heat Exchanger by Finite Volume Method. *Energies* **2018**, *11*, 1542. [[CrossRef](#)]
39. Kumar Borah, A.; Singh, P.K.; Goswami, P. Advances in Numerical Modeling of Heat Exchanger Related Fluid Flow and Heat Transfer. *Am. J. Eng. Sci. Technol. Res. Am. J. Eng. Sci. Technol. Res.* **2013**, *1*, 156–166.

Capítulo 5. Caso de estudio: Diseño un sistema de refrigeración por absorción para conservación de leche

5.1 Resumen

Este análisis se centra en el diseño de un sistema de refrigeración para el almacenamiento de leche en el ejido Adolfo López Mateos, ubicado dentro del Bosque de “La Primavera”, Jalisco. Se propone una unidad de refrigeración por absorción H₂O/LiBr que utiliza una fuente de calor geotérmico para impulsar el ciclo de absorción del proceso de refrigeración. Se presenta un análisis económico y su comparativo contra un sistema convencional y un sistema solar.

Luego de exponer la revisión de los trabajos relacionado con sistemas de absorción para diversas aplicaciones de refrigeración y aire acondicionado, se explica el campo geotérmico, y se exhibe el problema a resolver. Posteriormente, se describe a detalle el almacén propuesto incluyendo diseño, materiales y cálculo de las cargas térmicas, además del dimensionamiento y análisis económico del equipo de absorción. En la sección final se ofrecen los resultados y conclusiones de este análisis.

Se presenta el análisis de un sistema de simple efecto y de doble efecto para su comparación. El sistema propuesto debe conservar leche a 10°C y proporcionar la refrigeración al almacén (cuarto frío) con una carga de enfriamiento de 5 kW, una fuente de calor geotérmica de 80°C para el sistema simple efecto y 163°C para el sistema de doble efecto. Para el diseño del almacén se obtuvieron las cargas térmicas a través de techos, muros, por iluminación, infiltración y por ocupación a través del software EnergyPlus.

Los resultados mostraron que el sistema de simple efecto ofrece un COP de 0.85, a un costo total aproximado de \$13,083 USD, mientras que para el sistema de doble efecto el COP es de 1.38 con un costo de \$18,144 USD. Los valores de cargas térmicas mensuales oscilan entre 0.94 y 1.1 kW.

5.2 Artículo

Case Studies in Thermal Engineering

Case study: Design of an absorption refrigeration system for milk preservation in Jalisco, Mexico --Manuscript Draft--

Manuscript Number:	
Article Type:	Case study
Keywords:	Absorption refrigeration system; Geothermal energy; Thermal loads; Cooling load; Economic analysis
Corresponding Author:	Gedy Luz Gutiérrez, PhD Autonomous University of San Luis Potosi San Luis Potosí, San Luis Potosí MEXICO
First Author:	Juliana Saucedo-Velázquez
Order of Authors:	Juliana Saucedo-Velázquez Gedy Luz Gutiérrez, PhD Alejandro Pacheco Wilfrido Rivera
Abstract:	<p>This article presents a case study focused on the design of a refrigeration system for milk storage in a town located in Jalisco, Mexico. An absorption refrigeration unit is proposed, activated with a geothermal heat source from an existing well. An economic analysis of the proposal and its comparison with a conventional system and a solar system is presented. The proposed system must provide refrigeration to the warehouse (cold room) with a cooling load of 5 kW, with a geothermal heat source temperature of 80°C for the single effect system and 163°C for the double effect system. For the design of the warehouse, the thermal loads were obtained through ceilings and walls, by lighting, infiltration, and by occupation, through the EnergyPlus software. The results show values of monthly thermal loads ranging between 0.94 and 1.1 kW. The single-effect system offers a COP of 0.85 at a total cost of approximately \$13,083 USD, while the double-acting system offers a COP of 1.38 at the cost of \$18,144 USD.</p>
Suggested Reviewers:	Maria Venegas, PhD mvenegas@ing.uc3m.es Rajagopal Saravanan, PhD Anna University rs.ishrae@gmail.com
Opposed Reviewers:	

Case Studies in Thermal Engineering

Editorial Office

Dear Sr. or Madame,

Please find enclosed the manuscript of the paper entitled “Case study: Design of an absorption refrigeration system for milk preservation in Jalisco, Mexico” To be submitted for publication in Case Studies in Thermal Engineering.

The paper has not been published previously or submitted for publication elsewhere.

The authors express their interest in publishing this work and thank for the time in reviewing it.

Sincerely yours

Dr. Geydy Gutiérrez-Urueta

Autonomous University of San Luis Potosí, Faculty of Engineering,

San Luis Potosí, SLP, 78290, México

e-mail:geydy.gutierrez@uaslp.mx

Case study: Design of an absorption refrigeration system for milk preservation in Jalisco, Mexico

J. Saucedo-Velázquez, G. Gutiérrez-Urueta^{2*}, A. Pacheco¹ and W. Rivera¹

¹ Instituto de Energías Renovables, Universidad Nacional Autónoma de México, Privada Xochicalco S/N, Col. Centro, Temixco C.P. 62580, Morelos, México; jusave@ier.unam.mx (J.S.-V.); parea@ier.unam.mx; wrgf@ier.unam.mx

² Facultad de Ingeniería, Universidad Autónoma de San Luis Potosí, Av. Dr. Manuel Nava No. 8, Col. Zona Universitaria Poniente, San Luis Potosí C.P. 78290, San Luis Potosí, México; geydy.gutierrez@uaslp.mx

* Correspondence: geydy.gutierrez@uaslp.mx

Abstract:

This article presents a case study focused on the design of a refrigeration system for milk storage in a town located in Jalisco, Mexico. An absorption refrigeration unit is proposed, activated with a geothermal heat source from an existing well. An economic analysis of the proposal and its comparison with a conventional system and a solar system is presented. The proposed system must provide refrigeration to the warehouse (cold room) with a cooling load of 5 kW, with a geothermal heat source temperature of 80°C for the single effect system and 163°C for the double effect system. For the design of the warehouse, the thermal loads were obtained through ceilings and walls, by lighting, infiltration, and by occupation, through the EnergyPlus software. The results show values of monthly thermal loads ranging between 0.94 and 1.1 kW. The single-effect system offers a COP of 0.85 at a total cost of approximately \$13,083 USD, while the double-acting system offers a COP of 1.38 at the cost of \$18,144 USD.

Keywords: Absorption refrigeration system, Geothermal energy, Thermal loads, Cooling load, Economic analysis.

1. Introduction:

One of the main current challenges is to meet the world's growing energy demands, making it accessible to all social sectors and, simultaneously, reducing greenhouse gas emissions due to global warming derived from such growing demand. Therefore, a more rational and efficient use of energy is necessary [1], as well as the use of energy sources that, in turn, contribute to reducing greenhouse gas emissions.

The energy problem is both one of supply and the search for new energy sources. The demand is a challenge that must be analyzed [2] since it is necessary to cover food needs due to population growth worldwide, which entails food conservation using refrigeration systems. For instance, perishable foods such as milk, meat, fruits, and vegetables, among others, are heat-sensitive products, so it is necessary to maintain them under certain thermal requirements, by storing them in a refrigerated space.

Food security is one of the most prominent global problems and is strongly related to food waste and losses. Globally, 33% of food production is wasted, affecting food security and the

environment, and wasting the earth's resources. Around 1.4 million hectares are globally occupied by uneaten food [3].

The lack of refrigeration in remote or rural places is one of the main causes of food waste and loss. Therefore, the development of sustainable refrigeration systems using local resources to meet the demand for refrigeration is very important [4]. Furthermore, the need for cooling and refrigeration is related to the ability to slow down the decomposition of food to allow its production, transport, and storage [5].

It is estimated that of 100% of the energy consumed worldwide, approximately 50% is consumed by refrigeration processes [6] and cold rooms are widely used throughout the world for food preservation. The most widely used cold storage is mainly based on a conventional vapor compression system, in which the compressor consumes electrical energy. The latter is obtained, in general, from fossil fuels and in combination with the use of refrigerants, implies a high economic and environmental cost [6].

Using alternative energy sources and cooling systems could contribute significantly to decreasing electricity consumption and the negative environmental impact. In this context, absorption refrigeration systems powered by renewable energies are an alternative that has been implemented more over time, as presented in Best & Rivera [7]. Work has been carried out on absorption refrigeration systems for various refrigeration and air conditioning applications, driven mainly by solar energy or in cascade. Among these alternatives is also geothermal energy, which can be used to drive absorption refrigeration systems for space conditioning and other refrigeration applications. However, its direct application for food preservation purposes is still scarce.

In Breindel et al. [8], a first approach is presented on the potential of using absorption systems for freezing or storing food, using geothermal energy in cascade. Best et al. [9] developed an experimental ammonia/water absorption chiller installed in a geothermal field, which could be used for food storage. The system operated at temperatures close to 91 °C achieving a coefficient of performance (COP) of 0.433. In Keçeciler et al. [10], the design of an absorption refrigeration system using water-lithium bromide was presented. The results showed that the geothermal resource in the studied site could not be used efficiently for electricity generation, but it could be used for storing fruits and vegetables at 4–10°C and for air conditioning. Ábrago Castillo [11] proposed a cascade absorption refrigeration system for tropical climates, which can be used for daily product storage, such as cured meat, to hydroponic plantations, with a COP of 0.6. Isaza C. et al. [12] simulated the performance and analyzed the feasibility of simple-effect solar absorption refrigeration systems using monomethylamine-H₂O solutions for applications in food preservation in rural regions. They reported that the maximum COP was achieved at a generation temperature of around 70°C. Uwera et al. [13] designed a refrigeration system to store agricultural products. A simple-effect absorption refrigeration unit driven by geothermal energy with a thermal load of 140 kW achieved COP values from 0.49 to 0.6. In Yopez & Ramos[14], a prototype of an intermittent absorption refrigeration system driven by solar energy was designed and built to conserve tropical fruits. The system obtained a COP of 0.35. De & Ganguly [15] compared the performance of a

single-effect and a double-effect vapor absorption system for the operation of a cold storage facility operating by a combination of a grid-interactive photovoltaic solar system and parabolic trough collectors. The COP of the double-effect system was 1.32. El Haj Assad [16] presented the use of cascade to take advantage of the residual heat of a simple flashing geothermal plant to activate a simple-effect absorption system for the cooling of a residential building. The results showed that with a geo-fluid temperature of 120 °C, a COP of 0.87 can be obtained. Ozcan et al. [17] designed an ammonia-water refrigeration system using a geothermal source for cooling a single-family house. The system was analyzed through an energy and exergy analysis. A COP of 0.30 was attained at a $T_G = 90^\circ\text{C}$ and a $T_E = 2^\circ\text{C}$. Sofyan et al. [18] examined the performance of an absorption refrigeration system operating with a lithium bromide-water mixture using residual heat from a power plant for the cold storage of fish. The results evaluated the system performance by varying the temperatures of the system components. Jimenez-Garcia and Rivera [19] built a new absorption refrigeration system driven by solar energy built with plate heat exchangers using the $\text{NH}_3/\text{H}_2\text{O}$ mixture. The system could be used for air conditioning and food preservation. The results showed that it was possible to obtain cooling power close to 3 kW achieving a COP of 0.61 at temperatures as low as -19°C . Sadi et al. [20] proposed a solar single-effect absorption cooling system with lithium bromide to store apples and potatoes. The results showed the performance of different solar collectors, and a maximum COP of 0.7 was obtained. Sur et al. [21] designed a system for milk storage using an activated carbon-methanol adsorption refrigeration driven by solar energy. The results showed that the maximum COP varied between 52 and 57 kW/kg at a desorber temperature of 80°C . Pilatowsky et al. [22] analyzed the performance of a monomethylamine-water absorption refrigeration system using solar energy to cool milk in rural regions. The evaporator temperature varied from -5 to 10°C at T_G from 60 to 80°C , achieving COP varying from 0.15 to 0.7.

The literature review showed that although absorption refrigeration systems have been investigated for about 3 decades, their use in projects for direct applications such as food preservation is scarce. In addition, the existing developments are mainly based on solar energy.

This article proposes the design of a warehouse (cold room) and an absorption refrigeration system to conserve milk from Ejido Adolfo López Mateos, with geothermal energy supplied from the nearest geothermal well. The purpose is that the settlers can continue this productive activity. Two absorption system configurations are presented, a simple and double-effect system, comparing their performance and cost.

2. Description of the geothermal field

The Cerritos Colorados geothermal field is located in the central-southern portion of “La Primavera forest” [23], within the “Ejido Adolfo Lopez Mateos” (Figura 1,2). This area is a volcanic caldera about 11 km in diameter, with an approximate age of 95,000 years [24]. As a remnant of the volcanic activity, a strong hydrothermal activity occurred, and a geothermal system developed, which currently manifests itself with fumaroles, hot springs, solfataras, and hot soils,

which outcrop in various parts of the volcanic complex, such as in Cerritos Colorados, Las Barrancas, La Azufrera, and El Nejahuete, as well as outcrops of springs in Rio Caliente [25].

Given its geothermal potential, the Federal Electricity Commission (CFE, for its initials in Spanish) of Mexico, during the period 1980-1989, developed civil works to explore the geothermal zone called Cerritos Colorados. The works consisted of the opening of access roads, the construction of platforms and mud dams, as well as the drilling of 12 geothermal wells. Unfortunately, these works were suspended, so the existing wells are inoperative (Figure 1). The Cerritos Colorados geothermal field has great potential for direct use, as well as for electricity production.

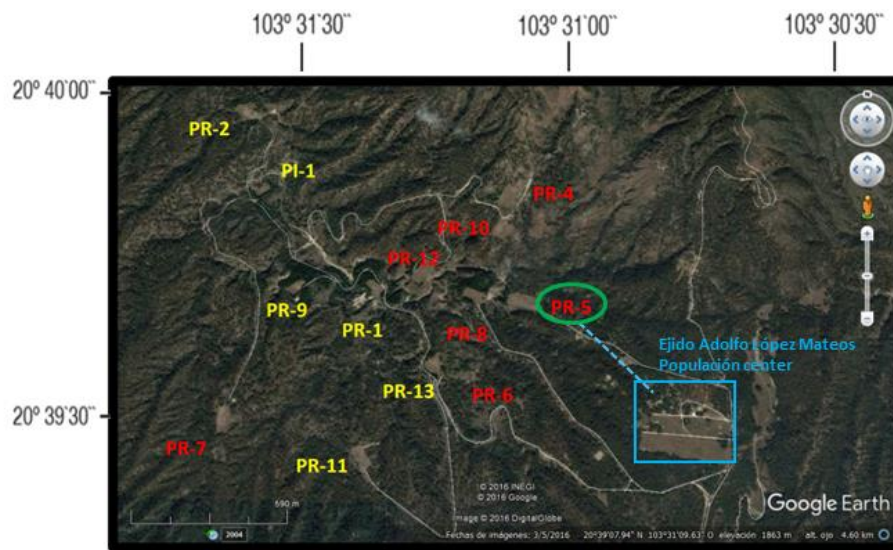


Figure 1. Location of platforms and wells within the Cerritos Colorado geothermal field in “La primavera” (image edited from google earth)

2.1 Statement of the problem and need for the study.

The location “Ejido Adolfo López Mateos” is within the La Primavera Forest (Figure 2), in the municipality of Zapopan, with coordinates of latitude 20.65 and longitude -103.512. It has 1,500 hectares with 94 settlers, of which only around 30 partially live in the ejido, there is no electricity within the ejido, and hence they do not have refrigeration systems. On the other hand, those with the economic capacity have a power plant, or gas refrigerator, and some brick ovens (cement coolers). Among the productive activities are pig farming, planting of corn, lemon orchards, avocado, and dairy cattle.

The lack of means to preserve the milk was identified. There were 90 dairy cows which were mostly sold due to a lack of refrigeration systems.

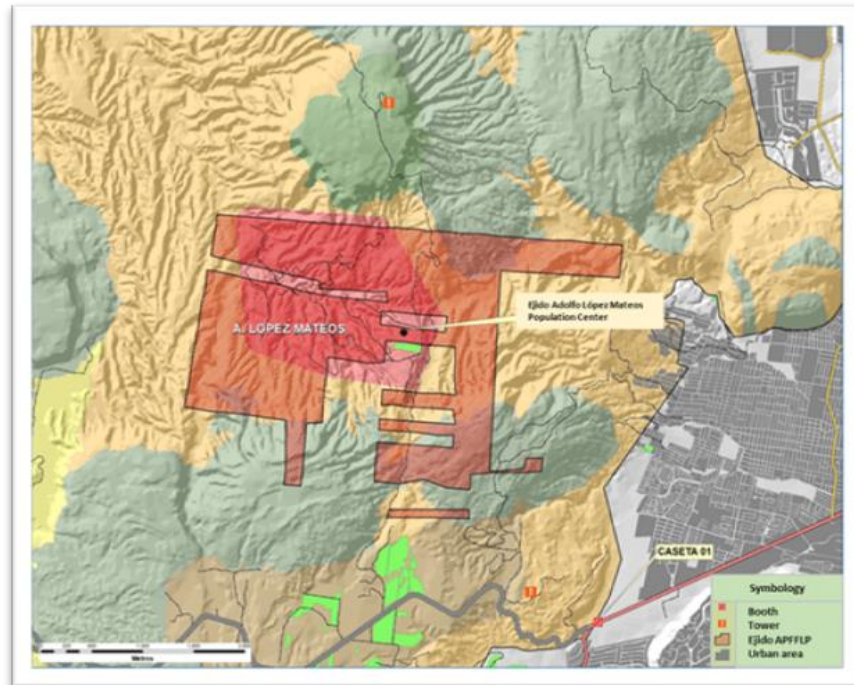


Figure 2. Location of the “Ejido Adolfo López Mateos” (Image modified, provided by the Decentralized Public Organization Bosque de la Primavera)

Once the needs of the place have been identified, a warehouse (cold room) is proposed to conserve milk at 10°C, based on an absorption refrigeration system with geothermal energy supplied from the nearest geothermal well. This corresponds to well PR5 with an approximate distance of 600 meters from the ejido (Figure 1), with the objective that the inhabitants can resume this productive activity.

2.2 Conditions for milk storage

The temperature of freshly milked milk is 37°C. The frequency with which the milk is collected, and its amount determine the necessary heat load to be removed to keep the milk at the desired temperature. When the collection is done twice a day, the milk must be cooled within two hours of milking to a temperature below 15°C. If the collection takes place only once a day, the refrigeration and storage temperature must be close to 10°C. Lastly, if the collection is carried out every 48 hours, the milk should be kept at around 4°C [5]. In the location, milk will be collected once a day, so the design temperature for the cold store was established at 10°C.

To keep the milk at that temperature, it is necessary to calculate the refrigeration cooling load and to determine the heat transfer rate necessary to remove the heat from a space to lower its temperature to the desired value. The cooling or refrigeration load is calculated with equation 1

[26]; where: M_d corresponds to the maximum reception per day (kg/day), C_p to the specific heat of the product (J/kg°C), T_1 is the entry temperature of the product (milking temperature = 37°C) and T_2 the storage temperature (10°C).

$$Q_R = M_d * C_p * (T_1 - T_2) \quad (1)$$

3. Warehouse description

This section describes the warehouse design, including materials, the construction budget, and the calculation of thermal loads.

Based on the information provided by the community inhabitants, a dairy cow needs 1 hectare for grazing. The ejido has 1,500 hectares; therefore, the maximum production would be 150 cows. Each cow produces around 20-25 liters a day in two milkings. Thus, there would be a maximum production of 3750 liters/day with 150 cows. With this information, the necessary storage capacity was calculated, considering the maximum milk production, and it was concluded that 20 containers of 200 liters each one would be needed for total storage. Then, the warehouse was dimensioned based on the arrangement of the drums inside the warehouse, considering an additional 10%. The measures proposed for the warehouse design are 3.6m*5m*2.3m. (Figure 3).

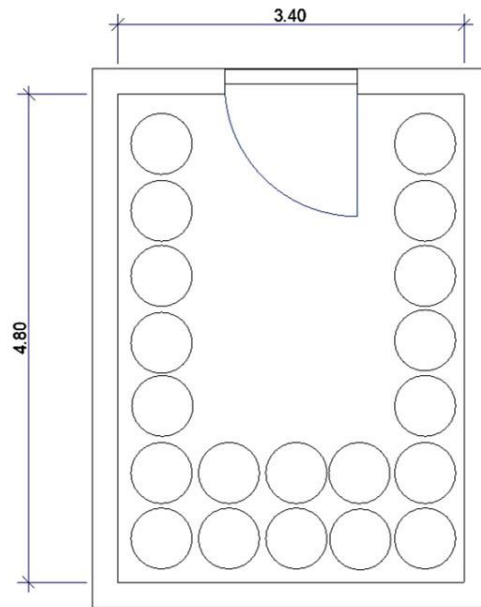


Figure 3. Plan layout of the warehouse for milk conservation.

The materials proposed for the construction of the warehouse are:

- Concrete floor of 10 cm.
- Brick walls with polystyrene plate (as insulation) and galvanized sheet.
- Lightened roof with partition.

Next, the detailed design and engineering of the milking warehouse is presented, which was modeled using ArchiCad:

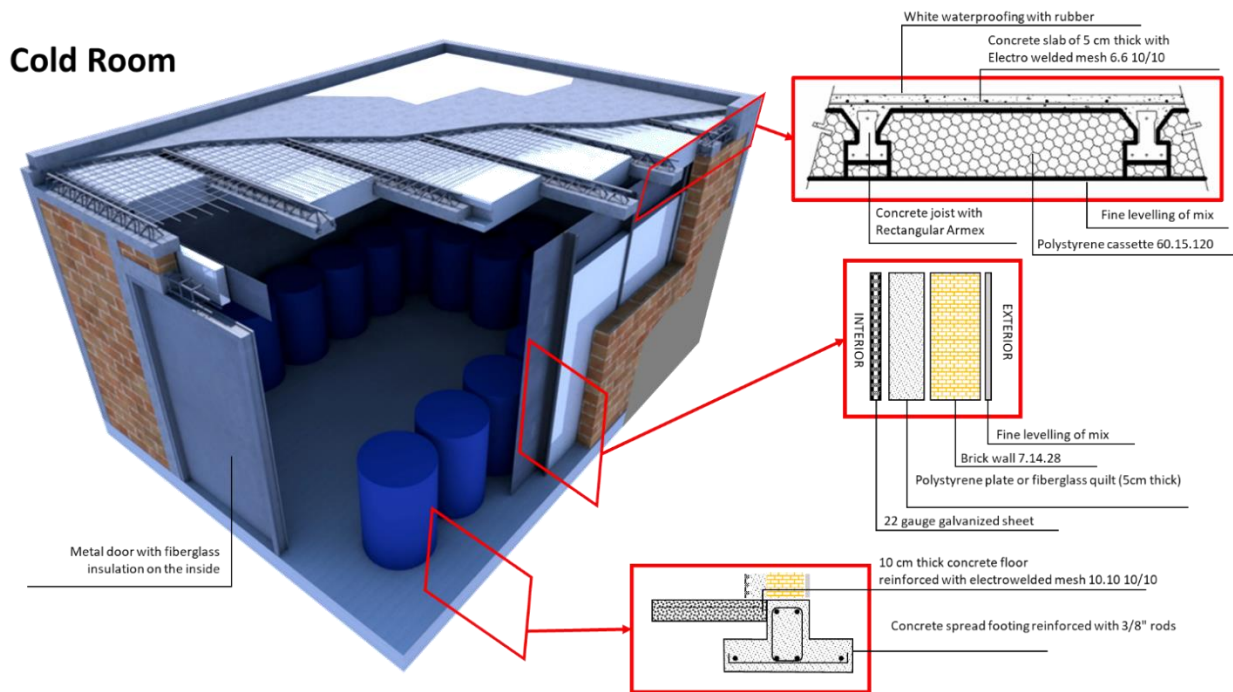


Figure 4. Detailed model of the milk storage warehouse

Once the sizing and construction design was conducted, the budget for the unit and the total price was obtained for the warehouse construction based on local prices.

4. Calculation of the thermal loads of the warehouse

Once the warehouse was designed, the total thermal loads (sensible and latent) were calculated monthly to compare their behavior at different periods of the year. The climatological data for this model were obtained from the Climate.OneBuilding.Org database from the closest meteorological station to the study area: the Zapopan-766015 station.

Thermal loads consist of the amount of heat that must be removed from the space to be cooled during a given period. It depends on two main factors: heat leakage or heat transfer load and heat

use or service load [13]. The following thermal loads have been considered in the design of this warehouse: loads through ceilings and walls, lighting loads, infiltration loads, and occupation loads.

The modeling of the construction system was carried out in the Sketchup and OpenEstudio software, in which the design characteristics are loaded, such as dimensions, type of materials, thickness, quantity and type of luminaires, number of people, the activity to be carried out, machinery or equipment to be used, window characteristics if applicable, etc. With this information, the total thermal loads were calculated in the EnergyPlus software (equation 2).

$$\dot{Q}_{\text{load}} = \sum_{i=1}^{N_{\text{sl}}} \dot{Q}_i + \sum_{i=1}^{N_{\text{surfaces}}} h_i A_i (T_{s_i} - T_Z) + \sum_{i=1}^{N_{\text{surfaces}}} \dot{m}_i C_P (T_{z_i} - T_Z) + \dot{m}_{\text{inf}} C_P (T_{\infty} - T_Z) \quad (2)$$

Where: $\sum_{i=1}^{N_{\text{sl}}} \dot{Q}_i$ is the sum of the internal convective loads,

$\sum_{i=1}^{N_{\text{surfaces}}} h_i A_i (T_{s_i} - T_Z)$ is the heat transfer by convection from the surfaces,

$\dot{m}_{\text{inf}} C_P (T_{\infty} - T_Z)$ is heat transfer due to infiltration of outside air

$\sum_{i=1}^{N_{\text{surfaces}}} \dot{m}_i C_P (T_{z_i} - T_Z) + \dot{m}_{\text{inf}} C_P (T_{\infty} - T_Z)$ transfer of heat due to air mixing between zones,

T_Z corresponds to the desired zone temperature.

The EnergyPlus program performs an integrated simulation of program modules working together to calculate the energy required to heat and cool a building using various energy sources and systems. This means that the three main parts, building, system, and equipment, must be solved simultaneously. It does this by simulating the building and associated energy systems when they are exposed to different environmental and operating conditions. The core of the simulation is a model of the building that is based on the fundamental principles of heat balance. EnergyPlus provides three different solution algorithms to solve the energy and humidity balance equations of the air (*ZoneAirHeatBalanceAlgorithm*): *3rdOrderBackwardDifference*, *EulerMethod*, and *AnalyticalSolution*. The first two methods use the finite difference approximation, while the third uses an analytical solution.

EnergyPlus takes advantage of the climatological database to determine the amount of energy entering or leaving the storage room as a function of the temperature of the air in the zone. Thus, the net charge of the area is given by equation (2). A detailed description of how the software calculates thermal loads is presented in the Engineering Reference manual, 2022 [27].

5. Sizing of the absorption equipment

This section describes in detail the dimensioning of the absorption system, which includes the determination of the design conditions of each system (simple and double). The average logarithmic temperatures are used to obtain the cost of the absorption equipment.

For the supply of cold to the warehouse, and thus keep the milk at the desired temperature, it is necessary to dimension the capacity of the refrigeration system and model it under specific design conditions. The single-effect water/LiBr refrigeration system consists of two circuits: a refrigerant circuit consisting of a condenser, an expansion valve, and an evaporator, and a solution circuit consisting of a generator, an absorber, a heat exchanger solution heat, a pump, and a valve. A double-effect system, in addition to these components, has a second generator-condenser, which works as a generator in one stage and as a condenser in another, which operates at higher pressure and temperature, and has a second solution heat exchanger. A detailed description of the teams is given in [28].

The following table shows the design conditions proposed for the single and double-effect systems.

Table 1: Design conditions

Component	Single effect	Doble effect
Evaporator	4 °C	4°C
Condenser	35°C	35°C
Absorber	35°C	35°C
Generator	80° C	164°C
Condenser-generator	-	105°C
COP	0.85	1.38
HX efficiency	0.8	0.8

A condensation temperature (T_C) of 35°C was chosen considering a ΔT of 7°C with respect to the ambient temperature T_{amb} . This was established based on the histogram of T_{amb} records, which determined that 95% of the year, there are T_{amb} less than or equal to 28 ° C (Figure 5).

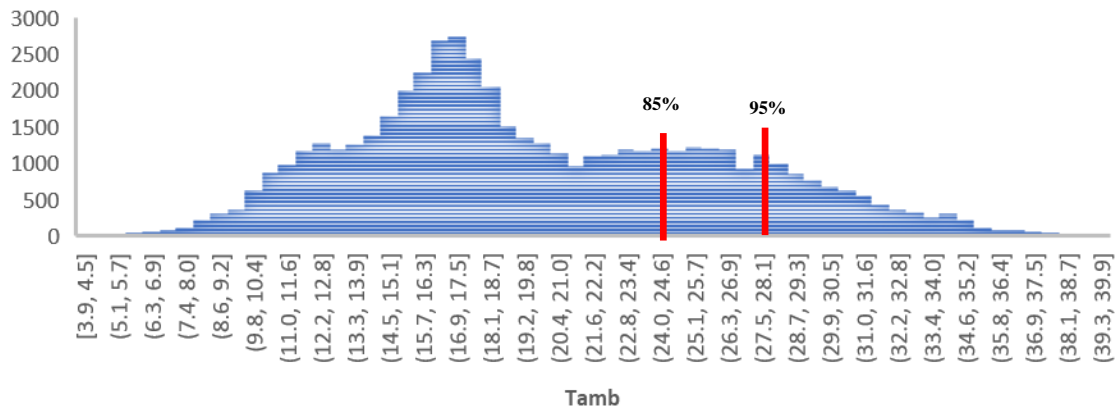


Figure 5. Histogram of the ambient temperature of the study area

The evaporation temperature (T_E) of 4°C was established based on the thermal requirements for milk storage at 10°C , considering a ΔT of 6°C .

The temperature supplied to the generator (T_G) for the simple-effect system was chosen as the minimum value with which this system can operate (80°C), based on the established considerations. Besides being the most optimal value, as shown in Figure 6, with an increase to a maximum of 120°C in the T_G , the COP value increases only 0.5, that is, with a ΔT of 40°C the increase in COP is minimal so it is not affordable to use a higher generation temperature.

In the case of the double effect system, the minimum operating temperature is not the most optimal temperature. As can be seen in Figure 6, the COP values show a significant change in slope as the T_G increases, unlike the simple effect system that showed an almost linear trend. Based on this, a T_G of 163°C was chosen, in which this change in the slope of the COP is observed.

Together with these temperature values, favorable COPs are achieved based on simulations carried out in [28,29]

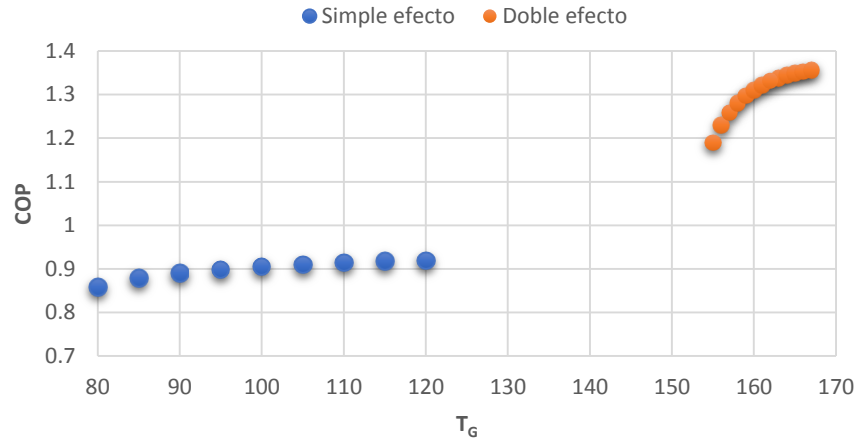


Figure 6. Coefficient of performance as a function of T_G

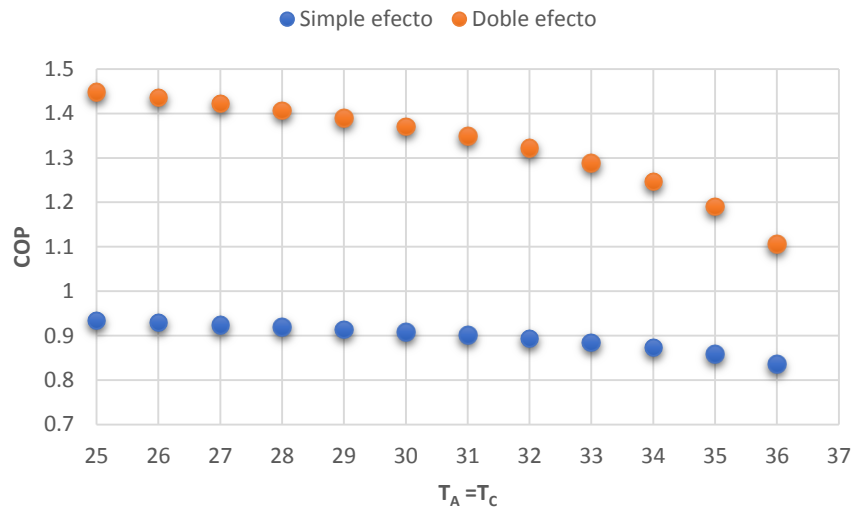


Figure 7. Coefficient of performance as a function of T_C

As can be seen in Figure 7, if a condensation temperature lower than 35°C is considered, for example, 31°C, the system would have an increase in performance (COP); however, it could only operate 85% of the year (Figure 5). From this, a $T_A = T_C$ of 35°C was established, even though the performance slightly decreased. It is a value with which it is possible to operate most of the year practically, being the most useful characteristic in practice.

Once the design conditions were established, the thermal loads per component were calculated with the energy balances in the EES (Engineering Equation Solver) software. Appendix A shows the corresponding energy balances for each of the components of the absorption system.

Subsequently, the logarithmic mean temperature difference (ΔT_{ML}) was obtained. This parameter is used to determine the heat loads in the components helping to size equipment and cost estimation.

The average logarithmic temperatures are calculated with equation (3), except for the evaporator, since the cold and hot currents remain constant at the inlet and outlet.

$$\Delta TML = \frac{\Delta T_1 - \Delta T_2}{\ln(\Delta T_1 / \Delta T_2)} \quad (3)$$

with: $\Delta T_1 = T_{c,ent} - T_{f,sal}$ y $\Delta T_2 = T_{c,sal} - T_{f,ent}$

6. Economic analysis of the absorption system

Mathematical correlations proposed in [30] were used to determine the cost of the absorption equipment based on the thermal loads and the ΔTML of each component. These correlations are presented in Equations 4-11.

Generator cost:
$$Z_G = 309.14 \left[\frac{Q_G}{0.2\Delta T_G} \right]^{0.85} \quad (4)$$

Condenser cost:
$$Z_C = 516.62 \left[\frac{Q_C}{0.15\Delta T_C} \right] \quad (5)$$

Evaporator cost:
$$Z_E = 309.14 \left[\frac{Q_E}{0.2\Delta T_E} \right]^{0.85} \quad (6)$$

Absorber cost:
$$Z_A = 516.62 \left[\frac{Q_A}{0.2\Delta T_A} \right] \quad (7)$$

Pump cost:
$$Z_P = 1120[\dot{W}_P]^{0.80} \quad (8)$$

Solution heat exchanger cost
$$Z_{EC} = 12500 \left[\frac{A_{shx}}{100} \right]^{0.60} \quad (9)$$

Valve cost
$$Z_V = 114.5[\dot{m}_v] \quad (10)$$

Total cost
$$Z_{Total} = Z_{componentes} \quad (11)$$

A more detailed economic analysis includes determining various parameters to have an overview of the investment and the capital recovery time compared to other systems. These parameters are presented in Table 2.

Table 2. Economic analysis equations

Capital recovery factor	$CRF = \frac{i(1+i)^n}{(1+i)^n - 1} \quad (12)$
sinking fund factor	$SFF = \frac{i}{(1+i)^n - 1} \quad (13)$
Annual capital cost	$ACC = Z_{Total} \times CRF \quad (14)$
Salvage value	$SV = 0.20 \times Z_{Total} \quad (15)$
Annual salvage value	$ASV = SV \times (SFF) \quad (16)$
Maintenance cost	$CM = ACC \times 0.1 \quad (17)$

The system's operating time was established at 24 hours a day, with a lifetime of the equipment of 10 years. The Interbank interest rate was 8.50% based on the latest update from the Bank of Mexico. For the comparison of costs and capital recovery time, actual quotes were obtained from specialized suppliers.

7. Results and Discussion

7.1. Milk storage

The result of calculating the refrigeration load necessary to keep the milk at the desired temperature based on equation (1) is presented.

$$Q_R = 4.65 \text{ kW}$$

Considering a safety factor of 10%, a refrigeration load of 5.11 kW is required, equivalent to 1.45 tons of refrigeration.

7.2. Warehouse analysis

7.2.1. Calculation of thermal loads in the warehouse

Figure 8 shows the monthly thermal loads calculated in Energyplus.

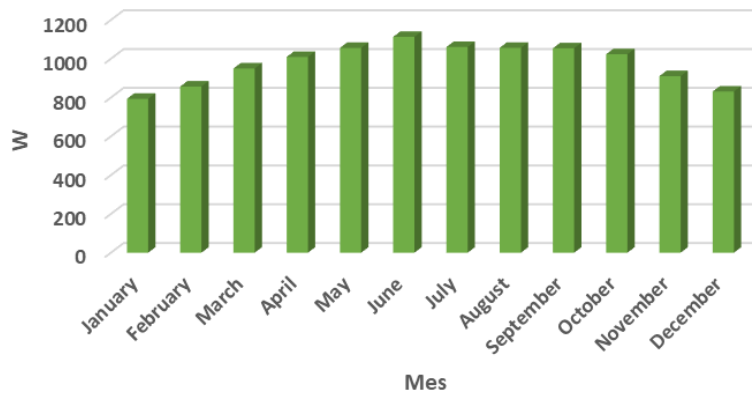


Figure 8. Monthly thermal load

As can be seen, the highest values occur in the months of May to September, when the ambient temperature is higher. Therefore, removing more heat from the outside is necessary to preserve the product at the desired conditions. The thermal load values range between 0.94 and 1.1 kW.

7.2.2. Sizing of the absorption equipment

The ΔTML values for each component are shown in Table 3 for the single-acting system and in Table 4 for the double-acting system, based on their respective diagrams shown in Figures 9 and 10.

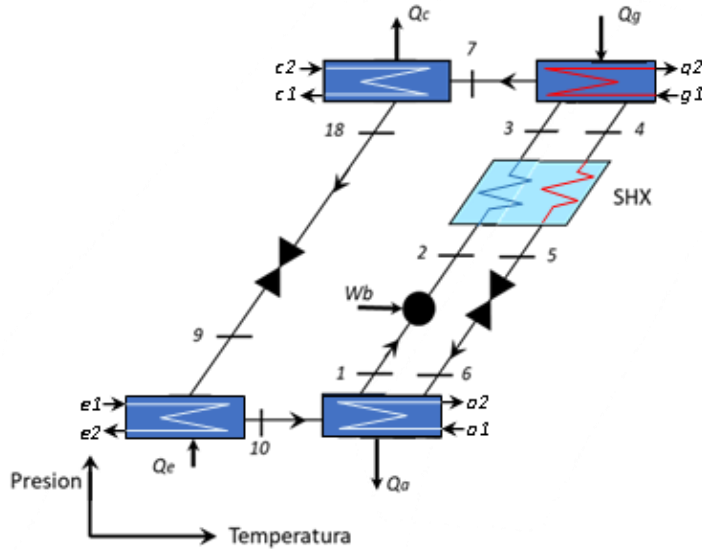


Figure 9. Single-effect system

Table 3. Loads by component and ΔTML for the simple-effect system

Component	Q (kW)	punto	Temperature °C	ΔTML °C
Condenser	8.48	8	80	24.5
		9	35	
		c1	26	
		c2	28	
Absorber	8.83	1	4	10.3
		2	35	
		7	43.8	
		a1	26	
		a2	28	
Generator	9.31	8	80	9.7
		4	70.5	
		5	80	
		g1	90	
		g2	87	
Evaporator	8	10	4	6.0
		1	4	
		e1	10	
		e2	10	
Heat exchanger	4	3	35	9.2
		4	70.5	
		5	80	
		6	44	

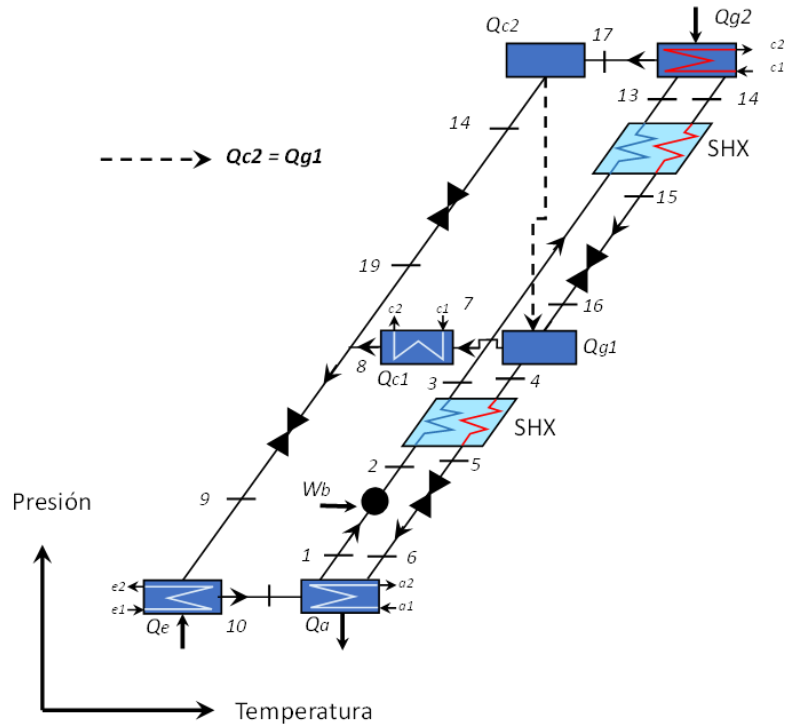


Figure 10. Double effect system

Table 4. Loads per component and ΔTML for the double effect system.

Componente	Q (Kw)	punto	Temperatura °C	ΔTML °C
Condenser 2	4.8	17	163	37.9
		18	105	
Generator 1	4.8	16	80.4	37.9
		7	91.7	
Generator 1	4.8	4	91.7	37.9
		3	91.7	
Condenser 1	4.1	7	91.7	28.0
		8	35	
		c2	28	
		c1	26	
Absorber	9.8	10	4	14.8
		1	35	
		6	54.6	
		a2	28	
		a1	26	
Generator 2	5.98	17	163	13.9
		13	146.5	
		14	163	

		g1	173	
		g2	170	
Evaporator	8	9	4	6.0
		10	4	
		e1	10	
		e2	10	
Heat exchanger 1	2.3	2	35	11.3
		3	80.4	
		4	91.7	
		5	46.4	
Heat exchanger 2	2.3	3	80.35	16.5
		13	146.5	
		14	163	
		15	96.9	

For both systems, the highest values of ΔT_{ML} are obtained for the condenser, where more heat is transferred.

7.2.3. Economic analysis of the absorption system

Below, the results of the economic analysis of the warehouse construction and the absorption refrigeration cost based on the mathematical correlations are presented. Also, it is shown the comparison of the proposed systems against a conventional compression system driven with solar panels.

Table 5 shows the budget for the construction of the warehouse (cold room), including materials and labor, based on local prices.

Cold Room Budget					
	Item	U	Amount	PU	Subtotal
1	Excavation, fine-tuning, and compaction of a trench for continuous cementation	ml.	17	\$15.00	\$255.00
2	Construction of continuous cementation based on: Concrete footing of 60 x 15 cm with 3/8" rods and a 15 x 15 cm footing with 3/8" rods.	ml.	17	\$45.00	\$765.00
3	10 cm concrete floor reinforced with 10.10 10/10 electro-welded mesh.	m2	17.5	\$12.50	\$218.75
4	Red annealed partition wall (7.14.28), grouted with a mixture of cement, lime, and sand.	m2	36.55	\$22.50	\$822.38
5	Concrete castle with Armex 15.15cm	ml.	19.35	\$14.00	\$270.90
6	Button and top concrete beam 15.15 cm	ml.	34	\$15.50	\$527.00

7	Lightened slab: Concrete reticule with 3/8" rebar and wire rod stirrups, with 20 cm cant plus 5 cm thick compression slab with 6.6 10/10 electro-welded mesh (slope total cant 25 cm)	m2	17.5	\$75.00	\$1,312.50
8	Exterior and soffit plastering of a fine mix	m2	54.05	\$11.00	\$594.55
9	Insulation system based on: Galvanized profile, fiberglass quilt (5cm), and 22 gauge galvanized sheet.	m2	36.55	\$50.00	\$1,827.50
10	Waterproofing with white rubber	m2	17.5	\$7.50	\$131.25
11	Iron door with counter frame and glass fiber insulation on the inside	.	1	\$250.00	\$250.00
12	solvent-based enamel white paint on exterior walls	m2	36.55	\$7.50	\$274.13
Total					\$7,248.95

From equations 4-11, the cost per component for the two systems was obtained. As shown in Table 6, the total cost of the double-effect system is higher than the single-effect system as it has additional components; however, it has better performance, as can be observed in Figure 7.

Table 6. Cost of absorption refrigeration equipment by component

Component	Costo (USD)	
	Simple-effect	Double-effect
Generator	1169.2	594.5
Condenser	1191.4	505
Evaporator	1550.5	1550.5
Absorber	2942.1	2285
Valves	5.3	13.6
Pump	10.6	10.45
Heat exchangers	57.9	41.6
Generator-condenser	NA	645.1
Total	6926.9	7931
Total with 10%	7619.6	8724.1

The following table shows some of the most used parameters for the economic project analysis, considering the annual interest as well as the lifetime of the system. With this, annual values can be determined and an estimate of the maintenance cost and buffering at the project end.

Table 7. Parameters for economic analysis

	Simple-effect	Double-effect
Capital recovery factor	0.15	0.15
sinking fund factor	0.07	0.07

Annual capital cost (\$USD)	1161.3	1329.7
Maintenance cost (\$USD)	116.1	133
Salvage value (\$USD)	1524	1744.8
Annual salvage value (\$USD)	102.8	117.6
Annual total cost (\$USD)	1174.8	1345

Finally, a comparison between the proposed absorption system with a conventional system and against a solar system is presented.

Table 8. Comparison of costs of refrigeration systems

System	Cost (USD)	Annual electricity cost (USD)	Annual maintenance cost (USD)	Pipe cost (USD)	Total cost (USD)
Simple effect	\$7,619.6	N/A	\$109.49	\$5,354	\$13,083
Double effect	\$8,724.00	N/A	\$133	\$9,287	\$18,144.
Conventional	\$10,091	\$2,916	\$201.00	N/A	\$13,208
Solar	\$101,987	N/A	\$678	N/A	\$102,665

Concerning the total cost, as a first investment, the simple-effect absorption system and the conventional system have a similar cost. However, the absorption system has the advantage that it will not generate an annual cost of electricity consumption, so at the end of the lifetime of 10 years, both absorption systems will represent significant savings, as shown in Table 9. The increase in the cost of the double-effect system, in contrast to the simple-effect, is reflected in the piping since, by requiring higher temperatures, the cost of specialized piping is higher. In the case of a solar system, the investment is too high, so this system for this case study is not competitive. These costs may vary according to inflation and suppliers.

Table 9. Savings of absorption systems

Sistema	Savings at 10 years (USD)	
	Simple-effect	Double-effect
conventional	\$27,192.48	\$21,920.00
solar	\$94,693.48	\$89,421.00

8. Conclusions

The design and economic analysis of an H₂O/LiBr absorption refrigeration system for milk conservation at 10°C were conducted in Mexico using a geothermal heat source obtained from

a well. The analysis of a simple effect and double effect system is presented to select the most suitable from its comparison.

For the design of the proposed warehouse, a refrigeration load of 5 kW is needed (1.45 tons of refrigeration) with a geothermal heat source of 80°C for the simple-effect system and 163°C for the double-effect system.

In the design of this warehouse, the following were calculated: loads through roofs, walls, lighting loads, infiltration loads, and occupation loads. The highest values in thermal loads occur in the months of May to September, when the ambient temperature is higher. Therefore, it is necessary to remove more heat from the outside to preserve the product at the desired conditions. The thermal load values range between .094 and 1.1 kW.

The single-effect system achieves a COP of 0.85 at 10°C, at a total cost of approximately \$13,083 USD, while the double-effect system reaches a COP of 1.38 at the cost of \$18,144 USD. Although the cost of the double-effect system was around 27% higher than the single-effect system, also achieved a 61% increase in the COP.

The solar system offers no advantage against the proposed absorption systems.

The heat exchanger size influences the costs for each component in the case of the absorption system. For example, if geothermal energy is used, the distance from the well to the place of application, since the cost of the pipe necessary to transport the fluid is derived from this.

Nomenclature

A= area

COP= coefficient of performance

C_p= specific heat

m= mass flow

h= enthalpy

M_d= maximum reception per day

Q= heat load

Q_R = cooling refrigeration load

T = temperature

T₁= temperature of the product

T₂ = storage temperature

T_{G,I}=temperature supplied to the generator

T_z = desired zone temperature

W= work

Subscript

A= absorber

amb = environmental

p=pump

c= condenser

e= evaporator

g= generator

inf= infiltration

s = surface
 SHX = Heat exchangers

Greek

ε = Effectiveness

Apéndice A

Table A1. Energy balances for each one of the components of the single-effect absorption cooling system.

Component	Balances
Generator	$Q_g = \dot{m}_4 h_4 + \dot{m}_7 h_7 - \dot{m}_3 h_3$
Condenser	$Q_c = \dot{m}_7 (h_7 - h_8)$
Evaporator	$Q_e = \dot{m}_{10} (h_{10} - h_9)$
Absorber	$Q_a = \dot{m}_{10} h_{10} + \dot{m}_6 h_6 - \dot{m}_1 h_1$
Effectiveness of the SHE	$\varepsilon_{SHE} = \frac{h_3 - h_2}{h_4 - h_2}$
Pump Work	$W_p = v_1 (P_8 - P_{10})$
<i>COP</i>	$COP = \frac{Q_e}{Q_g + W_b}$

Table A2. Energy balances for each one of the components of the double-effect absorption cooling system.

Component	Balances
Generator	$Q_{g2} = \dot{m}_{14} h_{14} + \dot{m}_{17} h_{17} - \dot{m}_3 h_3$
Condenser	$Q_{c1} = \dot{m}_7 h_7 - \dot{m}_8 h_8$
Generator-Condenser	$Q_{g1} = \dot{m}_7 h_7 + \dot{m}_4 h_4 - \dot{m}_{16} h_{16}$ $Q_{c2} = \dot{m}_{17} h_{17} - \dot{m}_{18} h_{18}$
Evaporator	$Q_e = \dot{m}_{10} (h_{10} - h_9)$
Absorber	$Q_a = \dot{m}_6 h_6 + \dot{m}_{10} h_{10} - \dot{m}_1 h_1$
Effectiveness of the SHE	$\varepsilon_{SHX} = \frac{h_3 - h_2}{h_4 - h_2}$ $\varepsilon_{SHX} = \frac{h_{13} - h_3}{h_{14} - h_3}$
Pump Work	$W_p = v_1 (P_2 - P_1)$
<i>COP</i>	$COP = \frac{Q_e}{Q_{g2} + W_b}$

References

- [1] M.D. Mastrandrea, S.H., Schneider, Resource Letter GW-2: Global Warming, , Am. J. Phys.76, 608-614. (2008).
- [2] L. Iannelli, S. Gil, Acondicionamiento térmico de aire usando energía geotérmica-ondas de calor, Am. J. Phys. Educ. 6 (2012). <http://www.lajpe.org>.
- [3] Food and Agriculture Organization., Food wastage footprint Impacts on natural resources. 2013 , [Www.Fao.Org/Publications](http://www.Fao.Org/Publications). (2013).
- [4] Food and Agriculture Organization., Agroindustry Policy Brief: developing the cold chain in the agrifood sector in sub-Saharan Africa., 2016.
- [5] Hernandez Benedi, La refrigeracion de la leche, n.d.
- [6] J.† Valle-Hernandez, R.-A. Nieto-Peña, A.Y. Morales-Ortega, E. Enrique, Análisis energético de un sistema de refrigeración solar por absorción, 4 (2017) 58–65. www.ecorfan.org/bolivia.
- [7] R. Best, W. Rivera, A review of thermal cooling systems, Appl Therm Eng. 75 (2015) 1162–1175. <https://doi.org/10.1016/j.applthermaleng.2014.08.018>.
- [8] B. Breindel, R.L. Harris, G.K. Olson, Geothermal absorption refrigeration for food processing industries, in: 1979.
- [9] R. Best, C.L. Heard, H. Fernández, J. Siqueiros, Developments in geothermal energy in Mexico—Part five: The commissioning of an ammonia/water absorption cooler operating on low enthalpy geothermal energy, Journal of Heat Recovery Systems. 6 (1986) 209–216. [https://doi.org/10.1016/0198-7593\(86\)90004-4](https://doi.org/10.1016/0198-7593(86)90004-4).
- [10] A. Keçeciler, H.İ. Acar, A. Doğan, Thermodynamic analysis of the absorption refrigeration system with geothermal energy: an experimental study, Energy Convers Manag. 41 (2000) 37–48. [https://doi.org/10.1016/S0196-8904\(99\)00091-6](https://doi.org/10.1016/S0196-8904(99)00091-6).
- [11] J.C. Ábrego Castillo, Cost estimation of using an absorption refrigeration system with geothermal energy for industrial applications in el Salvador, (2007).
- [12] Isaza C., Isaac Pilatowsky, Rosemberg J. Romero, Farid B. Cortés, Análisis termodinámico de un sistema de refrigeración solar por absorción usando soluciones de monometilamina - agua para la conservación de alimentos, (2010).
- [13] J. Uwera, R. Itoi, S. Jalilinasrabad, T. Jóhannesson, D.Ö. Benediktsson, Design of a cooling system using geothermal energy for storage of agricultural products with emphasis on Irish potatoes in Rwanda, Africa, Transactions - Geothermal Resources Council. 39 (2015) 157–164.
- [14] J. Yepez, F. Ramos, Diseño y construcción de un sistema de refrigeración por absorción intermitente empleando energía solar para la Universidad De Córdoba Facultad De Ingeniería Ingeniería Mecánica , 2015.
- [15] R.K. De, A. Ganguly, Performance comparison of solar-driven single and double-effect LiBr-water vapor absorption system based cold storage, Thermal Science and Engineering Progress. 17 (2020) 100488. <https://doi.org/10.1016/J.TSEP.2020.100488>.
- [16] M. el Haj Assad, M. Sadeghzadeh, M.H. Ahmadi, M. Al-Shabi, M. Albawab, A. Anvari-Moghaddam, E. Bani Hani, Space cooling using geothermal single-effect water/lithium bromide absorption chiller, Energy Sci Eng. 9 (2021) 1747–1760. <https://doi.org/10.1002/ese3.946>.
- [17] B. Ozcan, I.E. Aykurt, M. Akpak, T. Tacer, N. Yildirim, A. Hepbasli, H.G. Ozcan, Thermodynamic analysis and assessment of a geothermal cooling system for a house,

- International Journal of Exergy. 29 (2019) 350–369.
<https://doi.org/10.1504/IJEX.2019.100370>.
- [18] S.E. Sofyan, M. Farhan, Khairil, Jalaluddin, Akram, Theoretical Study of the Absorption Refrigeration Cycle Using Water-Lithium Bromide as Working Pair for Cold Storage Application, IOP Conf Ser Mater Sci Eng. 796 (2020) 012015.
<https://doi.org/10.1088/1757-899X/796/1/012015>.
- [19] J.C. Jiménez-García, W. Rivera, Parametric analysis on the experimental performance of an ammonia/water absorption cooling system built with plate heat exchangers, Appl Therm Eng. 148 (2019) 87–95.
<https://doi.org/10.1016/J.APPLTHERMALENG.2018.11.040>.
- [20] M. Sadi, A. Arabkoohsar, A.K. Joshi, Techno-economic optimization and improvement of combined solar-powered cooling system for storage of agricultural products, Sustainable Energy Technologies and Assessments. 45 (2021) 101057.
<https://doi.org/10.1016/J.SETA.2021.101057>.
- [21] A. Sur, R.P. Sah, S. Pandya, Milk storage system for remote areas using solar thermal energy and adsorption cooling, Mater Today Proc. 28 (2020) 1764–1770.
<https://doi.org/10.1016/J.MATPR.2020.05.170>.
- [22] I. Pilatowsky, W. Rivera, J.R. Romero, Performance evaluation of a monomethylamine–water solar absorption refrigeration system for milk cooling purposes, Appl Therm Eng. 24 (2004) 1103–1115. [https://doi.org/10.1016/S1359-4311\(03\)00087-5](https://doi.org/10.1016/S1359-4311(03)00087-5).
- [23] Gutierrez-Negrin L.C., The La Primavera, Jalisco, México, Geothermal Field, Geothermal Resources Council. 2 (1988) 35–38.
- [24] G.A. Mahood, Geological evolution of a pleistocene rhyolitic center — Sierra La Primavera, Jalisco, México, Journal of Volcanology and Geothermal Research. 8 (1980) 199–230. [https://doi.org/10.1016/0377-0273\(80\)90105-5](https://doi.org/10.1016/0377-0273(80)90105-5).
- [25] P. Kruegfl, A. Aragon, R. Maciel, C. Residencia, G.C. Lucio, J. Villa, Preproduction simulation of thermal decline atlaprimaverafirst5-mwellheadunits abstract, Geothermal Resources Council, TRANSACTIONS. 12 (1988).
- [26] Eduardo. Hernández Goribar, Fundamentos de aire acondicionado y refrigeracion, Editorial Limusa, 1973.
- [27] Department of Energy U.S., EnergyPlus™ Documentation Engineering Reference , (2022).
- [28] J. Saucedo-Velázquez, G.G. Urueta, J.A. Wong-Loya, R. Molina-Rodea, W. Rivera, Cooling Potential for Single and Advanced Absorption Cooling Systems in a Geothermal Field in Mexico, Processes. (2022). <https://doi.org/10.3390/pr10030583>.
- [29] J.I. Saucedo-Velázquez, W.R.G. Franco, E. Gómez-Arias, G.G. Urueta, Evaluation of the cooling potential for a single effect absorption cooling system in the PR2 well of Cerritos Colorados geothermal field, Mexico, Energy Exploration and Exploitation. 38 (2020) 2521–2540. <https://doi.org/10.1177/0144598720927458>.
- [30] R. Shankar, W. Rivera, Analysis of an integrated thermal separation and flashing cooling cogeneration cycle, Appl Therm Eng. 190 (2021).
<https://doi.org/10.1016/j.applthermaleng.2021.116773>.

Declaration of interests

The authors declare that they have no known competing financial interests or personal relationships that could have appeared to influence the work reported in this paper.

The authors declare the following financial interests/personal relationships which may be considered as potential competing interests:

Conclusiones

En esta tesis doctoral se evaluó el potencial de utilización y viabilidad de sistemas de enfriamiento por absorción operando con energía geotérmica en una localidad en México. El estudio se llevó a cabo usando datos reales del pozo PR2 Y PR5 del campo geotérmico Cerritos Colorados en el bosque de “La primavera”, Jalisco.

A continuación, se presenta un resumen de las principales conclusiones de esta tesis.

Con respecto a la simulación del potencial de enfriamiento para un sistema de simple efecto:

- Las simulaciones, desarrolladas en el software EES, permitieron analizar la influencia que tienen las temperaturas de entrada de los distintos componentes sobre el rendimiento (COP) y el potencial de enfriamiento de los sistemas. Se observó que cuando la temperatura ambiente es mayor (en primavera y verano), y por ende la T_{AC} , se produce una disminución del potencial y del COP. Se evaluaron temperaturas de evaporación (T_E) de 6°, 8°, 10° y 12°C para un rango de temperatura de generación (T_G) de 77-110°C. La profundidad requerida para la mínima recuperación de calor a 77° C se obtiene a 260 m en primavera, 270 m en verano, 290 m en otoño y 310 m en invierno. Para el caso de la temperatura máxima de 110° C, las profundidades son 590 m en primavera, 600 m en verano, 620 m y 640 m, en otoño e invierno respectivamente.
- Para una temperatura de generación fija, se podría obtener un potencial de enfriamiento máximo de 71 594 GW, 70 649 GW, 71 164 GW, 70 859 GW en invierno, primavera, verano y otoño con una T_E de 12°. Los valores de potencial de enfriamiento son de gran magnitud debido a que en los cálculos se considera un área de 2km² que abarca todo el yacimiento.

Con base a la evaluación de sistemas avanzados de absorción:

- El pozo analizado puede alcanzar temperaturas de 59° C a 190° C, dependiendo de la profundidad del tubo en U y el espesor del aislamiento.
- A una $T_E = 8^\circ\text{C}$, el rango de temperaturas de funcionamiento fue de 59-80°C para el medio efecto, de 77°-110 °C para el simple efecto; 135-162°C para el doble efecto y de 180-187°C para el triple efecto.
- El máximo potencial de refrigeración fue de 99,334 GW el cual se obtuvo con el sistema de doble efecto, seguido de 92,995 GW con el sistema de triple efecto, 70,939 GW con el sistema de simple efecto y 38,721 GW con el sistema de medio efecto.
- El rango de los COP para los cuatro sistemas fue: 0.43–0.49 para el de medio efecto, de 0.89–0.97 para simple efecto, de 1.27–1.47 para doble efecto y 1.78–1.95 para el sistema de triple efecto.
- Los valores máximos de los COPs obtuvieron en otoño e invierno cuando las temperaturas ambientales eran más bajas.

- Se observó que, sin colocar una capa aislante en el tubo de retorno del intercambiador en U, es posible obtener temperaturas alrededor de los 60°C, las cuales son suficientes para accionar un sistema de medio efecto. Sin embargo, es necesario el aislamiento en el tubo para alcanzar temperaturas más altas y así poder impulsar los otros sistemas, especialmente los sistemas de doble y triple efecto.

Con respecto al caso de estudio:

- Para el diseño del almacén (cuarto frío) propuesto, se necesita una carga de refrigeración de 5 kW, con una fuente de calor geotérmica de 80°C para el sistema simple efecto y 163°C para el sistema de doble efecto.
- El sistema de simple efecto ofrece un COP de 0.85, a un costo total aproximado de \$13,083 USD, mientras que el sistema de doble efecto ofrece un COP de 1.38 con un costo de \$18,144 USD.
- El sistema más idóneo es el sistema de doble efecto, ya que ofrece un incremento en el COP de 61%, con un costo total 27% más alto comparado con el sistema de simple efecto.
- El sistema solar no ofrece ventaja contra los sistemas de absorción propuestos activados con energía geotérmica.
- Se calcularon las cargas a través de techos, muros, por iluminación, por infiltración y por ocupación mediante el software Energyplus. Los valores de cargas térmicas totales oscilan entre .94 y 1.1 kW.
- Los valores más altos en las cargas térmicas se presentan en los meses de mayo a septiembre donde la temperatura ambiente es mayor, por tanto, es necesario retirar más calor del exterior para conservar el producto a las condiciones deseadas.
- Los principales parámetros que influyen el costo total son el tamaño de los intercambiadores de calor que componen el sistema de absorción y la distancia del pozo al lugar de aplicación ya que de eso se deriva el costo de la tubería necesaria para transportar el fluido.

Con base a estos argumentos se demostró la viabilidad del uso de los sistemas de refrigeración por absorción para la refrigeración y/o acondicionamiento de espacios, mediante el uso de energía geotérmica como fuente de calor impulsora.

Los resultados de la presente tesis doctoral pueden usarse en las zonas con activada productiva que requiera almacenamiento de productos perecederos para su conservación por más tiempo, carente de suministro de energía.

Mediante esta evaluación se demostró la factibilidad de instalar una unidad de enfriamiento a través de sistemas de refrigeración por absorción en una zona remota donde existe la

disponibilidad de calor de una fuente geotérmica cercana, aún con potencial para su aprovechamiento.

El trabajo a futuro de la línea de investigación puede ser dirigido al desarrollo un caso práctico para su comparación con este trabajo teórico y la búsqueda de tecnología para transportar largas distancias el fluido geotérmico a bajo costo. Esto debido a que alrededor del mundo existen numerosos pozos geotérmicos que pueden ser aún aprovechados para diversas aplicaciones, sin embargo, las largas distancias resultan en la inviabilidad económica.

Referencias

- Andraca Gutiérrez F. H., & Rodríguez Marian J. R. (2012). *Modelado inicial para yacimientos geotérmicos durante la etapa de exploración*. Universidad Nacional Autónoma De México.
- Armstead, H. C. H., & and J.W. Tester. (1987). Heat Mining: a new source of energy. *E&FN Spon Ltd*.
- Augustine, C. , Tester, J. W. , & Anderson, B. ,. (2006). A comparison of geothermal with oil and gas well drilling costs. In , *en Thirty–First Workshop on Geothermal Reservoir Engineering, Proceedings: Stanford, California, Stanford University, SGP–TR–179*,.
- b. Dorgan, C., Dorgan, C. E., & Leight, S. (1995). ASHRAE’s new application guide for absorption cooling/refrigeration using recovered heat. *Ashrae Journal*, 37, 31–37.
- Best, R., & Rivera, W. (2015). A review of thermal cooling systems. *Applied Thermal Engineering*, 75, 1162–1175. <https://doi.org/10.1016/j.applthermaleng.2014.08.018>
- Delgado, C. D., & Juarez, O. R. I. (2014). “*Procesos de perforación y terminación de pozos geotérmicos*. UNAM.
- Dickson, M. H., & Fanelli, M. (2003). *Geothermal energy, utilization and technology*.
- Dickson, M. H., & M. Fanelli. (2003). *Geothermal energy: Utilization and technology*. Publication of UNESCO, Renewable Energy Series, Paris, 205 p.
- Dimas, A., López, C., Victor, M., Ruiz, I., & González Pérez, F. (2018). *Refrigeración: por absorción*.
- ESMAP, (Programa de Asistencia para la Gestión del Sector Energético). (2012). *Manual de geotermia: cómo planificar y financiar la generación de electricidad*.
- Gupta, H. K., & S. Roy. (2007). *Geothermal energy: an alternative resource for the 21st century*, . Ámsterdam, Elsevier Science.
- Gutiérrez-Negrín, L., Canchola Félix, I., Romo-Jones, J. M., & Quijano-León, J. (2020). Geothermal energy in Mexico: update and perspectives. In *Mexican Geothermal Association* (Vol. 466, Issue 4). <https://www.researchgate.net/publication/343111483>
- Gutiérrez-Negrín, L., Canchola Félix, I., Romo-Jones, J. M., & Quijano-León, J. (2020). Geothermal energy in Mexico: update and perspectives. In *Mexican Geothermal Association* (Vol. 466, Issue 4). <https://www.researchgate.net/publication/343111483>
- Hernández Magallanes, J. A. (2017). *Desarrollo y evaluación de un sistema de enfriamiento solar tipo vertical operando con la mezcla nitrato de litio-amoniaco*. UNAM.
- Herold keith E., Radermacher Reinhard, & Sanford A. Klein. (2016). *Absorption-Chillers-and-Heat-Pumps*. Taylor & Francis Group, LLC.

- Hiriart, G. (2013). *Llaman a invertir en energía geotérmica en México*.
[Http://Www.Razon.Com.Mx/IMG/Mk/InfoLR/Mex7291013.Jpg](http://Www.Razon.Com.Mx/IMG/Mk/InfoLR/Mex7291013.Jpg).
- Hiriart, G., & Bert, L. (2011). *Tecnologías de punta y costos asociados para generación distribuida, autoabastecimiento y cogeneración con recursos geotérmicos en México*.
- IDAE, I. para la D. y A. de la E., & IGME, I. G. y M. de E. (2008). *Manual de geotermia Geotermia*.
- IEA, I. E. A. (2018). *The Future of Cooling Opportunities for energy-efficient air conditioning Together Secure Sustainable*. www.iea.org/t&c/
- IGME, I. G. y M. de E. (n.d.). *Roca caliente seca y Sistemas geotérmicos estimulados*.
[Https://Www.Igme.Es/Geotermia/Yacimientos-Rocacalienteseca.Htm](https://Www.Igme.Es/Geotermia/Yacimientos-Rocacalienteseca.Htm).
- Morgado Ruiz, P. (2009). *Construcción y perforación de pozos geotérmicos en el área de Cerro Prieto Mexicali, Baja California Inst.*
- Orús, A. (2022, July 14). *Ranking mundial de los países con mayor potencia geotérmica instalada en 2021*. <https://Es.Statista.Com/Estadisticas/600568/Potencia-Geotermica-Instalada-Par-Paises/#statisticContainer>.
- Perez-Blanco, H. (1984). Absorption heat pump performance for different types of solutions. *International Journal of Refrigeration*, 7(2), 115–122.
[https://doi.org/https://doi.org/10.1016/0140-7007\(84\)90024-0](https://doi.org/https://doi.org/10.1016/0140-7007(84)90024-0)
- Prol-Ledesma, R.-M., Carrillo-De La Cruz, J.-L., Torres-Vera, M.-A., Membrillo-Abad, A.-S., Espinoza-Ojeda, O.-M., Prol-Ledesma, R. M., Carrillo-De La Cruz, J. L., Torres-Vera, M. A., Membrillo-Abad, A. S., & Espinoza-Ojeda, O. M. (2018). *Heat flow map and geothermal resources in Mexico \$ Mapa de flujo de calor y recursos geotérmicos de México*. <https://doi.org/10.22201/igg.25940694.2018.2.51.105>
- REN21, R. 2020 G. S. R. (2020). *Renewables 2020 Global Status Report*.
- Robins, J. C., Kolker, A., Flores-Espino, F., Pettitt, W., Rising, G., Schmidt, B., Beckers, K., Pauling, H., & Anderson, B. (2021). *2021 U.S. Geothermal Power Production and District Heating Market Report*.
- Sánchez-Upton, P., Sánchez-Velasco, R. A., Frost, J. A., & León-Vivar, J. S. (2010). Recuperación secundaria de energía en el campo geotérmico de Cerro Prieto, BC. *Geotermia*, 23(2).
- Santoyo, E., & Barragán-Reyes, R. M. (2010). *Energía Geotérmica*.
- Sureshchandra Bhurat, S., Ranjit Pasupuleti, S., Kunwer, R., Kumar Gugulothu, S., & Joshi, A. (2022). Technical challenges and opportunities for milk chilling unit based on vapor absorption refrigeration systems. *Materials Today: Proceedings*.
<https://doi.org/https://doi.org/10.1016/j.matpr.2022.09.155>
- Trillo, L., & Angulo, R. (2008). *Guía de la energía geotérmica*